INFORMATION TO USERS

This manuscript has been reproduced from the microfilm master. UMI films the text directly from the original or copy submitted. Thus, some thesis and dissertation copies are in typewriter face, while others may be from any type of computer printer.

The quality of this reproduction is dependent upon the quality of the copy submitted. Broken or indistinct print, colored or poor quality illustrations and photographs, print bleedthrough, substandard margins, and improper alignment can adversely affect reproduction.

In the unlikely event that the author did not send UMI a complete manuscript and there are missing pages, these will be noted. Also, if unauthorized copyright material had to be removed, a note will indicate the deletion.

Oversize materials (e.g., maps, drawings, charts) are reproduced by sectioning the original, beginning at the upper left-hand corner and continuing from left to right in equal sections with small overlaps. Each original is also photographed in one exposure and is included in reduced form at the back of the book.

Photographs included in the original manuscript have been reproduced xerographically in this copy. Higher quality 6" x 9" black and white photographic prints are available for any photographs or illustrations appearing in this copy for an additional charge. Contact UMI directly to order.

UMI

University of Alberta

Ubiquitin Conjugating Enzymes: Relating Form to Function

by

Christopher Ptak Ⓒ

A thesis submitted to the Faculty of Graduate Studies and Research in partial fulfillment of the requirements for the degree of Doctor of Philosophy

Department of Biochemistry

Edmonton, Alberta

Fall, 1997

National Library
of Canada

Bibliothèque nationale
du Canada

Acquisitions and
Bibliographic Services

Acquisitions et
services bibliographiques

395 Wellington Street
Ottawa ON K1A 0N4
Canada

395, rue Wellington
Ottawa ON K1A 0N4
Canada

The author has granted a non-exclusive licence allowing the National Library of Canada to reproduce, loan, distribute or sell copies of this thesis in microform, paper or electronic formats.

The author retains ownership of the copyright in this thesis. Neither the thesis nor substantial extracts from it may be printed or otherwise reproduced without the author's permission.

L'auteur a accordé une licence non exclusive permettant à la Bibliothèque nationale du Canada de reproduire, prêter, distribuer ou vendre des copies de cette thèse sous la forme de microfiche/film, de reproduction sur papier ou sur format électronique.

L'auteur conserve la propriété du droit d'auteur qui protège cette thèse. Ni la thèse ni des extraits substantiels de celle-ci ne doivent être imprimés ou autrement reproduits sans son autorisation.

0-612-23058-9

Canada

University of Alberta

Library Release Form

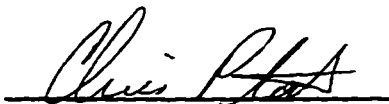**Name of Author:**   Christopher Ptak

Title of Thesis: Ubiquitin Conjugating Enzymes: Relating Form to Function

Degree: Doctor of Philosophy

Year this Degree Granted: 1997

Permission is hereby granted to the University of Alberta Library to reproduce single copies of this thesis and to lend or sell such copies for private, scholarly, or scientific research purposes only.

The author reserves all other publication and other rights in association with the copyright in the thesis, and except as hereinbefore provided, neither the thesis nor any substantial portion thereof may be printed or otherwise reproduced in any material form whatever without the author's prior written permission.

#902 10101 Saskatchewan Drive
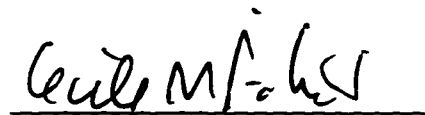Edmonton, Alberta, Canada
T6E 4R6

Sept. 2/1997

University of Alberta

Faculty of Graduate Studies

The undersigned certify that they have read, and recommend to the Faculty of Graduate Studies and Research for acceptance, a thesis entitled Ubiquitin Conjugating Enzymes: Relating Form to Function submitted by Christopher Ptak in partial fulfillment of the requirements for the degree of Doctor of Philosophy.
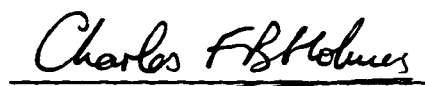
Supervisor: Dr. Michael Ellison

Dr. Cecile Pickart

Dr. Colin Rasmussen

Dr. Charles Holmes

Dr. Richard Rachubinski

Dated: Aug. 31, 19.97

Abstract

The ubiquitin proteolytic system controls the steady state levels of many proteins including such key cellular regulators as cyclins, kinases, and tumor suppressers. In the current model of protein ubiquitination assembly of a multiubiquitin chain is the last step in a cascade reaction where ubiquitin (Ub) is transferred from a Ub activating enzyme (E1), to Ub conjugating enzyme (E2), and finally to the protein target upon which the multiUb chain is assembled. At times a third enzyme, the Ub protein ligase (E3) may accept Ub from the E2 prior to chain assembly. Inherent to this model is that proteolysis is regulated at the level of target recognition and chain assembly; functions of both E2s and E3s. E2s constitute a highly conserved protein family. It is expected that conserved regions of E2s carry out conserved functions such as interactions with E1 or Ub. Conversely, unconserved regions would be expected to take part in functions specific to each E2, for example in target recognition. The E2, CDC34 from the yeast *Saccharomyces cerevisiae* allows these cells to pass through the G1 phase to the DNA replication or S phase of the cell cycle. Deletion analysis identified unique regions within both the catalytic and carboxy terminal domains of CDC34 that were required for its cell cycle function. In particular, CDC34 self-association was shown to be dependent upon the carboxy terminal domain, while multiUb chain assembly by CDC34 was regulated by regions within its catalytic domain. Amino acid substitutions were also introduced at conserved positions within a second E2 from yeast, namely UBC1. Unexpectedly, changes at these conserved residues affected the ability of UBC1 to assemble multiUb chains. Furthermore, multiUb chain assembly by UBC1 was found to be E1 dependent. In this capacity E1 preferentially transferred Ub to a modified form of UBC1, and was also found to play a catalytic role during chain assembly. In contrast to the prevailing model these novel roles for E1 indicate a potential regulatory and direct catalytic role for E1 during chain assembly, indicating that under certain circumstances the Ub conjugation system is poised for immediate action.

Table of Contents

List of Tables

List of Figures

List of Abbrevaiations

A	the nucleotide adenine ot the amino acid alanine
AMP	adenosine monophosphate
APC	anaphase promoting complex
ATP	adenosine triphosphate
BS^3	bis(sulfosuccinimidyl) suberate
BSA	bovine serum albumin
BCA	bicinchoninic acid
C	the nucleotide cytosine or the amino acid cysteine
°C	degrees celsius
CCD	cell cycle determinant
CDC	cell division cycle
CLN	cyclin
CPM	counts per minute
CUP1	copper metallothionine promoter
CYC1	transcriptional terminator
D	aspartic acid
DHFR	dihydrofolate reductase
DNA	deoxyribonucleic acid
DTT	dithiothreitol
E	glutamic acid
E1	ubiquitin activating enzyme
E2	ubiquitin conjugating enzyme
E3	ubiquitin protein ligase
E6	human pappilomavirus oncoprotein
E6-AP	E6 associated protein
E. coli	*Escherichia coli*

EDTA	ethylenediaminetetraacetic acid
EF	elongation factor
F	phenylalanine
FAR	factor arrest
FOA	5-fluoroorotic acid
FPLC	fast pressure liquid chromatography
FUR4	uracil permease
G	the nucleotide guanine or the amino acid glycine
G1	first growth phase of the cell cycle
G2	second growth phase of the cell cycle
GAP1	general amino acid permease
GST	glutathione-S-transferase
H	histidine
HCl	hydrochloric acid
HEPES	4-(2-hydroxyethyl)-1-piperazineethanesulfonic acid
HIS	histidine requiring
hr	hour
I	isoleucine
K	lysine
kDa	kilodaltons
L	leucine
LB	lauria broth
LEU	leucine requiring
MAT	mating type locus
Met	methionine
meUb	reductively methylated ubiquitin
$MgCl_2$	magnesium chloride

mg	milligram
ml	milliliter
mM	millimolar
Mono S	cation exchange column
Mono Q	anion exchange column
M phase	mitosis phase of the cell cycle
multiUb	multiubiquitin
N	asparginine
NaCl	sodium chloride
N-end	amino end
nM	nanomolar
nm	nanometer
ORF	open reading frame
P	proline
PEST	proline, glutamic acid, serine, threonine rich sequence
PP_i	pyrophosphate
R	arginine
RAD	radiation sensitive
RC	RAD6-CDC34 chimera
rpm	revolutions per minute
S	serine
SAC	suppressor of actin mutations
SD	synthetic defined
SDS-PAGE	sodium dodecyl sulphate-polyacrylamide gel electrophoresis
Superdex	gel exclusion column
S phase	replication phase of the cell cycle
T	threonine

TCA	trichloroacetic acid
Tris	tris(hydroxymethyl)aminoethane
TRP	tryptophan requiring
ts	temperature sensitive
Ub	ubiquitin
UBA	ubiquitin activating enzyme
UBC	ubiquitin conjugating enzyme
UBI	ubiquitin gene
UBR	ubiquitin protein ligase
URA	uracil requiring
V	valine
W	tryptophan
Y	tyrosine
Δ	deletion
μCi	microcurie
μg	microgram
μM	micromolar
5'	five prime end
3'	three prime end
%	percent

Chapter 1

General Introduction: Protein Ubiquitination

Intracellular protein levels are regulated to ensure that they are present in sufficient quantities to carry out their cellular functions. At times this requires that the level of a protein be increased, while other situations require that a protein be absent from the cell, or remain at a low level as its presence becomes inhibitory to key cellular processes.

The means by which cells regulate protein levels are varied. Often, a protein will have an 'on' and an 'off' state. In these situations, the 'on' state will be representative of a high cellular level while the 'off' state that of a low cellular level. Covalent modifications such as phosphorylation, or the binding of a ligand to a protein can function to regulate proteins in this way.

A less subtle approach functions to directly increase or decrease protein levels. In this respect, cells regulate the dynamic relationship between protein synthesis and degradation. While much study has gone into defining the processes involved in protein synthesis, such as transcription and translation, protein degradation has only recently received serious attention. From these studies it has been shown that within eukaryotes, the covalent modification of a protein with the small polypeptide ubiquitin (Ub) leads to the eventual degradation of that protein.

Ubiquitin (Ub) may form an isopeptide bond between its carboxy terminus and the ε-amino group of a lysine residue found in either a second Ub molecule or that of another protein (Busch and Goldknopf, 1981). Although this linkage is a simple amide bond the process involved in covalently linking Ub to another protein has proven to be complex. This complexity stems primarily from the requirement of specificity in protein ubiquitination. In other words, a cell must be able to distinguish between proteins that should be ubiquitinated from those that should not. A consequence of this requirement is that the number of proteins involved in facilitating the ubiquitin system is fairly large. Of these, three distinct protein classes have been shown to be directly involved in the formation of an isopeptide bond between Ub and another protein.

The first of these is the ubiquitin activating enzyme (UBA, or E1) which functions to chemically activate the carboxy terminus of Ub in an ATP dependent manner. Upon activation Ub is then transferred from the E1 to a ubiquitin conjugating enzyme (UBC or E2). The E2 will then identify a protein target and subsequently transfers Ub to it. In many cases the ability of an E2 to recognize a target is facilitated through the action of a third component referred to as the ubiquitin protein ligase (E3) (Hershko *et al.*, 1983). As

1

E2s and E3s are responsible for target recognition it is not surprising to note that these enzymes comprise protein families. Each member of the E2 or E3 family is involved in the ubiquitination of a distinct subset of targets.

In most cases it has been found that the process of protein ubiquitination results in the attachment of many Ubs to a target. These Ubs are usually found linked to one other forming a multiubiquitin (multiUb) chain which is in turn linked to a protein target (Chau *et al.*, 1989). Once assembled on a target, the multiUb chain is recognized by a specific subunit(s) of the large proteolytic complex referred to as the 26S proteosome (van Nocker *et al.*, 1996; Devereaux *et al.*, 1994). The proteosome unfolds the target and subsequently degrades it into peptide fragments (Lowe *et al.*, 1995; Seemuller *et al.*, 1995). Upon degradation the multiUb chain is released from one of the peptide fragments (Papa and Hochstrasser, 1993) and subsequently processed into Ub monomers (Wilkinson *et al.*, 1995; Hadari *et al.*, 1992) through the action of a ubiquitin hydrolase. In this way Ub is recycled and may once again be used in the assembly of chains and eventual protein degradation.

The biological importance of the Ub system has been borne out many times through mutational analysis. These studies have identified roles for the Ub system in such diverse cellular processes as the stress response (Seufert and Jentsch, 1990), cell cycle (Seufert *et al.*, 1995; Glozter *et al.*, 1991; Goebl *et al.*, 1988), oncogenesis (Sheffner *et al.*, 1990), DNA repair (Jentsch *et al.*, 1987), protein compartmentalization (Hicke and Riezman, 1996), and peroxisome biogenesis (Wiebel and Kanau, 1992). In most cases the connection between the Ub system and these cellular processes occurs on the level of protein degradation. For example, during the stress response the ubiquitination of damaged proteins leads to their degradation and removal from the cell (Seufert and Jentsch, 1990). In another example, degradation of cyclin B by the Ub system is required in order for cells to pass through mitosis and enter another cell cycle (Holloway *et al.*, 1993; Surana *et al.*, 1993).

While protein degradation appears to be the principal function of the Ub system other studies have shown that Ub does not always function as a degradation signal. In this regard Ub has been found to function as a chaperonin (Baker *et al.*, 1994; Finley *et al.*, 1989), a phosphorylation signal (Chen *et al.*, 1996), a compartmentalization signal (Hicke and Riezman, 1996), and a signal for protein processing (Orian *et al.*, 1995; Palombella *et al.*, 1994). Thus, Ub may function as a multipurpose signal either directing proteins for degradation or defining the manner in which proteins are utilized by a cell.

The work presented in this volume relates directly to two distinct questions. First, what are the structural elements within E2s that are key in defining their function, and second,

2

what is the mechanism involved in the assembly of multiUb chains. As such, this introductory section will focus on those aspects of the Ub pathway pertinent to the discussion of this work. To begin with, specific structural and chemical features of Ub itself are presented, followed by discussions of multiUb chains, the signals leading to protein ubiquitination, and the enzymes responsible for this process.

1.1. Ubiquitin.

Early fractionation experiments identified a small heat stable polypeptide required for the ATP dependent proteolysis of misfolded proteins (Ciechanover et al., 1978; Etlinger and Goldberg, 1977). Subsequent analysis identified this protein to be Ub (Wilkinson et. al., 1980); at the time, a protein of unknown function found both free and covalently linked to histones (Busch and Goldknopf, 1981). It was shown that the addition of radiolabeled Ub to a reticulocyte lysate resulted in its covalent linkage to many proteins (Ciechanover et al., 1980). Furthermore, linkage of Ub to these proteins also stimulated their degradation (Hershko et al., 1980).

The nature of the Ub-protein linkage had been determined for the Ub-histone H2A adduct which was composed of an isopeptide bond between the carboxy terminus of Ub and the ε-amino group of H2A's K119 residue (Busch and Goldknopf, 1981). As such, it was proposed that the same isopeptide linkage occurred within other Ub-protein conjugates (Ciechanover et al., 1980). In fact, linkage of Ub to calmodulin (Gregory et al., 1985) and other proteins was found to require the presence of at least one lysine residue. Furthermore, chemical cleavage of Ub's carboxy terminal residues eliminated its ability to become conjugated, and as such could not stimulate protein degradation (Wilkinson and Audhya, 1981).

Often, multiple Ubs were found to be conjugated to a protein. At first it was thought that these multiUb conjugates consisted of Ubs singly conjugated to multiple lysine residues. However, the number of Ubs conjugated to certain proteins including lysozyme (Hough et al., 1986; Hershko et al., 1984) and a β-galactosidase derivative (Bachamir et al., 1986) was in excess of the number of lysine residues found in these proteins. To account for these observations it was suggested that Ub conjugated to a protein could itself become a site for ubiquitination. As such, the carboxy terminus of an incoming Ub could form an isopeptide bond with an amino group of the conjugated Ub (Hershko and Heller, 1985). Reiteration of this process would result in the formation of a multiUb chain.

The amino groups found in Ub could be chemically blocked by reductive methylation (meUb). As the carboxy terminus of meUb is not affected it may still become singly

3

conjugated to a target protein, but would not be able to function as a site for the assembly of a multiUb chain given that its amino groups have been blocked. Through the use of meUb it was found that the number of Ubs linked to a protein target was reduced in comparison to the use of unmodified Ub. This implied that multiUb chains were in fact being assembled and that assembly could be blocked through the use of meUb (Hershko and Heller, 1985).

Subsequent studies were used to definitively show that multiUb chains could become attached to a single lysine residue within a protein target. In this work, chemical cleavage analysis revealed that a multiUb chain conjugated to β-galactosidase test proteins consisted of Ubs linked together through isopeptide bonds. Furthermore, the isopeptide bonds linking these Ubs were uniform in that the carboxy terminus of one Ub was linked to the ε-amino group of residue K48 found in another Ub (Chau et al., 1989; Gregori et al., 1990). Recent studies have found that alternative lysine residues found in Ub may also be used in multiUb chain assembly. The nature and significance of these alternate linkages is discussed in section 1.2.

Elucidation of the Ub crystal structure has provided a structural basis for its various chemical and functional characteristics. Ub was shown to be a 76 amino acid polypeptide whose structure consisted of one α-helix, five β-strands, and seven reverse turns. The relatively large number of turns allows Ub to take up a compact structure which is stabilized through extensive hydrogen bonding and a hydrophobic core (Vijay-Kumar et al., 1987; 1985). These interactions account for the comparatively high degree of chemical and thermal stability exhibited by Ub. In fact, high temperatures and low pHs have been used during Ub purification (Wilkinson et al., 1987; Haas and Wilkinson, 1985).

Out of this compact, stable structure extrudes the carboxy terminus of Ub consisting of residues G75-G76. This allows the carboxy terminus of Ub to be made available for its conjugation to other proteins (Vijay-Kumar et al., 1987; 1985).

Folding of the Ub polypeptide also places all of its acidic and basic side chains at the protein surface. These residues cluster on the surface of Ub generating distinct acidic and basic patches. Recent studies have indicated that some of the arginine residues making up the basic patch are important for interactions with E1 (Burch and Haas, 1994). The presence of each lysine residue on the protein surface also makes these residues available for chain assembly.

Of the hydrophobic residues, all but three remain buried within the Ub structure. Those residues which are solvent exposed include L8, I44, and V70. Together these residue produce a hydrophobic patch on the surface of Ub. Mutational analysis has found that the

4

principal role of these residues is in protein degradation, possibly by defining a site of interaction between Ub and the 26S proteosome (Beal et al., 1996).

Comparison of both the amino acid sequence and the crystal structure of Ub from a variety of organisms identifies Ub to be the most conserved eukaryotic protein (Vijay-Kumar 1997a; Ozkaynak et al., 1994). This conservation has placed structural constraints on some of the other components of the Ub system. For example, E2s (ubiquitin conjugating enzymes) also show a high degree of sequence and structural conservation (Jentsch et al., 1990).

Ub conservation is not relegated to its protein structure, but extends to the structure of its genes. As a result, the following discussion of the ubiquitin genes from the yeast *Saccharomyces cerevisiae* is generally true of Ub genes from all other organisms. Four separate genes encoding for Ub have been identified in yeast, and are referred to as *UBI 1-4* (Ozkaynak et al., 1987). *UBI 1-3* encode for proteins consisting of Ub bearing carboxy terminal extensions. These fusions are processed to generate free Ub and polypeptides found in the ribosome (Finley et al., 1989; Redman and Reichsteiner, 1989). Apparently, Ub functions as a nucleation site for the folding of the carboxy terminal extensions increasing their intracellular levels (Finley et al., 1989). In fact, Ub amino terminally fused to a number of proteins has been found to have a similar effect (Baker et al., 1994). As such, Ub is thought to possess a chaperonin function along with its function in protein degradation.

Unlike the other Ub genes, *UBI4* encodes for a contiguous polypeptide consisting of five Ub repeats linked head to tail (Ozkaynak et al., 1984). This polypeptide is also unique in that an additional residue is found at the carboxy terminus of the last Ub in the chain (Ozkaynak et al., 1987). Processing of the multiUb chain encoded by *UBI4* occurs essentially co-translationally such that the chain is split into monomeric Ubs, and the additional carboxy terminal residue is removed. Rapid processing of this multiUb chain is generally thought to preclude its conjugation to proteins. The conjugation of any unprocessed chains is also blocked by the presence of the additional carboxy terminal residue blocking the access of E1 to residue G76 thereby inhibiting activation of this chain (Ozkaynak et al., 1987, 1984).

The promoter region of *UBI4* possesses a heat shock element (Ozkaynak et al., 1984) allowing for its expression under conditions of stress such as elevated temperature or DNA damage (Treger et al., 1988; Ozkaynak et al., 1987). A *UBI4* deletion strain has also been found to be highly sensitive to these same stresses (Finley et al., 1987). As such, the multiple copies of Ub encoded by *UBI4* function to rapidly increase the intracellular concentration of Ub under conditions of stress. This ensures that the relatively large

amount of damaged proteins produced under these conditions continue to be degraded by the ubiquitin system without severely depleting the intracellular levels of free Ub (Finley *et al.*, 1987).

1.2. MultiUb chains.

The previous section identified two distinct forms of multiUb chains, namely: the head to tail arrangement encoded by the *UBI4* gene and the K48 linked chain found conjugated to a β-galactosidase derivative. For reasons cited above, the primary function of the *UBI4* encoded chain is to provide a means of rapidly increasing Ub protein levels.

A derivative of Ub, namely UbR48 has been used to probe the importance of assembling K48 linked multiUb chains. As UbR48 bears the K48R amino acid substitution its use functions to effectively block the extension of K48 linked multiUb chains. *In vitro* studies have shown that the use of UbR48 blocks the assembly of multiUb chains conjugated to β-galactosidase test proteins. Furthermore, blocking chain assembly was also shown to inhibit degradation of these proteins. As the carboxy terminus of UbR48 remained intact it was observed to become singly conjugated to these targets. Even so, the monoubiquitinated versions of these test proteins were not degraded. These results implied that the conjugation of a single Ub to a target was insufficient for signaling its degradation, rather the presence of a multiUb chain was required (Chau *et al.*, 1989).

The biological importance of K48 linked chains was also assessed using the yeast *S. cerevisiae*. In this study each of the four Ub genes, namely *UBI 1-4* were knocked out. As simultaneous deletion of these genes is lethal, the ectopic expression of Ub within these cells was required for cell viability. The ectopic expression of UbR48 within this deletion strain proved to be lethal. Furthermore, these cells were found to arrest in late G2 or M phase, and overall protein degradation, as well as the degradation of damaged proteins was also shown to be inhibited. These results suggested that *in vivo*, K48 linked chains play a vital role in protein degradation and in this capacity are critical for maintaining cell viability (Finley *et al.*, 1994).

One possible role played by multiUb chains in protein degradation appears to involve targeting the ubiquitinated protein to the 26S proteosome. Using purified K48 linked multiUb chains a component of the 26S proteosome referred to as S5a was found to specifically bind these chains (Devereaux *et al.*, 1994). Furthermore, the binding of chains to S5a was dependent upon chain length. It was shown that as chain length is increased from Ub$_3$ to Ub$_4$ the binding affinity of the chain to S5a was also found to dramatically increase. Similar observations were made for chains with lengths greater than four Ubs.

These results indicated that chains consisting of four or more Ubs bind to S5a in a cooperative manner (Devereaux *et al.*, 1994; Baboshina and Haas, 1996).

Crystal structures of the K48 linked Ub_2 and Ub_4 chains provide a possible explanation for this observation. The Ub_2 structure is characterized by a two fold symmetry between the two Ubs in the chain. This structure is stabilized through hydrogen bonding, and hydrophobic interactions. While hydrophobic residues L8, I44, and V70 form a patch on the surface of Ub, this patch becomes buried within the Ub_2 structure as a consequence of hydrophobic contacts (Cook *et. al.*, 1992). It has also been shown that this patch defines an element within Ub that is required for the interaction of multiUb chains with the proteosome. The fact that these residues remain buried may in part explain the poor affinity of Ub_2 for the proteosome subunit S5a (Beal *et al.*, 1996).

Although the Ub_2 structure provides a free carboxy terminus and K48 residues, the addition of a third Ub to extend the chain could not be accommodated by the conformation taken up by Ub_2. Elucidation of the Ub_4 crystal structure showed that this problem is overcome by a conformational shift within each Ub_2 moiety found in the Ub_4 chain. Furthermore, the distinct Ub_2 conformation within the Ub_4 chain places the L8, I44, V70 hydrophobic patch of each Ub on the surface of the chain (Cook *et al.*, 1994). The redundancy of this patch throughout multiUb chains consisting of four or more Ubs may account for their increased affinity for, and co-operative binding to proteosome subunit S5a (Beal *et al.*, 1996).

Recent studies have also shown that the linkage between the carboxy terminus of one Ub and K48 of another Ub does not define the sole manner in which Ubs may be linked. *In vivo* studies carried out in yeast indicate a role for K63 linked Ubs in both DNA repair (Spence *et al.*, 1995), and the stress response (Arnason and Ellison, 1994). The conjugation of multiUb chains and the degradation of the Ub-β-galactosidase and Ub-dihydrofolate reductase (Ub-DHFR) fusion proteins was shown to be dependent upon Ub residue K29 in yeast (Johnson *et al.*, 1995). *In vitro* work has also shown that residues K11, K6 (Baboshina and Haas, 1996), as well as the amino terminus (Hodgins *et al.*, 1996) may be used to link Ubs.

While these studies have identified novel Ub linkages, and shown that at least the K29 and K63 links have some biological significance the precise role of these links in the formation of a multiUb chain remains to be determined. Furthermore, it has not been definitively established whether these links are: propagated uniformly through a chain, define the initial linkage in a chain, or are part of chains bearing mixed linkages (Arnason and Ellison, 1994). Concrete proof will require direct chemical mapping of multiUb chains

bearing these alternative linkages as previously carried out for K48 linked chains (Chau *et al.*, 1989).

It also remains to be determined what role these alternative linkages play in protein degradation. In particular, how are these chains recognized by the 26S proteosome. In the case of test proteins it has been shown that their *in vivo* degradation is inhibited through the use of UbK29R indicating a role for the K29 linkage in degradation (Johnson *et al.*, 1996). Within the Ub structure, the surface which bears K29 is found opposite to that bearing K48. As such it would be expected that a uniform K29 linked multiUb chain would be structurally distinct from a K48 linked chain. If so, then do other proteosome subunits function to recognize elements within the K29 chain or for that matter chains bearing linkages other than K48.

1.3. Ubiquitination signals.

Just as the conjugation of a multiUb chain to a protein signals its degradation, there must be some determinant within each protein target that signals its ubiquitination. Of the signals which have been elucidated the N-end rule is the best characterized. Simply, the N-end rule states that the susceptibility of a protein to degradation via the Ub dependent proteolytic pathway is dependent upon the residue found at its amino terminus. The *in vivo* half-lives of various β-galactosidase test proteins were measured as a function of which residue was present at their amino terminus. This study showed that the amino terminal residues could be broadly classified into stabilizing, i.e. provided the test protein with a long half life, or destabilizing, i.e. provided the test protein with a short half life. In particular, basic (K, R, H) or bulky hydrophobic (I, L, F, W, Y) groups were found to be destabilizing (Bachamir *et al.*, 1986).

When using a similar set of amino terminally distinct DHFR test proteins the N-end rule did not appear to operate as each derivative remained stabilized. This indicated that along with the amino terminal residue some other element within the β-galactosidase derivatives functioned to direct ubiquitination. It was determined that this secondary element was the actual ubiquitination site, namely the K residue to which the multiUb chain becomes conjugated. Furthermore, the use of such a ubiquitination site via the N-end rule pathway requires that it be spatially close to the amino terminus (Bachamir and Varshavsky, 1989).

Although the N-end rule has been shown to operate in yeast as well as in mammalian systems (Gonda *et al.*, 1989) its general utilization and biological importance as a ubiquitination signal remains debatable given that first, there is little diversity among the amino termini of most proteins (Arfin and Bradshaw, 1989) such that destabilizing

residues are generally not presented and second, deletion of the yeast genes which encode for enzymes of the ubiquitin system involved in the recognition and ubiquitination of N-end rule targets is not lethal and does not effect the overall degradation of proteins *in vivo* (Varshavsky, 1992; Bartel *et al.*, 1990).

Most proteins are found to be modified *in vivo* through the acetylation of their amino termini (N^α-acetylation; Brown and Roberts, 1976). A subset of these N^α-acetylated proteins including histone H2A, and actin are degraded via the ubiquitin system (Gonen *et al.*, 1991). Their degradation is mediated through the action of the translation elongation factor, EF-1α. In this process EF-1α directs ubiquitinated N^α-acetylated proteins to the 26S proteosome (Gonen *et al.*, 1994). Given that some 80% of all cellular proteins are N^α-acetylated, as a degradation signal this modification would likely result in a futile cycle of bulk protein synthesis and degradation. To avoid such a cycle it is possible that additional elements within N^α-acetylated proteins are also required to signal their ubiquitination and degradation.

Another protein modification, namely phosphorylation also functions in certain cases as a ubiquitination signal. In yeast, ubiquitination of the G1 cyclin CLN2 (Deshaies *et al.*, 1995; Willems *et al.*, 1996), and the cyclin dependent kinase inhibitor SIC1 (Schneider *et al.*, 1996) is dependent upon their phosphorylation. In the case of CLN2, its phosphorylation appears to direct it to a multi-component complex where upon binding it becomes ubiquitinated (Willems *et al.*, 1996). A third example involves the phosphorylation dependent ubiquitination of IκBα, an inhibitor of the transcription factor NF-κB (Chen *et al.*, 1995; Scherer *et al.*, 1995; Alkalay *et al.*, 1995). This presents an interesting case as the phosphorylation of IκBα is dependent upon an initial ubiquitination event, distinct from the ubiquitination event leading to IκBα degradation (Chen *et al.*, 1996). It remains to be seen if the same lysine residues within IκBα are utilized in both its ubiquitin dependent phosphorylation and degradation.

A final category for ubiquitination signals comprise structural motifs found on the surface of target proteins. One such signal consists of peptide stretches within a target that are rich in the amino acid residues proline, glutamic acid, serine, and threonine, i.e. PEST elements. It is believed that PEST elements remain masked and that only through the action of some inducing event can they function as a signal for protein ubiquitination and degradation (Rechsteiner and Rogers, 1996). An interesting example involves the protein phytochrome. A light sensitive cofactor is covalently linked to phytochrome at a residue adjacent to its PEST region. Upon exposure to light the cofactor undergoes a conformational change which is thought to expose the PEST region (Rechsteiner, 1990). Degradation of the yeast cyclin CLN3 is also dependent upon its PEST regions. It appears

that the utilization of these regions as a ubiquitination and degradation signal initially requires the phosphorylation of a serine residue in one of its PEST elements (Yaglom *et al.*, 1995).

In an attempt to identify other potential peptide elements which function to signal protein ubiquitination and degradation, Sadis *et al.* (1995) introduced a random peptide library into a β-galactosidase test protein. Three distinct peptide families which decreased the test proteins half-life were identified. One set of signals functioned within the N-end rule discussed above, while the other two identified a role for hydrophobic residues in signaling. One of the hydrophobic set of peptides conformed to the characteristics expected of amphipathic helices. Using amino acid substitutions the putative hydrophobic face of these helices was shown to be critical in signaling ubiquitination and degradation. The biological relevance of such a signal has been inferred from the observation that the degradation signal found within the yeast transcriptional regulator MATα2 also conforms to the characteristics expected of an amphipathic helix (Ho *et al.*, 1995). The second set of hydrophobic peptides consisted of short homopolymers of amino acid residues such as I or L. These peptides are thought to mimic the unfolded state taken up by damaged proteins which are themselves degraded by the ubiquitin system (Seufert and Jentsch, 1990). It is thought that the presence of these residues on the protein's surface signals its ubiquitination and degradation; a premise supported by the observations of Sadis *et al.* (1995).

1.4. Ubiquitin activating enzyme.

Prior to the conjugation of Ub to a protein its carboxy terminus must become chemically activated. This activation is catalyzed by the first enzyme involved in protein ubiquitination, namely the ubiquitin conjugating enzyme (E1 or UBA). Early studies showed that E1 activates the carboxy terminus of Ub in an ATP dependent manner following the set of reactions shown below (Haas and Rose. 1982; Haas *et al.*, 1982; Ciechanover *et al.*, 1982)

$$E1 \ + \ ATP \ + \ Ub \ \rightleftharpoons \ E1 \cdot AMP\text{-}Ub \ + \ PP_i \qquad (1)$$

$$E1 \cdot AMP\text{-}Ub \ \rightleftharpoons \ E1\text{-}Ub \ + \ AMP \qquad (2)$$

$$E1\text{-}Ub \ + \ ATP \ + \ Ub \ \rightleftharpoons \ (E1\text{-}Ub) \cdot AMP\text{-}Ub \ + \ PP_i \qquad (3)$$
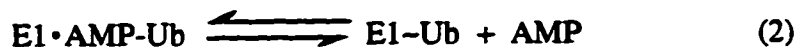
In reaction 1, the carboxy terminal glycine of Ub becomes activated through the hydrolysis of ATP resulting in the formation of the AMP-Ub adenylate (Haas *et al.*, 1983).

10

The adenylate binds strongly to E1 at a site close to one of the E1's cysteine residues. This allows for the transfer of Ub from AMP to the sulfhydryl group found in the cysteine side chain leading to the formation of the E1-Ub thiolester (reaction 2). Finally, a second molecule of AMP-Ub is synthesized and bound to E1-Ub (reaction 3).

Although E1 functions to activate Ub it does not directly participate in protein ubiquitination. Rather, a transthiolation reaction occurs in which Ub is transferred from the E1 thiolester to a sulfhydryl group found within a ubiquitin conjugating enzyme (E2 or UBC) as depicted in reaction 4.

$$E1\text{-}Ub + E2 \rightleftharpoons E1 + E2\text{-}Ub \quad (4)$$

This transthiolation reaction is stimulated through the binding of AMP-Ub to the E1-Ub thiolester as depicted in reaction 3, or by the binding of ATP at the same site (Pickart et al., 1994).

A number of mammalian cell lines carrying temperature sensitive alleles of E1 have been identified. At the non-permissive temperature these cells are shown to arrest at either the G2 or M phase of the cell cycle (Kulka et al., 1988; Finley et al., 1984). In the yeast *Saccharomyces cerevisiae* disruption of either the *UBA1* (McGrath et al., 1991), or *UBA2* (Dohmen et al., 1995) genes which encode for distinct E1 isoforms is lethal. A distinct terminal phenotype could not be associated with the *UBA1* disruption. As E1 function is pleiotropic in that it transfers Ub to a number of different E2s each of which is involved in distinct cellular pathways (see section 1.5) it is not surprising to find that disruption of *UBA1* leads to multiple terminal phenotypes (McGrath et al., 1991). Disruption of UBA2 on the other hand leads to arrest at a number of distinct stages of the cell cycle. This observation is in keeping with the nuclear localization of UBA2 indicating it is solely involved in cellular processes which occur in the nucleus (Dohmen et al., 1995). These mutational studies underscore the biological importance of both E1 and the ubiquitin system.

The identification of multiple E1s in yeast (Dohmen et al., 1995), wheat (Hatfield and Vierstra, 1992), and mammalian (Cook and Chock, 1992) cells also suggests that different E1s may be involved in different cellular pathways. As mentioned, yeast UBA2 appears to function solely within the nucleus. Other studies using human cell lines have identified distinct cytoplasmic and nuclear E1 populations (Handley-Gearhart, 1994), and that the localization of E1 to the nucleus varies over the cell cycle (Grenfell et al., 1994). Furthermore, retention of E1 in the nucleus is thought to be dependent upon its being phosphorylated (Stephen et al., 1996). Controlling the nuclear localization of E1 in a cell cycle dependent fashion may function to regulate the ubiquitination of nuclear proteins in a

cell cycle dependent manner as well (Stephen et al., 1996). These studies indicate that ubiquitination pathways may be regulated either through the use of distinct E1 isoforms or through the covalent modification of a single E1.

Chapter 4 presents work carried out in our lab which indicates that protein ubiquitination may be regulated through reactions carried out by E1. In particular, using in vitro reactions we found that bovine E1 preferentially transferred Ub to a covalently modified E2 over its unmodified counterpart. Similar reactions using wheat E1 showed that this E1 could only transfer Ub to the unmodified E2. The transfer of Ub from E1 to the modified E2 was also shown to be the key step in the assembly of multiUb chains. Therefore, the assembly of multiUb chains was contingent upon the ability of bovine E1 to recognize the modified E2 and subsequently transfer Ub to it. These observations along with the identification of: multiple E1 isoforms, and modified forms of E1 with distinct cellular activities suggests that E1 function may also be relegated to a subset of cellular pathways. It can be envisioned that distinct E1 isoforms or modified E1 derivatives drive protein ubiquitination through the formation of distinct E1/E2 combinations. Each of these combinations then would be involved in the ubiquitination of a specific subset of proteins. As such, E1s may not play a static role in the activation and transfer of Ub but may also play a regulatory role in the process of protein ubiquitination and multiUb chain assembly.

1.5. Ubiquitin conjugating enzymes.

Apart from being acceptors of Ub from E1 (see reaction 4, section 1.4) , E2s may also function as the immediate donors of Ub during protein ubiquitination and multiUb chain assembly (van Nocker and Vierstra, 1993; Chen and Pickart, 1990; Hershko et al., 1983). As the number of intracellular ubiquitination targets are numerous E2s must also be able to differentiate between these potential targets ensuring that protein ubiquitination and degradation occur at appropriate times. A consequence of this requirement is the existence of multiple E2s each responsible for the ubiquitination of a specific subset of proteins. As a result, target specificity confines the function of each E2 to a distinct cellular pathway.

Studies carried out in yeast were useful in identifying E2s, and through mutational and phenotypic analysis identifying which cellular pathway each is involved in. To date, ten E2s each involved in distinct cellular pathways have been identified in yeast. These include: RAD6 (UBC2), which functions in DNA repair, induced mutagenesis, sporulation (Jentsch et al., 1987), and the N-end rule (Sung et al., 1991; Dohmen et al., 1991) pathways; CDC34 (UBC3), which is required for the transition from G1 phase to S phase of the cell cycle (Goebl et al., 1988); UBC1, UBC 4, and UBC5 each of which is

involved in the stress response, and normal cell growth (Seufert and Jentsch, 1990; Seufert *et al.*, 1990), while UBC1 is also involved in spore germination (Seufert *et al.*, 1990); UBC6 which functions to regulate protein translocation (Sommer and Jentsch, 1993); UBC7 which functions in the resistance of cells to cadmium (Jungmann *et al.*, 1993); UBC9 which is required at the G2 and M phases of the cell cycle (Seufert *et al.*, 1995); PAS2 (UBC10) which is involved in peroxisome biogenesis (Wiebel and Kanau, 1992); and lastly, the cellular pathway in which UBC8 functions has not been determined (Qin *et al.*, 1991).

Associating an E2 with a distinct cellular pathway is indicative of its ability to ubiquitinate and target for degradation other proteins involved in the same pathway. For example, UBC1, UBC4, and UBC5 function to ubiquitinate and target damaged proteins for degradation, in keeping with their role in the stress response. Similarly, CDC34 is involved in the degradation of G1 cyclins (Willems *et al.*, 1996; Yaglom *et al.*, 1995; Deshaies *et al.*, 1995), and the cyclin dependent kinase inhibitor SIC1 (Schneider *et al.*, 1996; Schwob *et al.*, 1994) as part of its role in the G1 to S phase transition, while UBC9 is involved in the degradation of B-type cyclins in keeping with its function in the G2/M phases of the cell cycle (Seufert *et al.*, 1995).

All E2s are characterized by a conserved catalytic domain which contain the active site cysteine residue required for the formation of the E2~Ub thiolester (see reaction 4, section 1.4). At the primary sequence level these catalytic domains share anywhere from ninety-three percent to thirty-three percent identity (Seufert *et al.*, 1990). Sequence similarities are thought to reflect structures which are involved in functions that are common to all E2s, such as the formation of the E2~Ub thiolester. On the other hand, sequence differences would reflect specific E2 functions, such as target recognition.

Of the ten yeast E2s, four consist solely of the catalytic domain (Finley, 1992). The fact that E2 function can be carried out solely by these enzymes indicates that the E2 catalytic domain may contain the necessary information required for common and unique E2 functions. Comparing the crystal structures of two E2s that share 42 percent sequence identity and consist solely of the E2 catalytic domain showed that these structures may be superimposed (Cook *et al.*, 1993). This indicates that the catalytic domains of all E2s are structurally similar. Therefore, the structural features which determine functional specificity or similarity are defined not by gross E2 structure, but by the distribution of amino acids on a common E2 structure. Mapping the positions of conserved E2 residues onto these structures shows that they cluster within specific structural regions. It is expected that these conserved structures will be involved in functions common to all E2s.

Our first attempts at determining specific E2 functions that may be ascribed to such conserved regions is the focus of chapter 5.

CDC34 and UBC7 differ from the other yeast E2s in that they possess a polypeptide insertion found on the carboxy terminal side of their active site cysteines. The CDC34 catalytic domain insertion plays an important role in defining CDC34's cell cycle function (Liu *et al.*, 1995; Pitluk *et al.*, 1995). Chapter 3 extends these observations with evidence that the polypeptide insertion helps to define the *in vitro* activity of CDC34, and determines how the tail domain is utilized by CDC34 in these reactions.

Some of the yeast E2s consist not only of the conserved catalytic domain but also possess carboxy terminal extensions or tails. A functional role for some of these tail domains has been determined. The RAD6 tail is required for its sporulation function and does not appear to function in other RAD6 related pathways such DNA repair (Morrison *et al.*, 1988). *In vitro* ubiquitination reactions were used to show that the UBC1 tail functions to modulate the linkage used in the assembly of multiUb chains from K48 of Ub to the amino terminus of Ub. Deletion of this tail domain from UBC1 allows for the synthesis of K48 linked chains (Hodgins *et al.*, 1996). The UBC6 tail anchors this enzyme to the cytosolic side of the endoplasmic reticulum (Sommer and Jentsch, 1993). Finally, the cell cycle function associated with CDC34 requires its tail domain (Kolman *et al.*, 1992; Silver *et al.*, 1992). The work presented in chapter 2 shows that only a small portion of the CDC34 tail is required for carrying out its cell cycle function and that this same region of the tail is required for CDC34 self-association.

E2-E2 interactions is not relegated to CDC34 self-association. Other E2s have also been shown to interact forming either homodimers (Gwozd *et al.*, 1994; Girod and Vierstra, 1993; Haas and Bright, 1988; Pickart and Rose, 1985), or heterodimers (Chen *et al.*, 1993). The heterodimeric interaction between UBC6 and UBC7 is required in the degradation of the MATα2 repressor (Chen *et al.*, 1993), while the requirement of a UBC4 homodimer has been implicated in UBC4 autoubiquitination (Gwozd *et al.*, 1994). A definitive biological role for these E2 complexes remains to be determined. One possible function is presented in chapter 2, which suggests that multiUb chains are synthesized through the interaction of E2s carrying Ub at their active sites. A second possibility is that E2s interact to form target recognition sites. The ability of E2s to form heterodimers may introduce a combinatorial factor in the number of possible target recognition sites that could be formed between various E2-E2 pairs (Chen *et al.*, 1993).

1.6. Ubiquitin protein ligases.

While *in vitro* studies have shown that E2s may function alone in target recognition (van Nocker and Vierstra, 1993; Haas *et al.*, 1991; Sung *et al.*, 1988) it is thought that *in vivo* target recognition is mediated through the activity of auxiliary factors referred to as ubiquitin protein ligases or E3s (Hershko *et al.*, 1983). Inherent to this function is the requirement that E3s interact with both their E2 partner and the ubiquitination target. The E3 which mediates protein ubiquitination in the N-end rule pathway conforms to these criteria.

The N-end rule degradation signal is composed of two elements; the amino terminal residue and the lysine residue at which ubiquitination occurs (see section 1.3). *In vivo* studies have shown that the yeast N-end rule E3, namely UBR1 is required for the degradation of β-galactosidase test proteins carrying destabilizing residues at their amino termini (Bartel *et al.*, 1990). This function of UBR1 or its mammalian homologs may be inhibited by the presence of dipeptides containing destabilizing residues. As such, target recognition proceeds through a direct interaction between the N-end rule E3 and the amino terminus of the target. (Baker and Varshavsky, 1991; Reiss and Hershko, 1990; Gonda *et al.*, 1989; Reiss *et al.*, 1988). UBR1 also interacts with RAD6, the E2 responsible for the degradation of N-end rule targets (Dohmen *et al.*, 1991; Sung *et al.*, 1991). Through these two interactions UBR1 may bring RAD6 in close proximity to the target protein. In this configuration, RAD6 may then transfer Ub to the target lysine residue, and proceed to assemble the multiUb chain from this initial Ub moiety (Finley, 1992).

UBR1 and its mammalian homologues represent E3s which play structural roles in target recognition in that they mediate an interaction between an E2 and its ubiquitination target. Another potential candidate for this type of E3 is RAD18. RAD18 and RAD6 are both involved in the repair of UV damaged DNA (Prakash, 1981). The precise mechanism involved in this process remains undetermined, but the involvement of RAD6 in this process indicates that at least protein ubiquitination is involved (Jentsch *et al.*, 1987). RAD6 and RAD18 are found to strongly interact. Furthermore, RAD18 also possesses an ability to bind single stranded DNA even when complexed with RAD6. It is thought that RAD18 functions to bring RAD6 to sites bearing DNA lesions through its ability to bind single stranded DNA. RAD6 may then function to ubiquitinate proteins found at the same site, such as components of a stalled replication complex (Bailly *et al.*, 1994).

Apart from structural roles in target recognition, a subset of E3s have also been shown to play a direct catalytic role in protein ubiquitination. Ubiquitination of the tumor suppressor p53 is mediated by a complex consisting of the cellular E6-associated protein

15

(E6-AP) and the E6 oncoprotein of human pappilomavirus (Scheffner *et al.*, 1993; Huibregste, 1991). Ubiquitination of p53 requires the formation of a p53-E6-(E6-AP) ternary complex (Scheffner *et al.*, 1993) as well as the human homologue of the yeast E2 UBC4 (Rolfe *et al.*, 1995; Scheffner *et al.*, 1994). Surprisingly, it was shown that the UBC4-Ub thiolester was not the immediate donor of Ub during p53 ubiquitination. Rather, Ub was first transferred from the UBC4-Ub thiolester to E6-AP in a transthiolation reaction to form the (E6-AP)-Ub thiolester. As such, (E6-AP)-Ub functioned as the immediate donor of Ub during p53 ubiquitination (Scheffner *et al.*, 1995). It remains to be seen whether UBC4 interacts directly with the p53-E6-(E6-AP) ternary complex or whether a separate complex between UBC4 and E6-AP first forms to carry out the transthiolation reaction.

A catalytic role for E3s does not appear to be relegated to p53 ubiquitination. E6-AP has been shown to mediate the *in vivo* ubiquitination of other proteins. This activity does not require E6 suggesting that E6-AP may interact with targets alone or employs other proteins to mediate such interactions (Scheffner *et al.*, 1993). A number of yeast proteins have also been shown to share significant homology with the carboxy terminus of E6-AP; the region within E6-AP responsible for thiolester formation with Ub. The lack of homology between the amino termini of these proteins indicates that these regions are required for target recognition indicating that E6-AP like ligases are involved in the ubiquitination of a variety of proteins (Huibregste, 1995). In fact, one of the yeast homologues RSP5 is required for the ubiquitination of the general amino acid permease GAP1 as well as the uracil permease FUR4 (Galan *et al.*, 1996; Hein *et al.*, 1995).

Multisubunit complexes have also been implicated in the ubiquitination of cell cycle regulators in both yeast and mammalian cells. In yeast, ubiquitination of the G1 cyclin CLN2 requires four distinct proteins, CDC34, CDC4, CDC53, and SKP1 (Bai *et al.*, 1996; Willems *et al.*, 1996). Phosphorylation of CLN2 is shown to promote binding of CDC53 which in turn promotes CLN2 ubiquitination by CDC34. Furthermore, CDC53 has been shown to interact with CDC34. While these observations suggest that CDC53 functions as the E3 which mediates CLN2 ubiquitination by CDC34, CLN2 ubiquitination could not be reproduced *in vitro* using purified CLN2, CDC53, and CDC34 (Willems *et al.*, 1996). This suggested that other components such as CDC4 and SKP1 were also required. CDC4 contains a novel peptide motif referred to as an F-box that is required for interactions with SKP1 (Bai *et al.*, 1996). How the SKP1-CDC4 complex and the CDC53-CDC34 complex function to target CLN2 for ubiquitination remains to be fully elucidated.

Another multisubunit complex referred to as the anaphase promoting complex (APC) or cyclosome is required for the degradation of cyclin B in Xenopus or clam oocyte extracts (King et al., 1995; Sudakin et al., 1995). Through cyclin B degradation cells pass through mitosis and enter another cell cycle. King et al. (1995) showed that the APC comprises a 20S complex that contains at least two subunits, the Xenopus homologs of yeast CDC16 and CDC27 both of which function to promote progression of the cell cycle through anaphase (Iringer et al., 1995; Tugendreich et al., 1995). The APC is activated in a cell cycle dependent manner allowing for the ubiquitination of cyclin B by either the Xenopus homologue of yeast UBC4, or a novel as yet unidentified E2 (King et al., 1995).

The cyclosome is also a large complex being approximately 1500 kDa in size. Within this complex a novel E3 function has been identified which must first become activated through phosphorylation by CDC2 kinase. Upon phosphorylation, the cyclosome may direct an E2 to ubiquitinate cyclin B thereby targeting its destruction (Lava-Berates et al., 1995; Sudakin et al., 1995) While it is likely that the APC and cyclosome are the same complex this has yet to be rigorously proven.

The varied forms E3s coupled with the large number of E2s and their potential to synthesize multiUb chains of different linkages provides a combinatorial mechanism for the recognition of protein targets and the type of multiUb chain that becomes conjugated to that target.

1.7 Bibliography

Alkalay, I., Yaron, A., Hatzubai, A., Orian, A., Ciechanover, A., and Ben-Neriah, Y. (1995). Stimulation-dependent IκBα phosphorylation marks the NF-κB inhibitor for degradation via the ubiquitin-proteosome pathway. *Proc. Natl. Acad. Sci. USA* **92**, 10599-10603.

Arfin, S. M., and Bradshaw, R. A. (1988). Cotranslational processing and protein turnover in eukaryotic cells. *Biochemistry* **27**, 7979-7984.

Arnason, T., and Ellison, M. J. (1994). Stress resistance in *Sccharomyces cerevisiae* is strongly correlated with assembly of a novel type of multiubiquitin chain. *Mol. Cell. Biol.* **14**, 7876-7883.

Baboshina, O. V., and Haas, A. L., (1996). Novel multiubiquitin chain linkages catalyzed by the conjugating enzyms $E2_{EPF}$ and RAD6 are recognized by 26S proteosome subunit 5. *J. Biol. Chem.* **271**, 2823-2831.

Bachmair, A., Finley, D., and Varshavsky, A. (1986). In vivo half-life of a protein is a function of its amino-terminal residue. *Science* **234**, 179-186.

Bachmair, A., and Varshavsky, A. (1989). The degradation signal in a short-lived protein. *Cell* **56**, 1019-1032.

Bai, C., Sen, P., Hofmann, K., Ma, L., Goebl, M., Harper, W., and Elledge, S. J. (1996). *SKP1* connects cell cycle regulators to the ubiquitin proteolysis machinery through a novel motif, the F-box. *Cell* **86**, 263-274.

Bailly, V., Lamb, J., Sung, P., Prakash, S., and Prakash, L. (1994). Specific complex formation between yeast RAD6 and RAD18 proteins: a potential mechanism for targeting RAD6 ubiquitin-conjugating activity to DNA damage sites. *Genes & Dev.* **8**, 811-820.

Baker, R. T., and Varshavsky, A. (1991). Inhibition of the N-end rule pathway in living cells. *Proc. Natl. Acad. Sci. USA* **88**, 1090-1094.

Baker, R. T., Smith, S. A., Marano, R., Mckee, J., and Board, P. G. (1994). Protein expression using cotranslational fusion and cleavage of ubiquitin. *J. Biol. Chem.* **41**, 25381-25386.

Bartel, B., Wunning, I., and Varshavsky, A. (1990). The recognition component of the N-end rule pathway. *EMBO J.* **9**, 3179-3189.

Beal, R., Deveraux, Q., Xia, G., Rechsteiner, M., and Pickart, C. (1996). Surface hydrophobic residues of multiubiquitin chains essential for proteolytic targeting. *Proc. Natl. Acad. Sci. USA* **93**, 861-866.

Brown, J., and Roberts, W. (1976). Evidence that approximately eighty percent of the soluble proteins from Ehlrich ascites are N-alpha acetylated. *J. Biol. Chem.* **251**, 1008-1014.

Burch, T. J., and Haas, A. L. (1994). Site-directed mutagenesis of ubiquitin. Differential roles for arginine in the onteraction with ubiquitin-activating enzyme. *Biochemistry* **33**, 7300-7308.

Busch, H., and Goldknopf, I. L. (1981). Ubiquitin-protein conjugates. *Mol. Cell. Biochem.* **840**, 173-187.

Chau, V., Tobias, J. W., Bachamir, A., Marriot, D., Ecker, D. J., Gonda, D. K., and Varshavsky, A. (1989). A multiubiquitin chain is confined to specific lysine in a targeted short-lived protein. *Science* **243**, 1576-1583.

Chen, P., Johnson, P., Sommer, T., Jentsch, S., and Hochstrasser, M. (1993). Multiple ubiquitin-conjugating enzymes participate in the *in vivo* degradation of the yeast MATα2 repressor. *Cell* **74**, 357-369.

Chen, Z., and Pickart, C., M. (1990). A 25 kilodalton ubiquitin carrier protein (E2) catalyzes multi-ubiquitin chain synthesis via lysine 48 of ubiquitin. *J. Biol. Chem.* **265**, 21835-21842.

Chen, Z. J., Hagler, J., Palombella, V. J., Melandri, F., Scherer, D., Ballard, D., and Maniatis, T. (1995). Signal-induced site-specific phosphorylation targets IκBα to the ubiquitin-proteosome pathway. *Genes & Dev.* **9**, 1586-1597.

Chen, Z. J., Parent, L., Maniatis, T. (1996). Site-specific phosphorylation of IκBα by a novel ubiquitination-dependent protein kinase activity. *Cell* **84**, 853-862.

Ciechanover, A., Hod, Y., and Hershko, A. (1978). A heat-stable polypeptide component of an ATP-dependent proteolytic system from reticulocytes. *Biochem. Biophys. Res. Commun.* **81**, 1100-1105.

Ciechanover, A. Heller, H., Elias, S., Haas, A. L., and Hershko, A. (1980) ATP-dependent conjugation of reticulocyte proteins with the polypeptide required for protein degradation. *Proc. Natl. Acad. Sci. USA* **77**, 1365-1368.

Ciechanover, A., Elias, S., Heller, H., and Hershko, A. (1980). Covalent Affinity purifiaction of ubiquitin-activating enzyme. *J. Biol. Chem.* **257**, 2537-2542.

Cook, J. C., and Chock, P. B. (1992). Isoforms of mammalian ubiquitin-activating enzyme. *J. Biol. Chem.* **267**, 24315-24321.

Cook, W. J., Jeffery, L. C., Carson, M., Chen, Z., and Pickart, C. M. (1992). Structure of diubiquitin conjugate and a model for interaction with ubiquitin conjugating enzyme (E2). *J. Biol. Chem.* **267**, 16467-16471.

Cook, W. J., Jeffery, L. C., Xu, Y., and Chau, V. (1993). Tertiary structures of class I ubiquitin-conjugating enzymes are highly conserved: crystal structure of yeast UBC4. *Biochemistry* **32**, 13809-13817.

Cook, W. J., Jeffery, L. C., Kasperek, E., and Pickart, C. M. (1994). Structure of tetraubiquitin shows how multiubiquitin chains can be formed. *J. Mol. Biol.* **236**, 601-609.

Deshaies, R. J., Chau, V., and Kirschner, M. (1995). Ubiquitination of the G1 cyclin Cln2p by a Cdc34p-dependent pathway. *EMBO J.* **14**, 303-312.

Deveraux, Q., Ustrell, V., Pickart, C., and Rechsteiner, M. (1994). A 26S protease subunit that binds ubiquitin conjugates. *J. Biol. Chem.* **269**, 7059-7061.

Dohmen, R. J., Madura, K., Bartel, B., and Varshavsky, A. (1991). The N-end rule is mediated by the UBC2(RAD6) ubiquitin-conjugating enzyme. *Proc. Natl. Acad. Sci. USA* **88**, 7351-7355.

Dohmen, R. J., Stappen, R., McGrath, J. P., Forrova, H., Kolarov, J., Goffeau, A., and Varshavsky, A. (1995). An essential yeast gene encoding a homolog of ubiquitin-activating enzyme. *J. Biol. Chem.* **270**, 18099-18109.

Etlinger, J. D., and Goldberg, A. L. (1977). A soluble ATP-dependent proteolytic system responsible for the degradation of abnormal proteins in reticulocytes. *Proc. Natl. Acad. Sci. USA* **74**, 54-58.

Finley, D., Ciechanover, A., and Varshavsky, A. (1984). Thermolability of ubiquitin-activating enzyme from the mammalian cell cycle mutant ts85. *Cell* **37**, 43-55.

Finley, D., Ozkaynak, E., and Varshavsky, A. (1987) The yeast polyubiquitin gene is essential for resistance to high temperatures, starvation, and other stresses. *Cell* **48**, 1035-1046.

Finley, D., Bartel, B., and Varshavsky, A. (1989). The tails of ubiquitin precursors are ribosomal proteins whose fusion to ubiquitin facilitates ribosome biogenesis. *Nature* **338**, 394-401.

Finley, D. (1992). The yeast ubiquitin system. In *The Molecular and Cellular Biology of the Yeast Saccharomyces cerevisiae: Gene Expression*. Jones, E., Pringle, J., Broach, J., ed. (New York: Cold Spring Harbor Laboratory Press), 539-558.

Finley, D., Sadis, S., Monia, B. P., Boucher, P., Ecker, D. J., Crooke, S. T., and Chau, V. (1994). Inhibition of proteolysis and cell cycle progression in a multiubiquitination-deficient yeast mutant. *Mol. Cell. Biol.* 14, 5501-5509.

Galan, J. M., Moreau, V., Andre, B., Volland, C., and Haguenauer-Tsapis, R. (1996). Ubiquitination mediated by the Npi1p/Rsp5p ubiquitin-protein ligase is required for endocytosis of yeast uracil permease. *J. Biol. Chem.* **271**, 10946-10952.

Girod, P.-A., Vierstra, R. D. (1993). A major ubiquitin conjugation system in wheat germ extracts involves a 15 kDa ubiquitin-conjugating enzyme (E2) homologous to the yeast *UBC4/UBC5* gene products. *J. Biol. Chem.* **268**, 955-960.

Glotzer, M., Murray, A. W., and Kirschner, M. W. (1991). Cyclin is degraded by the ubiquitin pathway. *Nature* **349**, 132-138.

Goebl, M. G., Yochem, J., Jentsch, S., McGrath, J. P., Varshavsky, A., and Byers, B. (1988). The yeast cell cycle gene *CDC34* encodes a ubiquitin-conjugating enzyme. *Science* **241**, 1331-1335.

Gonda, D. K., Bachmair, A., Wunning, I., Tobias, J. W., Lane, W. S., and Varshavsky, A. (1989). Universality and structure of the N-end rule. *J. Biol. Chem.* **264**, 16700-16712.

Gonen, H., Schwartz, A. L., and Ciechanover, A. (1991). Purification and characterization of a novel protein that is required for degradation of N-α-acetylated proteins by the ubiquitin system. *J. Biol. Chem.* **266**, 19221-19231.

Gonen, H., Smith, C. E., Siegel, N. R., Kahana, C., Merrick, W. C., Chakraburtty, K., Schwartz, A. L., and Ciechanover, A. (1994). Protein synthesis elongation factor EF-1α is essential for ubiquitin-dependent degradation of certain N$^{\alpha}$-acetylated proteins and may

be substituted for ny the bacterial elongation factor EF-Tu. *Proc. Natl. Acad. Sci. USA* **91**, 7648-52.

Gregori, L., Poosch, M. S., Cousins, G., and Chau, V. (1990). A uniform isopeptide-linked multiubiquitin chain is sufficient to target substrate for degradation in ubiquitin-mediated proteolysis. *J. Biol. Chem.* **265**, 8354-8357.

Gregory, L., Marriott, D., West, C. M., and Chau, V. (1985). Specific recognition of calmodulin from D. discoideum by the ATP, ubiquitin-dependent degradative pathway. *J. Biol. Chem.* **261**, 5232-5235.

Grenfell, S. J., Trausch-Azar, J. S., Handley-Gearhart, P.M., Ciechanover, A., and Schwartz, A. L. (1994). Nuclear localization of the ubiquitin-activating enzyme, E1, is cell-cycle dependent. *Biochem. J.* **300**, 701-708.

Gwozd, C. S., Arnason, T. G., Cook, W. J., Chau, V., and Ellison, M. J. The yeast UBC4 ubiquitin conjugating enzyme monoubiquitinates itself in vivo: evidence for an E2-E2 homointeraction. *Biochemistry* **34**, 6296-6302.

Haas, A. L., Warms, J. V. B., Hershko, A., and Rose, I. A. (1982). Ubiquitin-activating enzyme. *J. Biol. Chem.* **257**, 2543-2548.

Haas, A. L., and Rose, I. A. (1982). The mechanism of ubiquitin activiaitng enzyme. *J. Biol. Chem.* **257**, 10329-10337.

Haas, A. L., Warms, V. B., and Rose, I. A. (1983). Ubiquitin adenylate: structure and role in ubiquitin activation. *Biochemistry* **22**, 4388-4394.

Haas, A. L., and Wilkinson, K. D. (1985). The large scale purification of ubiquitin from human erythrocytes. *Prep. Biochem.* **15**, 49-60.

Haas, A. L., and Bright, P. M. (1988). The resolution and characterization of putative ubiquitin carrier protein isozymes from rabbit reticulocytes. *J. Biol. Chem.* **263**, 13258-13267.

Haas, A. L., Reback, P. B., and Chau, V. (1991). Ubiquitin conjugation by the yeast RAD6 and CDC34 gene products: comparison to their putative rabbit homologs E2$_{20K}$ and E2$_{32K}$. *J. Biol. Chem.* **266**, 5104-5112.

Hadari, T., Warms, J. V. B., Rose, I. A., and Hershko, A. (1992). A ubiquitin C-terminal isopeptidase that acts on polyubiquitin chains. *J. Biol. Chem.* **267**, 719-727.

Handley-Gearhart, P. M., Stephen, A. G., Trausch-Azar, J. S., Ciechanover, A., and Schwartz, A. L. (1994). Human ubiquitin-activating enzyme, E1. Indication of potentail nuclear and cytoplasmic subpopulations using epitope-tagged cDNA constructs. *J. Biol. Chem.* **269**, 33171-33178.

Hatfield, P. M., and Vierstra, R. D. (1992). Multiple forms of ubiquitin-activating enzyme E1 from wheat. Identification of an essential cysteine by *in vitro* mutagenesis. *J. Biol. Chem.* **267**, 14799-14803.

Hein, C., Springael, J. Y., Volland, C., Haguenauer-Tsapis, R., and Andre, B. *Npl1*, an essential yeast gene involved in induced degradation of Gap1 and Fur 4 permeases, encodes the Rsp5 ubiquitin-protein ligase. *Molec. Microbiol.* **18**, 77-87.

Hershko, A., Ciechanover, A. Heller, H., Haas, A. L., and Rose, I. A. (1980) Proposed role of ATP in protein breakdown: conjugation od proteins with multiple chains of the polypeptide of ATP-dependent proteolysis. *Proc. Natl. Acad. Sci. USA* **77**, 1783-1786.

Hershko, A., Heller, H., Elias, S., and Ciechanover, A. (1983). Components of ubiquitin-protein ligase system: resolution, affinity purification, and role in protein breakdown. *J. Biol. Chem.* **258**, 8206-8214.

Hershko, A., Leshinsky, E., Ganoth, D., and Heller, H. (1984). ATP-dependent degradation of ubiquitin-protein conjugates. *Proc. Natl. Acad. Sci. USA* **81**, 1619-1623.

Hersko, A., and Heller, H. (1985). Occurrence of a polyubiquitin structure in ubiquitin-protein conjugates. *Biochem. Biophys. Res. Commun.* **128**, 1079-1086.

Hicke, L., and Riezman, H. (1996). Ubiquitination of a yeast plasma membrane receptor signals its ligand-stimulated endocytosis. *Cell* **84**, 277-287.

Ho, C. Y., Adamson, J. G., Hodges, S., and Smith, M. (1994). Heterodimerization of the yeast MATa1 and MATα2 proteins is mediated by two lecine zipper-like coiled-coil motifs. *EMBO J.* **13**, 1403-1413.

Hodgins, R., Gwozd, C., Arnason, T., Cummings, M., and Ellison, M. J. (1996). The tail of ubiquitin-conjugating enzyme redirects multi-ubiquitin chain synthesis from the lysine 48-linked configuration to a novel nonlysine-linked form. *J. Biol. Chem.* **271**, 28766-28771.

Holloway, S. L., Glotzer, M., King, R. W., and Murray, A. W. (1993). Anaphase is initiated by proteolysis rather than by the inactivation of maturation-promoting factor. *Cell* **73**, 1393-1402.

Hough, R., and Rechsteiner, M. (1986). Ubiquitin-lysozyme conjugates: Purification and suseptibility to proteolysis. *J. Biol. Chem.* **261**, 2391-2399.

Huibregtse, J. M., Scheffner, M., and Howley, P. M. (1991). A cellular protein mediates association of p53 with the E6 oncoprotein of human papillomavirus types 16 or 18. *EMBO J.* **13**, 4129-4135.

Huibregtse, J. M., Scheffner, M., Beaudenon, S., and Howley, P. M. (1995). A family of proteins structurally and functionally related to the E6-AP ubiquitin-protein ligase. *Proc. Natl. Acad. Sci. USA* **92**, 2563-2567.

Irniger, S., Piatti, S., Michaelis, C. and Nasmyth, K. (1995). Genes involved in sister chromatid separation are needed for B-type cyclin proteolysis in budding yeast. *Cell* **81**, 269-277.

Jentsch, S., McGrath, J. P., and Varshavsky, A. (1987). The yeast DNA repair gene RAD6 encodes a ubiquitin-conjugating enzyme. *Nature* **329**, 131-134.

Jentsch, S., Seufert, W., Sommer, T., and Reins, H-A. (1990). Ubiquitin-conjugating enzymes: novel regulators of eukaryotic cells. *Trends Biochem. Sci.* 15, 195-198.

Johnson, S. J., Ma, P. C. M., Ota, I. M., and Varshavsky, A. (1995). A proteolytic pathway that recognizes ubiquitin as a degradation signal. *J. Biol. Chem.* **270**, 17442-17456.

Jungmann, J., Reins, H. A., Schobert, C., and Jentsch, S. (1993). Resistance to cadmium mediated by ubiquitin-dependent proteolysis. *Nature* **361**, 369-371.

King, R. W., Peters, J-M., Tugendreich, S., Rolfe, M., Hieter, P., and Kirschner, M. W. (1995). A 20S complex containing CDC27 and CDC16 catalyzes the mitosis-specific conjugation of ubiquitin to cyclin B. *Cell* **81**, 279-288.

Kolman, C. J., Toth, J., and Gonda, D. K. (1992). Identification of a portable determinant of cell cycle function within the carboxy-terminal domain of the yeast CDC34 (UBC3) ubiquitin conjugating enzyme. *EMBO J.* **11**, 3081-3090.

Kulka, R. G., Raboy, B., Schuster, R., Parag, H. A, Diamond, G., Ciechanover, A., and Marcus, M. (1988). A chinese hamster cell cycle mutant arrested at G2 phase has a temperature-sensitive ubiquitin-activating enzyme, E1. *J. Biol. Chem.* **263**, 15726-15731.

Lahav-Baratz, S., Sudakin, V., Ruderman, J. V., and Hershko, A. (1995). Reversible phosphorylation controls the activity of cyclosome-associated cyclin-ubiquitin ligase. *Proc. Natl. Acad. Sci. USA* **92**, 9303-9307.

Liu, Y., Mathias, N., Steussy, N., and Goebl, M. G. (1995). Intragenic suppression among *CDC34 (UBC3)* mutations defines a class of ubiquitin-conjugating catalytic domains. *Mol. Cell. Biol.* **15**, 5635-5644.

Lowe, J., Stock, D., Jap, B., Zwickl, P., Baumeister, W., and Huber, R. (1995). Crystal structure of the 20S proteosome from the archeon *T. acidophilum* at 3.4 Å resolution. *Science* **268**, 533-539.

McGrath, J. P., Jentsch, S., and Varshavsky, A. (1991). *UBA1*: an essential gene encoding ubiquitin-activating enzyme. *EMBO J.* **10**, 227-236.

Morrison, A., Miller, E. J., and Prakash, L. (1988). Domain structure and functional analysis of the carboxy-terminal polyacidic sequence of the RAD6 protein of Saccharomyces cerevisiae. *Mol. Cell. Biol.* **8**, 1179-1185.

Orian, A., Whiteside, S., Isreal, A., Stancovski, I., Schwartz, A. L., and Ciechanover A. (1995). Ubiquitin mediated processing of NF-κB transcriptional activator precursor p105: reconstitution of a cell-free system and identification of the ubiqutin-carrier protein, E2, and a novel ubiquitin-protein ligase, E3, involved in conjugation. *J. Biol. Chem.* **270**, 21707-21714.

Ozkaynak, E., Finley, D., and Varshavsky, A. (1984) The yeast ubiquitin gene: head-to-tail repeats encoding a polyubiquitin precursor. *Nature* **312**, 663-666.

Ozkaynak, E., Finley, D., Solomon, M. J., and Varshavsky, A. (1987). The yeast ubiquitin genes: a family of natural gene fusions. *EMBO J.* **6**, 1429-1439.

Palombella, V., Rando, O. J., Goldberg, A. L., and Maniatis, T. (1994). The ubiquitin-proteosome pathway is required for processing the NF-κB1 precursor protein and the activation of NF-κB. *Cell* **78**, 773-85.

Papa, F. R., and Hochstrasser, M. (1993). The yeast *DOA4* gene encodes a deubiquitinating enzyme related to a product of the human *tre-2* oncogene. *Nature* **366**, 313-319.

Pickart, C.M., and Rose I.A. (1985). Functional heterogeneity of ubiquitin carrier proteins. *J. Biol. Chem.* **260**, 1573-1581.

Pickart, C. M., Kasperek, E. M., Beal, R., and Kim, A. (1994). Substrate properties of site-specific mutant ubiquitin protein (G76A) reveal unexpected mechanistic features of ubiquitin-activating enzyme (E1). *J. Biol. Chem.* **269**, 7115-7123.

Pitluk, Z. W., McDonough, M., Sangan, P., and Gonda, D.K. (1995). Novel *CDC34 (UBC3)* ubiquitin-conjugating enzyme mutants obtained by charge to alanine scanning mutagenesis. *Mol. Cell. Biol.* **15**, 1210-1219.

Prakash, L. (1981). Characterization of postreplication repair in *Saccharomyces cerevisiae* and effects of *rad6*, *rad18*, *rev3*, and *rad52* mutations. *Mol. Gen. Genet.* **184**, 471-478.

Qin., S., Nakajima, B., Nomura, M., and Arfin., S. M. (1991). Cloning and characterization of a *Saccharomyces cerevisiae* gene encoding a new member of the ubiquitin-conjugating protein family. *J. Biol. Chem.* **266**, 15549-15554.

Rechsteiner, M. (1990). PEST sequences are signals for rapid intracellualr proteolysis. *Sem. Cell. Biol.* **1**, 433-440.

Rechsteiner, M., and Rogers, S. W. (1996). PEST sequences and regulation by proteolysis. *Trends Biochem Sci.* **21**, 267-271.

Redman, K. L., and Rechsteiner, M., (1989) Identification of the long ubiquitin extension as ribosomal protein S27a. *Nature* **338**, 438-440.

Reiss, Y., Kaim, D., and Hershko, A. (1988). Specificity of binding of NH2-terminal residue of proteins to ubiquitin-protein ligase. *J. Biol. Chem.* **263**, 2693-2698.

Reiss, Y., and Hershko, A. (1990). Affinity purification of ubiquitin-protein ligase on immobilized protein substrates: evidence for existence of separate NH_2 terminal binding sites on a single enzyme. *J. Biol. Chem.* **265**, 3685-3690.

Rolfe, M., Beer-Romero, P., Glass, S, Eckstein, J., Berdo, I., Theodoras, A., Pagano, M., and Draetta, G. (1995). Reconstitution of p53-ubiquitinylation reactions from purified components: the role of human ubiquitin-conjugating enzyme UBC4 and E6-associated protein (E6AP). *Proc. Natl. Acad. Sci. USA* **92**, 3264-3268.

Sadis, S., Atienza, C. J., and Finley, D. (1995). Synthetic signals for ubiquitin-deoendent proteolysis. *Mol. Cell. Biol.* **15**, 4086-4094.

Scheffner, M., Werness, B. A., Huibregtse, J. M., Levine, A. J., and Howley, P. M. (1990). The E6 oncoprotein encoded by the human papilloma virus types 16 and 18 promotes the degradation of p53. *Cell* **63**, 1129-1136.

Scheffner, M., Huibregtse, J. M., Vierstra, R. D., and Howley, P. M. (1993). The HPV-16 E6 and E6-AP complex functions as a ubiquitin-protein ligase in ubiquitination of p53. *Cell* **75**, 495-505.

Scheffner, M., Huibregtse, J. M., and Howley, P. M. (1993). Identification of a human ubiquitin-conjugating enzyme that mediates the E6-AP dependent ubiquitination of p53. *Proc. Natl. Acad. Sci. USA* **91**, 8797-8801.

Scheffner, M., Nuber, U., and Huibregtse, J. M. (1995). Protein ubiquitination involving an E1-E2-E3 enzyme ubiquitin thiolester cascade. *Nature* **373**, 81-83.

Scherer, D. C., Brockman, J. A., Chen, Z. J., Maniatis, T., and Ballard, D. (1995). Signal-induced degradation of IκBα requires site-specific ubiquitination. *Proc. Natl. Acad. Sci. USA* **92**, 11259-11263.

Schneider, B. L., Yang, Q. H., and Futcher, A. B. (1996). Linkage of replication to start by the cdk inhibitor Sic1. *Science* **272**, 560-562.

Seemuller, E., Lupas, A., Stock, D., Lowe, J., Huber, R., and Baumeister, W. (1995). Proteosome from *Thermoplasma acidophilum*: a threonine protease. *Science* **268**, 579-582.

Seufert, W., and Jentsch, S., (1990). Ubiquitin-conjuagting enzymes UBC4 and UBC5 mediate selective degradation of of short-lived and abnormal proteins. *EMBO J.* **9**, 543-550.

Seufert, W., McGrath J. P., and Jentsch, S. (1990). *UBC1* encodes a novel member of an essential subfamily of yeast ubiquitin-conjugating enzymes involved in protein degradation. *EMBO J.* **9**, 4535-4541.

Seufert, W., Futcher, B., and Jentsch, S., (1995). Role of a ubiquitin-conjugating enzyme in degradation of S- and M-phase cyclins. *Nature* **373**, 78-81.

Silver, E. T., Gwozd, T. J., Ptak, C., Goebl, M., and Ellison M. J. (1992). A chimeric ubiquitin conjugating enzyme that combines the cell cycle properties of CDC34 (UBC3) and the DNA repair properties of RAD6 (UBC2): implications for the structure, function, and evolution of the E2s. *EMBO J.* **11**, 3091-3098

Sommer, T., and Jentsch, S. (1993). A protein translocation defect linked to ubqiutin conjugation at the endoplasmic reticulum. *Nature* **365**, 176-179.

Spence, J., Sadis, S., Haas, A. L., and Finley, D. (1995). A ubiquitin mutant with specific defects in DNA repair and multiubiquitination. *Mol. Cell. Biol.* **15**, 1265-1273.

Stephen, A. G., Trausch-Azar, J. S., Ciechanover, A., and Schwartz, A. L. (1996). The ubiquitin-activating enzyme E1 is phosphorylated and localized to the nucleus in a cell-cycle dependent manner. *J. Biol. Chem.* **271**, 15608-15614.

Sudakin, V., Ganoth, D., Dahan, A., Heller, H., Hershko, J., Luca, F. C., Ruderman, J. V., and Hershko, A. (1995). The cyclosome, a large complex containing ubiquitin ligase activity, targets cyclins for destruction at the end of mitosis. *Mol. Biol. Cell* **6**, 185-198.

Sung, P., Berleth, E., Pickart, C., Prakash, S., and Prakash, L. (1991). Yeast RAD6 encoded ubiquitin conjugating enzyme mediates protein degradation dependent on the N-end recognizing E3 enzyme. *EMBO J.* **10**, 2187-2193.

Surana, U., Amon, A., Dowzer, C., McGrew, J., Byers, B., and Nasmyth, K. (1993). Destruction of CDC28/CLB mitotic kinase is not required for metaphase to anaphase transition in budding yeast. *EMBO J.* **12**, 1969-1978.

Treger, J. M., Hiechman, K. A., and McEntree, K. (1988). Expression of the yeast *UBI4* gene increases in response to DNA-damaging agents and in meiosis. *Mol. Cell. Biol.* **8**, 1132-1136.

Tugendreich, S., Tomkiel, J., Earnshaw, W., and Hieter, P. (1995). CDC27Hs colocalizes with CDC16Hs to the centrosome and mititic spindle and is essential for the metaphase to anaphase transition. *Cell* **81**, 261-268.

van Nocker, S., and Vierstra, R. D. (1993). Multiubquitin chains linked through lysine 48 are abundant in vivo and are competent intermediates in the ubiquitin proteolytic pathway. *J. Biol. Chem.* **268**, 24766-24773.

van Nocker, S., Deveraux, Q., Rechsteiner, M., and Vierstra, R. D. (1996). *Arabidopsis MBP1* geneencodes a conserved ubiquitin recognition component of the 26S proteosome. *Proc. Natl. Acad. Sci. USA* **93**, 856-860.

Vijay-Kumar, S., Bugg, C. E., Wilkinson, K. D., and Cook, W. J. (1985). Three-dimensional structure of ubiquitin at 2.8 Å resolution. *Proc. Natl. Acad. Sci. USA* **82**, 3582-3585.

Vijay-Kumar, S., Bugg, C. E., and Cook, W. J. (1987). Structure of ubiquitin refined at 1.8 Å resolution. *J. Mol. Biol.* **194**, 531-544.

Vijay-Kumar, S., Bugg, C. E., Wilkinson, K. D., Vierstra, R. D., and Cook, W. J. (1987a). Comparison of three-dimensional structures of yeast and oat with human ubiquitin. *J. Biol. Chem.* **262**, 6396-6399.

Wiebel, F. F., Kunau, W-H. (1992). The Pas2 protein essential for peroxisome biogenesis is related to ubiquitin-conjugating enzymes. *Nature* **359**, 73-76.

Wilkinson, K. D., Urban, M. K., and Haas, A. L. (1980). Ubiquitin is the ATP-dependent factor I of rabbit reticulocytes. *J. Biol. Chem.* **255**, 7525-7528.

Wilkinson, K. D., and Audhya, T. K. (1981). Stimulation of ATP-dependent proteolysis requires ubiquitin with the COOH-terminal sequence Arg-Gly-Gly. *J. Biol. Chem.* **256**, 9235-9241.

Wilkinson, K. D., Cox, M. J., O'Conner, L. B., and Shapira, R. (1987), Structure and activities of a variant ubiquitin sequence from Baker's yeast. *Biochemistry* **25**, 4999-5004.

Wilkinson, K. D., Tashayev, V. L., O'Connor, L. B., larsen, C. N., Kasperek, E. M., and Pickart, C. M. (1995). Metabolism of the polyubiquitin degradation signal: structure, mechanism, and role of isopeptidase T. *Biochemistry* **34**, 14535-14546.

Willems, A. R., Lanker, S., Patton, E. E., Craig, K. L., Nason, T. F., Mathias, N., Kobayashi, R., Wittenberg, C., and Tyers, M. (1996). Cdc53 targets phosphorylated G1 cyclins for degradation by the ubiquitn proteolytic pathway. *Cell* **86**, 453-463.

Yaglom, J., Linskens, M. H. K., Sadis, S., Rubin, D. M., Futcher, B., and Finley, D. (1995). p34[cdc28]-mediated control of Cln3 cyclin degradation. *Mol. Cell. Biol.* **15**, 731-741.

[1]Chapter 2

Identification of a functional determinant within the CDC34 tail domain that facilitates self-association.

2.1 Introduction

All E2s identified to date share an evolutionarily conserved catalytic domain. Apart from this similarity, the functional uniqueness of many E2s is clearly reflected in their structures. The most obvious examples of these differences are found in E2s that have carboxy-terminal extensions or tails. These tails bear little or no resemblance to one another, therefore, unlike the catalytic domains, the tails probably did not evolve from a common ancestor but were acquired from abrupt, separate, and relatively recent mutational events (see Silver et al., 1992).

Recent evidence has indicated that E2 tails perform a variety of mechanistically distinct functions consistent with their diverse evolutionary origins. Early studies led to the suggestion that tails determined substrate specificity (Jentsch et al., 1990). This was based on the idea that E2s without tails may require accessory proteins such as Ub protein ligases (E3s), for substrate recognition and that therefore E2s with tails may circumvent the need for E3s by partitioning substrate recognition to the tail. Several findings are consistent with this notion. First, the sporulation function of the DNA repair enzyme RAD6 (UBC2) is dependent upon its acidic tail (Morrison et al., 1988). Second, the cell cycle function of the CDC34 (UBC3) enzyme depends upon a portion of its tail (Silver et al., 1992; Kolman et al., 1992). Third, the cell cycle function of CDC34 can be transferred to RAD6 by transposition of the CDC34 tail onto the catalytic domain of RAD6 (Silver et al., 1992; Kolman et al., 1992). Finally, in vitro experiments have shown that the acidic tails of several E2s are required for the ubiquitination of histones (Sung et al., 1988). With respect to these latter findings it should be noted that histones are basic proteins and there is currently no evidence to date that histone ubiquitination in vitro reflects anything more than a non-specific electrostatic interaction. Thus, although the above evidence is consistent with the idea that tails specifically target proteins for ubiquitination through their direct interaction, this idea remains to be proven.

---

[1]A version of this chapter has been previously published: Ptak, C., Prendergast, J.A., Hodgins, R., Kay, C.M., Chau, V, and Ellison, M.J. (1994) *J. Biol. Chem.* 269, 26539-26545

Two recent studies illustrate that tail function may not be simply restricted to substrate recognition. Dohmen *et al.* (1991) have shown for instance that the tail of RAD6 mediates the interaction of RAD6 with UBR1, an E3 that functions in the yeast N-end rule pathway (Bartel *et al.*, 1990). In other work, Sommer and Jentsch (1993) have shown that the tail of UBC6 contains a sequence that anchors this E2 to the cytosolic side of the endoplasmic reticulum. Based on these two examples, it is clear that different E2 tails can function in entirely unrelated ways.

Here we describe a new function for an E2 tail based on *in vivo* and *in vitro* studies of the cell cycle Ub conjugating enzyme CDC34 (Goebl *et al.*, 1988). CDC34 has a 14 kDa tail that is necessary for the transition of yeast cells from G1 phase to S phase (Silver *et al.*, 1992; Kolman *et al.*, 1992). Furthermore, genetic evidence suggests that CDC34 is capable of interacting with itself or with RAD6 *in vivo* (Silver *et al.*, 1992). In the present work we define a small region of the CDC34 tail that is necessary and sufficient for CDC34's cell cycle function as well as its ability to interact with itself.

2.2. Materials and Methods

2.2.1. Yeast plasmids and strains. All high copy expression plasmids for *CDC34* and its derivatives carry the *TRP1* marker and are identical in sequence except for the codon deletions indicated (Figure 2.1). Construction of the *CDC34*, *cdc34Δ170*, *cdc34Δ244*, and *cdc34Δ265*, plasmids has been previously described (Silver *et al.*, 1992). Plasmids for the remaining derivatives were constructed in the same manner. Protein coding sequences for all plasmids were verified using the double-stranded chain termination method on an Applied Biosystems automated sequenator operated by the DNA Synthesis and Sequencing Facility at the University of Alberta.

A low copy plasmid containing *cdc34Δ209* (pJP81) under the control of the *CDC34* promoter was created by introducing the SalI/BamHI fragment (containing the *CDC34* promoter and codons 1-105) from pGEM34 H/S (Goebl *et al.*, 1988) and the BamHI/ClaI fragment (containing codons 105-209 and the *CYC1* terminator) from the high copy version of *cdc34Δ209* described above, between the SalI and ClaI sites of pRS316 (Sikorski and Heiter, 1989).

All yeast plasmids were transformed into the congenic yeast strains YL10 (*MATa, ura3-52, trp1Δ63, leu2Δ1, his3Δ, cdc34-2*, - a gift of M. Goebl) and YES71 (*MATa, ura3-52, trp1Δ63, leu2Δ1, his3Δ, cdc34-2::HIS3*). YL10 carries the temperature sensitive *cdc34-2* allele. YES71 was constructed by disrupting the *cdc34-2* allele with the *HIS3* gene using the ApaI/EcoRI fragment from pGEM34 H/S as previously described (Goebl *et al.*, 1988).

31

Viability of YES71 is maintained by the presence of a *CDC34* expression plasmid carrying the *URA3* marker (Silver *et al.*, 1992). A strain of YES71 carrying the *cdcΔ$_{209}$-URA3* plasmid, pJP81, was created by first introducing the *CDC34-TRP1* plasmid (described above) into YES71 followed by the elimination of the *CDC34-URA3* maintenance plasmid by 5-fluoroorotic acid (FOA) selection (Silver *et al.*, 1992). pJP81 was then introduced into this strain and cells having lost the *CDC34-TRP1* plasmid were selected by their inability to grow in the absence of tryptophan.

2.2.2 Complementation experiments. Freshly transformed YL10 and YES71 cells were plated onto synthetic defined (SD) plates supplemented with all amino acids (Sherman *et al.*, 1986) except tryptophan or tryptophan and uracil and grown at 25 °C until colonies appeared. Individual colonies were then inoculated into liquid dropout media and grown to early exponential phase (1×10^7 cells/ml) prior to replating. In the case of YL10, 1×10^5 cells from individual cultures were spotted then streaked in duplicate onto SD plates supplemented as described above. One plate was incubated at the permissive temperature (30 °C) while the other was incubated at the non-permissive temperature (37 °C). In the case of YES71, 1×10^5 cells were spotted then streaked onto supplemented SD plates containing FOA (1 mg/ml) and uracil (12 µg/ml) to select for cells that had lost the *CDC34-URA3* maintenance plasmid. Colonies formed under these conditions indicated that a given *CDC34* derivative expressed from the remaining plasmid was capable of complementing for the loss of *CDC34* activity.

2.2.3. Protein overexpression. Gene cassettes encoding each *CDC34* derivative were excised from the yeast high copy plasmids described above using SstI and KpnI (see Silver *et al.*, 1992) and inserted in frame between the SstI and KpnI sites of a modified derivative of pET-3a (Studier *et al.*, 1990). The pET-3a derivative was created by inserting a fragment, synthesized using the polymerase chain reaction, between the NdeI and BamHI sites of pET-3a with the following sequence: <u>CATATGAGCTC</u>TCCCG <u>GGTACC</u>GA**TCC**. Underlined are the positions of the NdeI, SstI and KpnI sites and in bold type the remnants of the destroyed BamHI site. The Met-1 codon begins at the fourth nucleotide.

Expression plasmids were co-transformed into the *E. coli* strain BL21 along with the thermally induced T7 polymerase plasmid, pGP1-2 as previously described (Tabor and Richardson, 1985). Unlabeled CDC34 derivatives were produced by growing cells in one liter of LB liquid media (containing 50 µg/ml ampicillin and 75 µg/ml kanamycin) at 30 °C to a final absorbance of 0.4 at 590 nm. The culture was then shifted to 42 °C for 1 hr followed by a shift to 37 °C for 2 hr. Cells were harvested by centrifugation, resuspended in 25 ml of buffer A (50 mM Tris-HCl (pH 7.5), 1 mM EDTA, 2 mM DTT) and lysed

using a French press. The lysate was centrifuged at 40 000 rpm for 1 hr using a Beckman Ti 70 M rotor and the supernatant was saved for subsequent purification.

[35S]-methionine labeled derivatives were produced as above with the following modifications. Cells were grown in 6 ml of M9 media supplemented with 1 mM MgSO$_4$, 0.1 mM CaCl$_2$, 12 mM glucose, 18 µg/ml thiamine, 50 µg/ml ampicillin, 75 µg/ml kanamycin and all amino acids (40 µg/ml) except for cysteine and methionine. Cells were then induced at 42 °C for 20 minutes followed by the addition of rifampicin (300 µg/ml final). Cells were then incubated for 10 minutes at 42°C followed by a shift to 37°C for one hour. Trans [35S]-methionine (ICN) was then added (25 µCi/ml) followed by incubation for 10 minutes at 37 °C. Cells were harvested by centrifugation, resuspended in 500 µl of 25% sucrose, 50 mM Tris-Cl (pH 8.0) and lysed with lysozyme as previously described (Gonda et al., 1989).

2.2.4. Protein purification. Unlabeled CDC34 derivatives were purified using a FPLC system (Pharmacia) by passing clarified supernatants over a HiLoad Q sepharose 26/10 ion exchange column (Pharmacia) equilibrated with buffer A using gradients that ranged from 0 M NaCl to 2 M NaCl as previously described (Haas et al., 1991). Each derivative eluted as the major protein peak at NaCl concentrations that varied for each derivative: CDC34 - 470 mM, cdc34Δ$_{265}$ - 500 mM, cdc34Δ$_{244}$ - 420 mM, cdc34Δ$_{209}$ - 290 mM, cdc34Δ$_{185}$ - 230 mM. Peak fractions were pooled, concentrated and exchanged with buffer A by centricon (Amicon) filtration. Concentrated samples were then loaded onto a Superdex 75 HR 10/30 gel exclusion column (Pharmacia) equilibrated with buffer A and eluted with the same. Peak fractions were concentrated and the buffer was exchanged as described above prior to storage at -80 °C in the presence of 5% glycerol.

[35S]-labeled CDC34 derivatives were purified as described above except that ion exchange chromatography was performed on a MonoQ HR 5/10 column (Pharmacia).

2.2.5 Protein crosslinking. Prior to crosslinking all CDC34 derivatives were dialyzed into crosslinking buffer (50 mM HEPES (pH 7.5), 150 mM NaCl, 2 mM DTT). Aliquots (40 µl) were pre-incubated on ice for 5 minutes followed by the addition of a 0.1 volume of the crosslinker BS^3 [Bis(sulfosuccinimidyl) suberate (Pierce) in crosslinking buffer]. Samples were incubated an additional 30 minutes on ice and the reaction was quenched by the addition of 1M Tris-HCl (pH 7.5) to a final concentration of 50 mM.

In Figure 2.3, BS^3 was added to final concentrations of 0, 1 or 10 mM to reactions that contained [35S]- labeled CDC34 (15 µM, 2 x 10^4 CPM/µM) in the presence or absence of BSA (150 µM).

In Figure 2.4, BS^3 was added in final concentrations of 0 or 1 mM to reactions that contained [35S]- labeled CDC34 derivatives at final concentrations of either 30 µM (1 x 10^4

CPM/μM) or 0.6 μM (5 x 10^5 CPM/μM). Crosslinked species were detected by SDS-PAGE (6% acrylamide - Figure 2.3; 10% acrylamide - Figure 2.4) followed by autoradiography.

Molecular mass estimates of the proteins and their crosslinked products was determined on the basis of their migration on SDS-polyacrylamide gels relative to known molecular mass standards. Protein standards (BioRad) included: Myosin - 205 kDa, β-galactosidase - 116.5 kDa, Phosphorylase B - 106 kDa, BSA - 80 kDa, Ovalbumin - 49.5 kDa, Carbonic anhydrase - 32.5 kDa, Soybean trypsin inhibitor - 27.5 kDa, and Lysozyme - 18.5 kDa.

2.2.6. CDC34 proteolysis. 30 μl aliquots of various [^{35}S]-labeled CDC34 derivatives in buffer A plus 5 mM $MgCl_2$ (which unmasks a trace level of proteinase activity contained in each preparation) was incubated at 30 °C for 16 hours prior to electrophoresis and autoradiography as described above.

2.2.7. Circular dichroism (CD) spectroscopy. Secondary structural content of selected CDC34 derivatives was determined by CD spectroscopy using a Jasco J-720 spectropolarimeter. Samples (0.5 - 1 mg/ml) in buffer A plus 150 mM NaCl were scanned between 194 nm - 255 nm. Percent secondary structure for each derivative was determined from the calculated molar ellipticities using the Contin program - version 1 (Provencher and Glockner, 1980).

2.2.8. Axial ratio determinations. Molecular masses and sedimentation coefficients for CDC34 and cdc34Δ_{185} were determined by analytical ultracentrifugation on a Beckman Model E Analytical Ultracentrifuge using the methodology described by Chervenka (1969). Prior to analysis, samples of CDC34 and cdc34Δ_{185} in buffer A were dialyzed against buffer A plus 150 mM NaCl. Axial ratios were determined for both the oblate and prolate ellipsoids of revolution by the method of Schachman (1959) using a comparison of the Stoke's radii calculated from the molecular mass and sedimentation coefficient determined for each derivative (Tanford, 1961) with that of the Stoke's radii predicted for spherical proteins of corresponding molecular mass.

Axial ratios for CDC34, cdc34Δ_{265}, cdc34Δ_{244}, cdc34Δ_{209} and cdc34Δ_{185} were also determined using Stoke's radii obtained from gel exclusion chromatography and the method described above (Schachman et al., 1959). Samples in buffer A plus 150 mM NaCl were applied to a Superdex 75 HR 10/30 column and Stoke's radii were determined from a standard plot of (-logK_{AV})$^{1/2}$ vs Stoke's radii created from molecular mass standards with known Stoke's radii, (cytochrome C, carbonic anhydrase and BSA) that were chromatographed under identical conditions. Axial ratio values determined using gel exclusion chromatography and those determined using analytical ultracentrifugation were equivalent for CDC34 and differed by 7% in the case of cdc34Δ_{185}.

2.3 Results

2.3.1. The cell cycle function of CDC34 depends upon tail residues 171-209. Previous genetic studies suggested that the function of CDC34 is dependent upon its ability to physically interact with either itself or other E2s (Silver et al., 1992). This conclusion was based on the observation that the catalytic domains of CDC34 and RAD6 could partially complement a cdc34 temperature sensitive (ts) mutant strain but not a mutant in which the CDC34 allele had been disrupted. The inability of the catalytic domains to complement for the disruption mutation showed that partial complementation of the ts mutant required the presence of both the catalytic domain and the cdc34 ts polypeptide. This suggested that CDC34 function and thus cell viability was restored as a consequence of an interaction between the catalytic domain and the tail of the cdc34 ts polypeptide.

To assess the role of the CDC34 tail in this interaction, a series of 9 yeast plasmid borne CDC34 derivatives was constructed in which the tail coding sequence of CDC34 was truncated in 10-15 residue increments from the carboxy terminus towards the catalytic domain (Figure 2.1). Each plasmid was then introduced into the ts cdc34-2 yeast strain or a yeast strain carrying a disruption of the CDC34 coding sequence and tested for complementation of either mutation. In the case of the ts mutant, cell viability was measured at the non-permissive temperature of 37°C. In the case of the disruption mutant, cell viability was determined based on the ability of cells to survive the loss of a CDC34 maintenance plasmid by FOA selection (Silver et al., 1992).

The results presented in Figure 2.1 indicate that only a 14 residue stretch of the 125 residues contained within the tail (171-185) are required to restore full CDC34 function in the cdc34 ts strain but fails to function in the disruption strain whereas the additional stretch of 24 residues present in cdc34Δ_{209} restores function to both strains. Furthermore, the ability of cdc34Δ_{209} to restore full viability to the disruption strain even at low copy and under control of the native CDC34 promoter indicates that the cell cycle activity of the CDC34 tail falls exclusively within a 39 residue stretch between positions 171-209, hereafter referred to as the cell cycle determinant or CCD, and that the remaining 86 residues are inessential. These results demonstrate that cdc34Δ_{185} functions only in the presence of the cdc34-2 ts polypeptide, whereas cdc34Δ_{209} retains full functional activity on its own. The simplest interpretation of these results is that the cell cycle activity of CDC34 depends upon its self-association and that while cdc34Δ_{185} can interact with the full length cdc34 ts polypeptide, it cannot interact with itself. The fact that cdc34Δ_{209} is

capable of full functional activity in the absence of the cdc34 ts polypeptide argues that the 24 residues that span positions 186 to 209 play an important role in this interaction.

2.3.2. Self-association of CDC34 *in vitro* depends on tail residues 171-209. To test the self-associative properties of CDC34 and its derivatives *in vitro*, *E. coli* expression plasmids were created for the nine derivatives shown in Figure 2.1 and the proteins expressed from these plasmids were purified (Materials and Methods). Figure 2.2 shows the level of purity achieved for eight of the nine derivatives. When cdc34Δ_{170} was overexpressed all of the protein was found in inclusion bodies. Therefore, cdc34Δ_{170} was omitted from subsequent *in vitro* analyses. cdc34Δ_{200} on the other hand was found to be particularly sensitive to proteolysis, yielding a proteolytic product with the same molecular mass as cdc34Δ_{185}. Although cdc34Δ_{200} could be chromatographically separated from its proteolysed form (Figure 2.2), subsequent manipulation resulted in further proteolysis. Therefore, cdc34Δ_{200} was also omitted from the *in vitro* analyses described below. From Figure 2.2 it can be seen that full length CDC34 as well as the tail deletion derivatives run anomolously on SDS gels at molecular masses considerably higher than that predicted from their primary amino acid sequences.

CDC34's ability to self-associate was tested directly by a chemical crosslinking experiment using bacterially expressed and purified CDC34 in combination with the lysine-lysine crosslinker BS^3 (Figure 2.3). The addition of BS^3 generated a ladder of crosslinked products which included higher molecular mass species as the concentration of the crosslinker was increased. The multimeric interactions between CDC34 monomers is highly specific and is not the result of random interactions expected through mass action. This conclusion is based on the observation that in the presence of a 10-fold molar excess of BSA (added as a non-specific competitor), neither CDC34-BSA (Figure 2.3) or BSA-BSA (results not shown) crosslinked products could be detected.

The assignment of stoichiometry to these multimeric bands is complicated by the deviation of their calculated molecular masses from predicted values (Figure 2.3). These deviations likely arise from the anomalous hydrodynamic properties exhibited by branched crosslinked structures. Based on the apparent molecular mass of the CDC34 monomer (42 kDa) a dimer would be expected to have a molecular mass of 84 kDa, therefore the 95 kDa crosslinked species is most probably a dimer. Although the 116 kDa species is closer in molecular mass to that predicted for a trimer (126 kDa), we have tentatively assigned this species as a dimer. This designation is based partly on the observation that the larger 190 kDa and 240 kDa crosslinked species have molecular masses twice as great as the 95 kDa and 116 kDa bands respectively. This observation is most easily accounted for by assuming that the 95 kDa and 116 kDa dimers have been crosslinked into tetramers without

passage through a trimeric intermediate. Further support for these designations is based on the observation that progressive deletion of the CDC34 tail normalizes the apparent molecular mass of these dimer species to expected values (Figure 2.4 and Table 2.1).

Table 2.1.

Derivatives	Apparent Molecular Mass (kDa)			Dimer/Monomer	
	Monomer	Dimer A	Dimer B	A	B
CDC34	42	95	116	2.2	2.8
cdc34Δ_{244}	35	66	72	1.9	2.1
cdc34Δ_{209}	29	57	62	2.0	2.1
cdc34Δ_{185}	25	49	–	–	2.0

The presence of more than one band for any given multimer reflects differences in the sites that link monomers together giving rise to multimers having different hydrodynamic properties in the unfolded state.

We next examined the effect of the tail length on the crosslinking pattern produced using the crosslinker BS^3 (Figure 2.4). As expected both the monomer and the spectrum of crosslinked multimers shifts downward in molecular mass in correspondence with the number of residues deleted from the tail. Significantly, the efficiency of dimer formation via crosslinking for CDC34, cdc34Δ_{244} and cdc34Δ_{209} is unaffected by either tail deletion or protein concentration. By comparison, the single crosslinked species observed for cdc34Δ_{185} is formed less efficiently than for longer derivatives. Furthermore, its formation is critically dependent upon protein concentration. We conclude from these results that the 24 residues situated between positions 186-209 play an important role in mediating the self-association of CDC34 *in vitro*, an observation that is entirely consistent with the notion that these residues are necessary for the self-associative properties of CDC34 *in vivo*.

By comparison to the dimer crosslinking results, the efficiency of crosslinking for higher multimers diminishes progressively as the tail is deleted to position 209 but are nonetheless present. This fact suggests that at least some of the structural information required for higher order interactions is spread throughout the entire length of the tail including the CCD. The simplification of the crosslinking pattern for higher multimers that results from the deletion of the 35 residues from position 244 to position 209 suggests that some of the crosslinked lysines are situated in this region. The complete disappearance of

higher multimers that results from the deletion of the 24 residues of the CCD from position 209 to 185 may be accounted for by one or both of two possibilities. First, lysines that are required for higher multimer crosslinking may be located in this portion of the CCD. Second, this region may be necessary to facilitate the interaction between constituents that comprise higher order complexes

2.3.3. Structure of the CDC34 tail. The shape of proteins can be modeled by two types of ellipsoids: the prolate (rod-like) or oblate (disk-like) forms. Either form is defined by an axial ratio which is the ratio of the major and minor axes of an ellipse. Using a protein's molecular mass and Stoke's radius, its axial ratio may be determined. The axial ratio provides a measure of asymmetry in the overall structure of a protein where the larger the value of the axial ratio the greater the protein's asymmetry. By measuring the change in axial ratio as a function of tail length we have determined the relative contribution of the tail to the overall shape of the CDC34 monomer (Figure 2.5A).

The axial ratios shown in Figure 2.5A were derived from Stoke's radii which were in turn empirically determined using gel exclusion chromatography on selected purified derivatives as described (see section 2.2.8). The reliability of the values determined chromatographically were confirmed by comparing the extreme values from cdc34Δ_{185} and full-length CDC34 to their values determined under similar conditions by analytical ultracentrifugation. The axial ratios determined by both methods agreed to within 93% of each other for each of the two derivatives.

From Figure 2.5A, it is apparent that the axial ratio of both the prolate and oblate forms is almost a linear function of tail length, increasing three fold and four fold for the prolate and oblate forms respectively from position 185 to full-length. From these results it is evident that CDC34 is a highly asymmetric protein and that most of this asymmetry resides in its tail.

The basic structural composition of the CDC34 tail was also determined by using CD spectroscopy on selected CDC34 derivatives (Figure 2.5B). CD spectroscopic analysis provides secondary structural information that specifies the relative contribution of α-helix, β-structure and undefined structure to the protein. From Figure 2.5B, deletion of the tail from full length to position 185 results in an approximate 3-fold drop in β-structure (from 57% to 18%) with little effect on α-helical content and only a modest effect on undefined content. From these results, we conclude that the tail is predominantly composed of β-structure with the vast majority of α-helix residing in the catalytic domain.

It is also apparent from Figure 2.5B that the trends exhibited by both β-structure and undefined structure are complicated and in counterpoint to one another. β-structure for instance drops almost two-fold by removal of the carboxyl terminal 30 residues whereas

38

undefined structure rises by greater than two-fold. Curiously, further deletion of the acidic stretch of the tail actually increases the β-structural content at the apparent expense of the undefined structural content. These results suggest that residues downstream of the acidic stretch anchor this region in a defined conformation which is lost upon its removal. Taken together, the results from CD analysis illustrate that the tail of CDC34 is a highly ordered and unique structure.

The region of the tail defining the cell cycle function and self-associative properties of CDC34 (residues 171-209) is structurally unique with respect to the rest of the tail. In contrast to the preponderance of β-structure found at the carboxy terminal portion of the tail (residues 210-295), loss of the 24 residues from positions 210 to 185 results in only a modest decrease in each of the three structural parameters measured by CD such that the structural content of this region cannot be solely classified by any one of these criteria. Furthermore, this region is highly susceptible to proteolysis (Figure 2.6). As with cdc34Δ_{200} (Figure 2.2), limited proteolysis of CDC34 and its remaining derivatives occurs at principally one cleavage site situated at or near position 185. Cleavage at this site gives rise to a common catalytic fragment migrating identically with cdc34Δ_{185}, and a tail fragment that varies in size according to its deletion position. Together these results argue that the dimerization region is ordered and accessible to interaction.

2.4 Discussion

Two previous studies have established that the unique cell cycle properties of CDC34 are contained within its tail (Silver et al., 1992; Kolman et al., 1992). Furthermore, genetic evidence suggest that the function of CDC34 is dependent upon the close physical proximity of one CDC34 monomer with another (Silver et al., 1992). This study links these two observations mechanistically by showing that both the cell cycle function and self-associative properties of CDC34 share a common dependence on a small region of its tail (residues 171-209), referred to here as the cell cycle determinant or CCD. The dependence of CDC34 on the CCD for self-association in vivo is suggested by the observation that while cdc34Δ_{209} is capable of full cell cycle function in the absence of the cdc34 ts polypeptide, cdc34Δ_{185} can only restore full function in the presence of the cdc34 ts polypeptide (Figure 2.1). This observation also suggests that the 24 residues contained within the CCD that separate cdc34Δ_{185} from cdc34Δ_{209} are important in stabilizing the self-association of CDC34 monomers. The dependence of CDC34 on the CCD for self-association in vitro is demonstrated by the crosslinking experiments of Figures 2.3 and 2.4. Together, these results indicate that the function of CDC34 depends upon its ability to

interact with itself and that this interaction is facilitated by the CCD contained within the tail.

Physical analyses presented in Figure 2.5 demonstrate that the CDC34 tail comprises a highly structured and extended domain, yet only the CCD which constitutes the N-terminal third of the tail is required for full function *in vivo*. Little can be said about the structure of the CCD except that it is proteolytically accessible and structurally distinct from the C-terminal portion of the tail. These structural differences appear to be reflected in the observed crosslinking characteristics of the CDC34 derivatives.

Several pieces of evidence suggest that the dimeric interaction of CDC34 is symmetrical about a two-fold axis. This idea was originally put forward in a model that could account for the first steps in multi-Ub chain assembly (Silver *et al.*, 1992). In this model (Figure 2.7), two E2 monomers, each coupled to Ub at their active sites, were envisioned to interact with one another across a dyad axis. Each Ub molecule within the complex interacts with the other such that the carboxy terminus of one Ub molecule is close to K48 of the other Ub molecule allowing for the formation of a Ub dimer linked at K48. The crystallographic structure of a Ub dimer where one Ub is linked to the other at K48 has been solved and shows that the two Ub molecules interact across a pseudo-dyad axis (Cook *et al.*, 1992). This Ub dimer structure is compatible with the model described above where the two-fold symmetry between E2 monomers would allow one Ub monomer to interact with the other across a pseudo-dyad axis.

Evidence in favor of a symmetrical interaction is based on the observation that the catalytic domains of either CDC34 or RAD6 are capable of partial cell cycle function when expressed in combination with a full length cdc34 ts polypeptide but not when expressed alone (Silver *et al.*, 1992). The simplest interpretation of this result in light of evidence presented here is that interacting E2 monomers are stabilized by a contact between the CDC34 tail of one monomer and the catalytic domain of the other. In a situation involving a symmetrical interaction between monomers, the tail of each monomer would interact with the catalytic domain of the other resulting in two identical contact points. The deletion of the tail from one monomer would weaken the interaction through the loss of one contact point thereby explaining the partial function of the interacting pairs described above and the failure of the catalytic domains to function on their own. Furthermore, this symmetrical interpretation is fully consistent with the *in vivo* results of Figure 2.1. The ability of cdc34Δ_{185} and cdc34Δ_{200} to function in combination with the *cdc34-2* allele despite extensive deletion of the CCD can be easily accounted for by assuming that although one tail contact point is weakened by deletion, the other remains unperturbed in the cdc34 ts - cdc34Δ dimer. Similarly, the failure of cdc34Δ_{185} or cdc34Δ_{200} to function on their own

40

in the disruption mutant can be accounted for by the combined effects of two weakened contact points.

Although crosslinking analysis (Figure 2.3) indicates that the interaction of CDC34 with itself *in vitro* is specific, it is also weak. We have not detected appreciable complex formation in either sedimentation or gel exclusion studies using a variety of conditions (results not shown). Based on these observations it is reasonable to expect that such an interaction is stabilized *in vivo* by other factors not accounted for in the experiments described here. One possibility is that interacting Ub molecules that are tethered at each active site provide additional stabilization for the dimer. Recent support for this idea has come from the observation that the direct interaction of Ub with a CDC34 mutant protein presumed to be defective in dimer formation, suppresses the cell cycle effects of the *cdc34-2* allele (Prendergast *et al.*, 1995). Other obvious possibilities include the idea that dimer formation is facilitated by either the interaction of CDC34 with its natural substrate or with proteins involved in substrate recognition such as E3s.

While there is no absolute requirement for tails in homodimer interactions (Pickart and Rose, 1985; Haas and Bright, 1988; Girod and Vierstra, 1993), there may be a requirement for tails in heterodimer interactions. The formation of heterodimers between E2s has already been observed in two cases where such interactions may be tail dependent. In the first instance a case has already been made that CDC34 interacts with the catalytic domain of RAD6 *in vivo* in a manner that depends upon the tail of CDC34 (Silver *et al.*, 1992). In the second instance, Chen *et al.* (1993) have recently found *in vivo* evidence for the interaction of UBC6 with UBC7. Notably in each of these two examples, a monomer without a tail is paired with a monomer that has a tail. Hetero interactions between the catalytic domains of different E2s may generally be weaker than interactions of the homo variety since contacts across the pseudo two-fold axis are less likely to be duplicated. Contact between the tail of one monomer and the catalytic domain of the other may provide the means of reinforcing this interaction.

Interestingly, different heterodimers may be stabilized by their own structural equivalent of the CDC34 CCD. While E2 tails generally bear little or no resemblance to one another, examination of the yeast UBC1 and UBC6 tail sequences reveal a significant region of consensus with the CDC34 CCD (Figure 2.8). Furthermore, the distance that separates this common element from the carboxy terminal end of the catalytic domain differs by only a few amino acids for each of these E2s. Taken together, the above observations suggest that functionally unrelated E2 heterodimers may utilize a structurally conserved mode of interaction. Such a possibility could be a foundation for the dynamic interplay between different E2 partners.
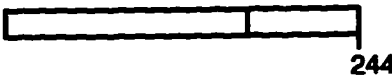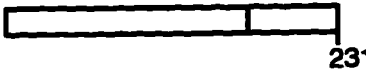
Figure 2.1. **Functional complementation of** *cdc34* **mutants by CDC34 tail-deletion derivatives.** The catalytic or core domain is shown in grey (residues 1-170). The tail (residues 171-295) is shown in white and contains a highly acidic region (residues 244-265) shown in black. Numbers designate the position of the C-terminal residue for each derivative. The ability of each derivative to confer viability to either a *cdc34* ts or disruption mutant under selective conditions was scored on the basis of colony size and plating efficiency. A positive score indicates viability and growth that is indistinquishable from full-length CDC34. A negative score indicates the absence of growth. All derivatives were expressed from gene cassettes contained within identical high copy plasmids using an uninduced *CUP1* promoter (see section 2.2.1). In addition, cdc34Δ_{209} (asterix) was expressed from a single copy plasmid under the control of the native *CDC34* promotor.

42
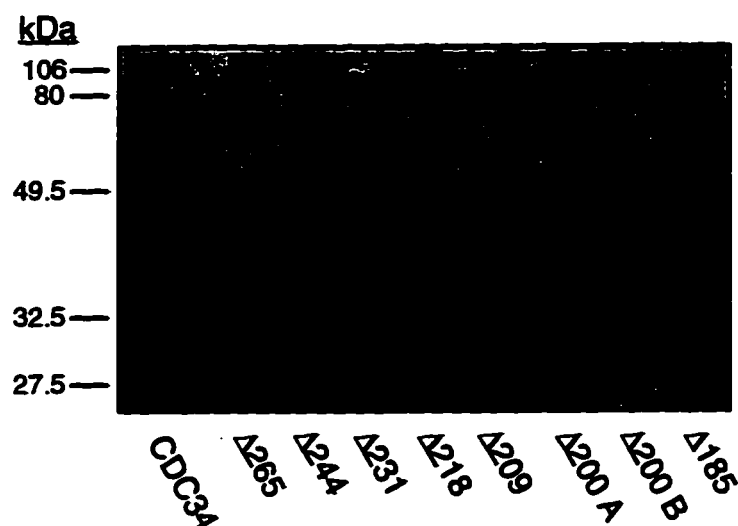
Figure 2.2. **Purified CDC34 and its derivatives.** Shown is a coomassie stained SDS-polyacrylamide gel of bacterially expressed and purified CDC34 and seven of the eight tail-deletion derivatives described in Figure 2.1. Also indicated are the positions of known molecular weight markers (from Bio-Rad; Phosphorylase B - 106 kDa; BSA - 80 kDa; Ovalumin - 49.5 kDa; Carbonic anhydrase - 32.5 kDa; Soybean trypsin inhibitor - 27.5 kDa). Lanes marked A and B refer to protein obtained from two closely spaced chromatographic peaks resulting from separation of $cdc34\Delta_{200}$ on a Superdex 75 (Pharmacia) gel exclusion column. Predicted molecular masses of CDC34 and its derivatives as calculated from the known peptide sequence are as follows : CDC34 - 34 kDa, $cdc34\Delta_{265}$ - 30 kDa, $cdc34\Delta_{244}$ - 28 kDa, $cdc34\Delta_{231}$ - 26 kDa, $cdc34\Delta_{218}$ - 25 kDa, $cdc34\Delta_{209}$ - 24 kDa, $cdc34\Delta_{200}$ - 23 kDa, $cdc34\Delta_{185}$ - 21 kDa. Apparent molecular masses of each species as determined electrophoretically are as follows: CDC34 - 42 kDa, $cdc34\Delta_{265}$ - 37 kDa, $cdc34\Delta_{244}$ - 35 kDa, $cdc34\Delta_{231}$ - 33 kDa, $cdc34\Delta_{218}$ - 31 kDa, $cdc34\Delta_{209}$ - 29 kDa, $cdc34\Delta_{200}$ - 27 kDa, $cdc34\Delta_{185}$ - 25 kDa.
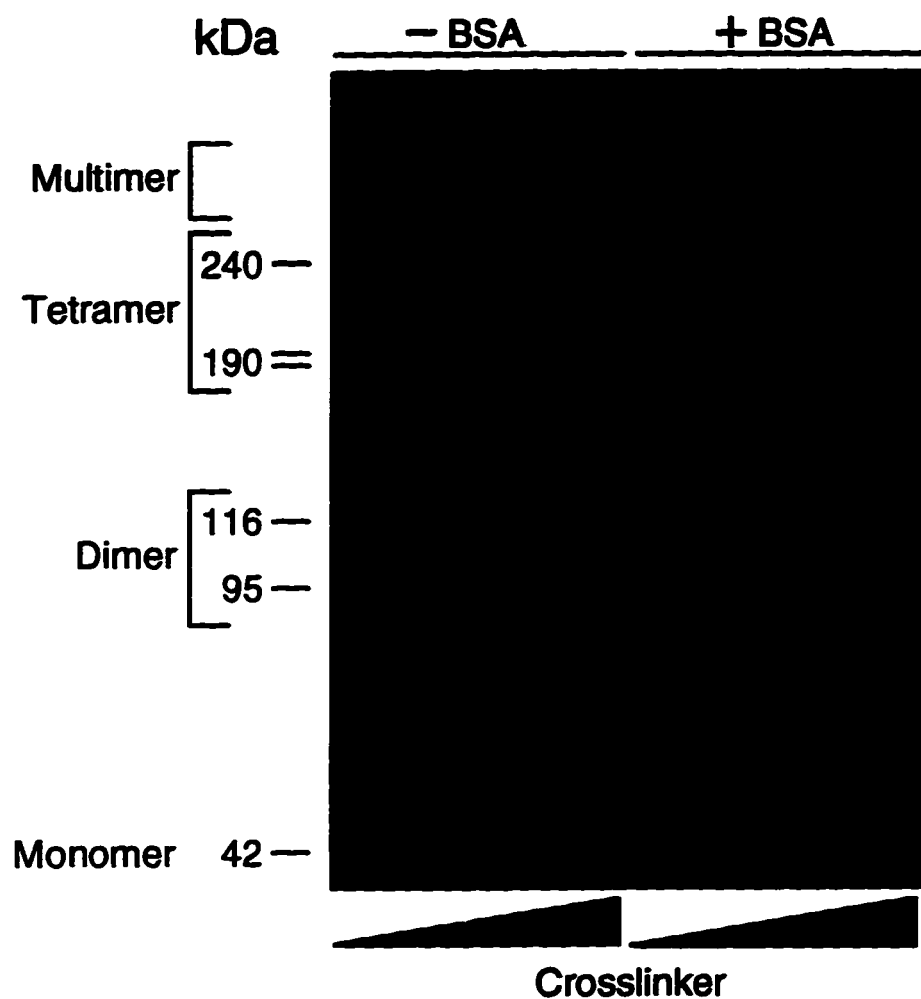
Figure 2.3. Self-association of CDC34 as detected by crosslinking analysis. Shown is an autoradiograph of a 6% SDS-polyacrylamide gel of purified radiolabeled CDC34 treated with 0, 1 or 10 mM of the crosslinker BS^3 in the presence or absence of the non-specific competitor BSA, (10-fold molar excess). The assignment of putative dimer and tetramer bands is based on the migration of each band relative to other crosslinked species in the same lane and to the migration of known molecular weight standards (see section 2.3.2).
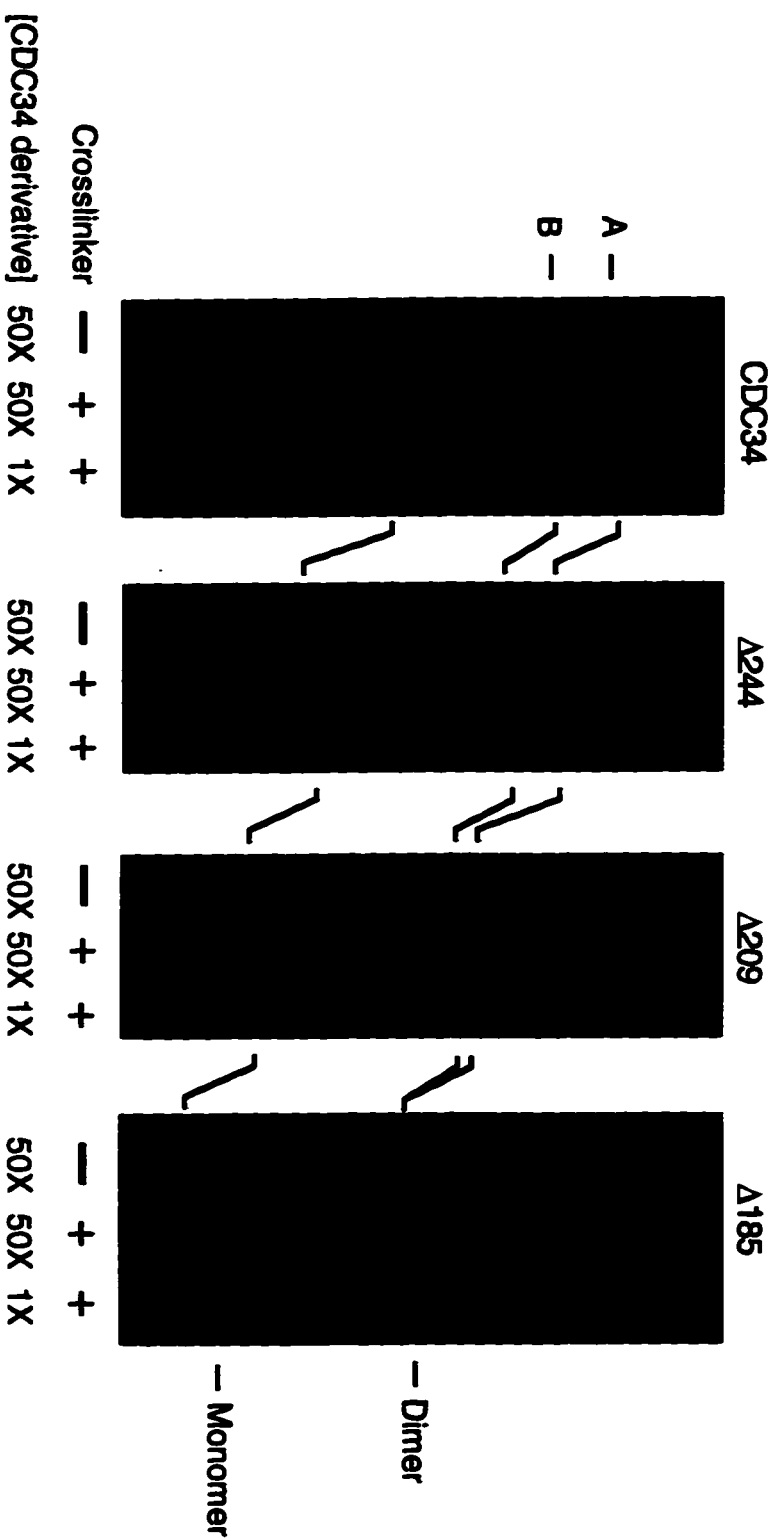
Figure 2.4. Dependence of CDC34 self-association on its tail. Crosslinking analysis of selected CDC34 tail deletion derivatives as a function of protein concentration was performed essentially as described for Fig. 2.3. One set of reactions used 1 mM crosslinker in combination with 0.6 μM (1X) of protein. A second set of reactions employed 0, or 1 mM crosslinker in combination with 30 μM (50X) of protein. Samples used were run on a 10% SDS-polyacrylamide gel in order to optimize resolution of the smaller derivatives and their crosslinked products.

45
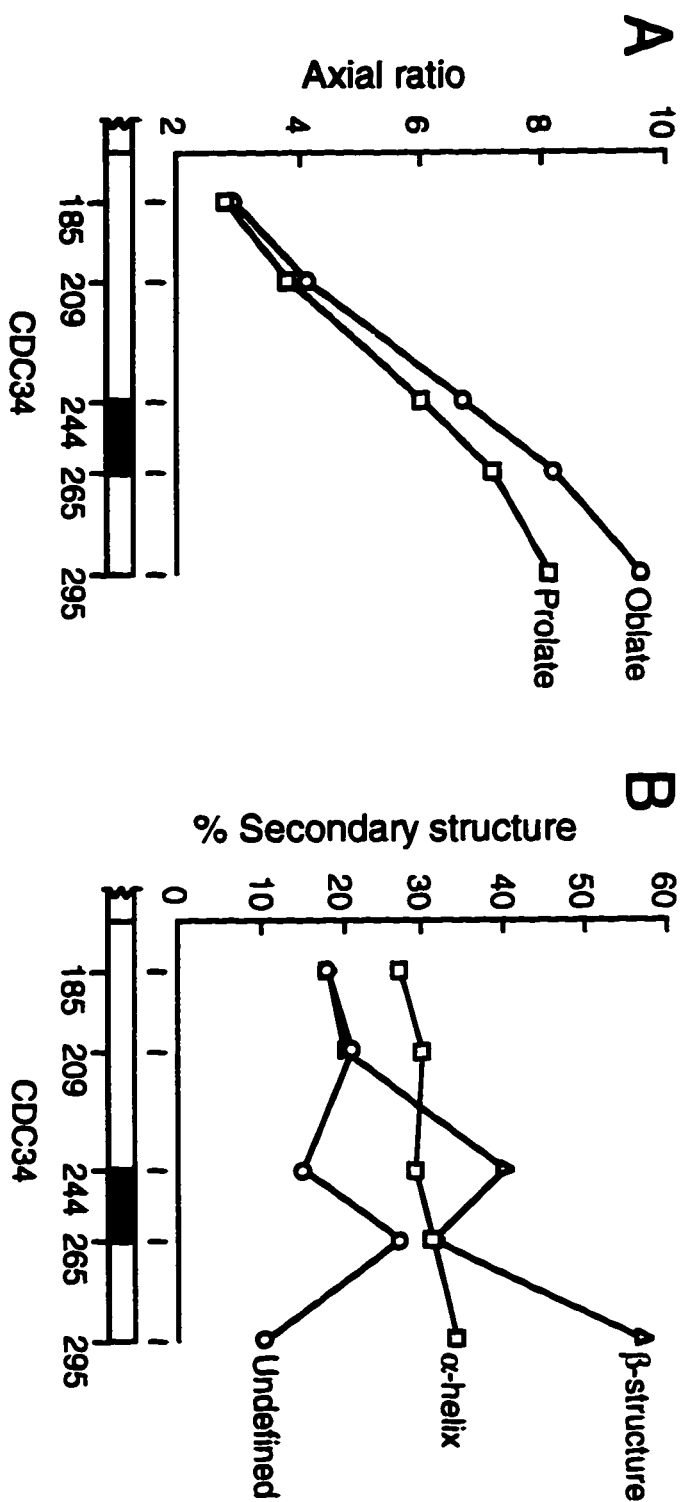
Figure 2.5. Structural analysis of the catalytic and tail domains. A) Shape determination. Elliptical axial ratios for selected CDC34 tail deletion derivatives were determined by either sedimentation velocity ultracentrifugation or by gel filtration chromatography and plotted as a function of tail length. Values were determined for the oblate (disk-like) and the prolate (rod-like) forms of the rotated ellipse. B) Secondary structure. Structural contents of the same tail deletion derivatives shown in panel A were determined by CD spectrum analysis and are shown plotted as a function of tail length. Values have been corrected for tail length to reflect structural content relative to full-length CDC34. β-structure represents the combined values for β-sheet and β-turn.

A
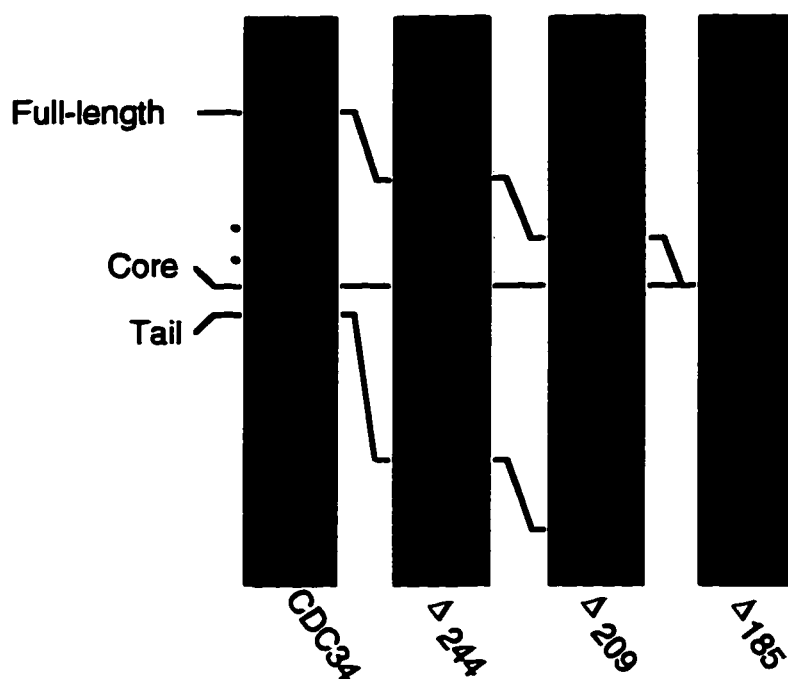
B
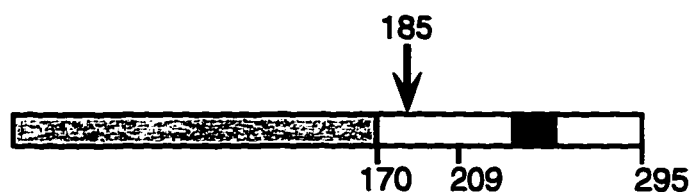
Figure 2.6. **Susceptibility of the interaction signal to proteolysis.** A) SDS-polyacrylamide gel of radiolabeled, purified CDC34 and selected tail deletion derivatives subjected to limited proteolysis (see section 2.2.6). Bands corresponding to unproteolyzed protein are indicated as full length. Core and tail refer to bands produced from a single cleavage. B) Proteolysis occurs at a principle cleavage site located within the interaction signal (residue 170-209) at or close to residue 185.
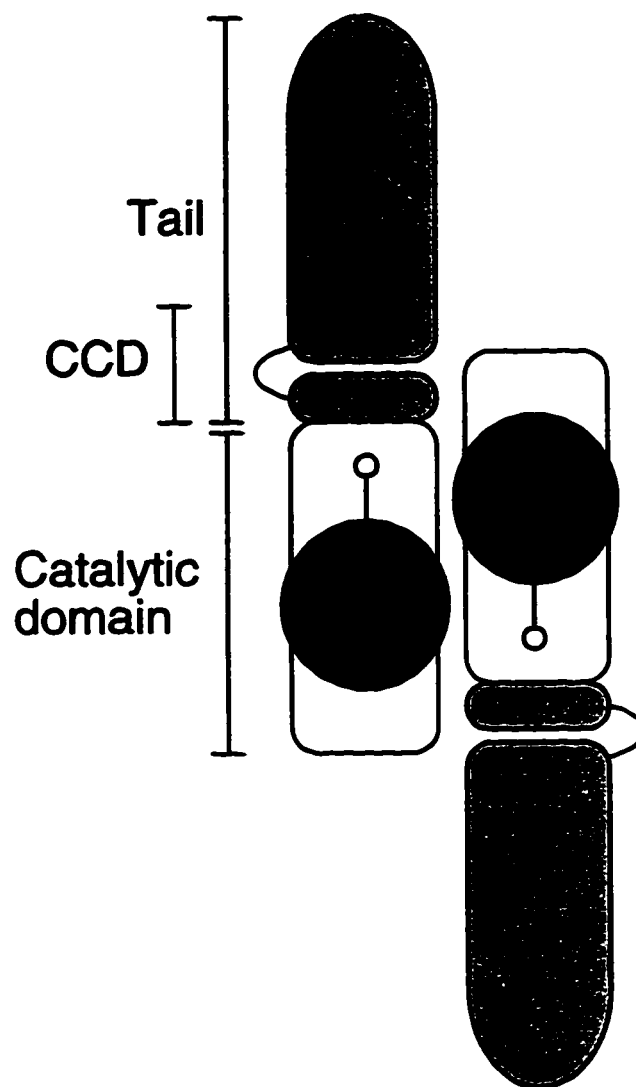
Figure 2.7. Model of a CDC34 homodimer interaction. Shown is a CDC34 dimer where monomers are stabilized through interactions between the tail (grey), catalytic domains (white) and Ub (black). Ub is shown coupled to each E2 monomer at the active site cysteine (circle). The loop within the tail indicates the proteolytically accessible site of the CCD.

```
CDC34 (14)  A Y I S Q S K L D E P E S N K D M A D ...
UBC6  (11)  E T L E K R K L D E G D A A N T G D E ...
UBC1  (16)  Y G I D H D L I D E F E S Q G F E K D ...
```

Figure 2.8. The tails of UBC1 and UBC6 share a common region with the CDC34 cell cycle determinant. Numbers indicate the distance of each region from the carboxy terminus of their respective catalytic domain. Boxed residues indicate identical or highly conserved residues shared between sequences (Goebl et al., 1988; Seufert et al., 1990; Sommer and Jentsch, 1993).

2.5 Bibliography

Bartel, B., Wunning, I, and Varshavsky, A. (1990). The recognition component of the N-end rule pathway. *EMBO J.* **9**, 3179-3189.

Chen, P., Johnson, P., Sommer, T., Jentsch, S., and Hochstrasser, M. (1993). Multiple ubiquitin-conjugating enzymes participate in the *in vivo* degradation of the yeast MATα2 repressor. *Cell* **74**, 357-369.

Chervenka, C. H. (1969). *A Manual of Methods for the Analytical Ultracentrifuge.* Spinco Division of Beckman Instrumants, Inc., Palo Alto, CA.

Dohmen, J. D., Madura, K., Bartel B., and Varshavsky A. (1991). The N-end rule is mediated by the UBC2(RAD6) ubiquitin-conjugating enzyme. *Proc. Natl. Acad. Sci. USA* **88**, 7351-7355.

Finley, D. The yeast ubiquitin system. In *The Molecular and Cellular Biology of the Yeast Saccharomyces cerevisiae: Gene Expression.* Jones, E., Pringle, J., Broach, J., ed. (New York: Cold Spring Harbor Laboratory Press), 539-558.

Girod, P.-A., Vierstra, R. D. (1993). A major ubiquitin conjugation system in wheat germ extracts involves a 15 kDa ubiquitin-conjugating enzyme (E2) homologous to the yeast *UBC4/UBC5* gene products. *J. Biol. Chem.* **268**, 955-960.

Goebl, M. G., Yochem, J., Jentsch, S., McGrath, J. P., Varshavsky, A., and Byers, B. (1988). The yeast cell cycle gene *CDC34* encodes a ubiquitin-conjugating enzyme. *Science* **241**, 1331-1335.

Gonda, D. K., Bachmair, A., Wunning, I., Tobias, J. W., Lane, S. W., and Varshavsky, A. (1989). Universality and structure of the N-end rule. *J. Biol. Chem.* **264**, 16700-16712.

Haas, A. L., and Bright, P. M. (1988). The resolution and characterization of putative ubiquitin carrier protein isozymes from rabbit reticulocytes. *J. Biol. Chem.* **263**, 13258-13267.

Haas, A. L., Reback, P. M., and Chau, V. (1991). Ubiquitin conjugation by the yeast RAD6 and CDC34 gene products. Comparison to their putative rabbit homologs, E2 (20K) and E2 (32K). *J. Biol. Chem.* **266**, 5104-5112.

Hershko, A., and Ciechanover, A. (1992). The ubiquitin system for protein degradation. *Annu. Rev. Biochem.* **61**, 761-807.

Hochstrasser, M. (1992). Ubiquitin and intracellular protein degradation. *Curr. Opin. Cell Biol.* **4**, 1024-1031.

Jentsch, S. (1992). The ubiquitin-conjugation system. *Annu. Rev. Genet.* **26**, 177-205.

Jentsch, S., Seufert, W., Sommer, T. and Reins, H. A. (1990). Ubiquitin-conjugating enzymes: novel regulators of eukaryotic cells. *Trends Biol. Sci.*, **15**, 105- 108.

Kolman, C. J., Toth, J., and Gonda, D. K. (1992). Identification of a portable determinant of cell cycle function within the carboxy-terminal domain of the yeast CDC34 (UBC3) ubiquitin conjugating enzyme. *EMBO J.* **11**, 3081-3090.

Morrison, A., Miller, E. J., and Prakash, L. (1988). Domain structure and functional analysis of the carboxy-terminal polyacidic sequence of the RAD6 protein of *Saccharomyces cerevisiae. Mol. Cell. Biol.*, **8**, 1179-1185

Pickart, C.M., and Rose I.A. (1985). Functional heterogeneity of ubiquitin carrier proteins. *J. Biol. Chem.* **260**, 1573-1581.

Schachman, H. K. (1959) *Ultracentrifugation in Biochemistry.* Academic Press, NY, 236-247

Seufert, W., McGrath J. P., and Jentsch, S. (1990). *UBC1* encodes a novel member of an essential subfamily of yeast ubiquitin-conjugating enzymes involved in protein degradation. *EMBO J.* **9**, 4535-4541.

Sherman, F., Fink, G. R., and Hicks, J. B., (1986) *Methods in Yeast Genetics.* Cold Spring Harbour Laboratory Press, Cold Spring Harbor, NY

Sikorski, R. S., and Hieter, P. (1989). A system of shuttle vectors and yeast host strains designed for efficient manupulation of DNA in *Saccharomyces cerevisiae. Genetics* **122**, 19-27.

Silver, E. T., Gwozd, T. J., Ptak, C., Goebl, M., and Ellison M. J. (1992). A chimeric ubiquitin conjugating enzyme that combines the cell cycle properties of CDC34 (UBC3) and the DNA repair properties of RAD6 (UBC2): implications for the structure, function, and evolution of the E2s. *EMBO J.* **11**, 3091-3098

Sommer, T., and Jentsch, S. (1993). A protein translocation defect linked to ubqiutin conjugation at the endoplasmic reticulum. *Nature* **365**, 176-179.

Studier, F. W., Rosenberg, A. H., Dunn, J. J., and Dubendorff, J. W. (1990). Use of bacteriophage T7 RNA polymerase to direct selective high-level expression of cloned genes. *Methods Enzymol.* **185**, 60-89

Sung, P., Prakash, S., and Prakash, L. (1988). Mutation of cysteine-88 in the Saccharomyces cerevisiae RAD6 protein abolishes its ubiquitin-conjugating activity and its various biological functions. *Genes & Dev.* **2**, 1476-1485.

Tabor, S., and Richardson, C. C. (1985). A bacteriophage T7 RNA poymerase/promoter system for controlled exclusive expression of specific genes. *Proc. Natl. Acad. Sci. USA* **82**, 1074-1078.

Tanford, C. (1961) *Physical Chemistry of Macromolecules.* John Wiley and Sons, NY, 317-456.

Varshavsky , A. (1992). The N-end rule. *Cell* **69**, 725-735.

Chapter 3

Deletion of the CDC34 catalytic domain insertion alters properties associated with the tail domain.

3.1. Introduction

While the tail domain of CDC34 plays a key role in its cell cycle function (Kolman *et al.*, 1992; Silver *et al.*, 1992; Ptak *et al.*, 1994) it is not the sole determinant that defines this activity. The catalytic domain also provides a cell cycle function beyond its catalytic role in thiolester formation. Previous studies have shown that an E2 chimera consisting of the RAD6 catalytic domain and the CDC34 tail domain can functionally replace CDC34 *in vivo* (Kolman *et al.*, 1992; Silver *et al.*, 1992). However, when expressed from a low copy plasmid this chimera could replace CDC34 function only to a limited degree. As such, while the RAD6 catalytic domain may functionally replace that of CDC34 it could only do so at elevated concentrations (Kolman *et al.*, 1992). Furthermore, replacing the catalytic domain of CDC34 with that of UBC1 or UBC4 generated chimeras completely lacking the ability to carry out CDC34 function (Kolman *et al.*, 1992). Each of these catalytic domains is capable of forming a thiolester with Ub (Seufert and Jentsch, 1990; Seufert *et al.*, 1990) but could not functionally replace the catalytic domain of CDC34. Therefore, the catalytic domain of CDC34 must also provide a necessary cell cycle function beyond thiolester formation (Kolman *et al.*, 1992; Silver *et al.*, 1992).

Comparison of the CDC34 amino acid sequence to that of other E2s showed that it not only possesses a unique carboxy terminal domain, but also contains unique elements within its catalytic domain. The most obvious of these is a short polypeptide stretch found on the carboxy terminal side of its active site cysteine. This twelve amino acid insertion is found in only one other E2 from yeast, UBC7 (Jungmann *et al.*, 1993; Vassal *et al.*, 1992). CDC34 also possesses a number of amino acid residues within its catalytic domain unique to itself and a small subset of E2s. For example, the sequence SPANVDAA comprising amino acid positions 139-146 of CDC34 is identical in RAD6 apart from a conservative D to E substitution. The corresponding stretch in UBC4 is considerably different consisting of the sequence DPLVPEIA. The importance of this region in the cell cycle function of CDC34 was borne out by replacing S139 with an D residue. This generates a derivative of CDC34 resembling UBC4 at the initial amino acid position of this stretch, and eliminates the ability of CDC34 to complement either a *cdc34* ts or disruption mutant when expressed from a low copy plasmid (Liu *et al.*, 1996). As such, the identity of this region between

CDC34 and RAD6 is thought to be partially responsible for allowing RAD6, but not UBC4 to functionally replace the catalytic domain of CDC34.

Mutational studies have also identified roles for the polypeptide insertion and residue S97 of CDC34 in defining the cell cycle function associated with its catalytic domain (Liu *et al.*, 1996; Pitluk *et al.*, 1995). This chapter extends these observations with evidence that the polypeptide insertion helps to define the *in vitro* activity of CDC34, and determines how the tail domain is utilized in these reactions. The CDC34 polypeptide insertion and residue S97 were also introduced into the corresponding positions of the RAD6 catalytic domain found in the RAD6-CDC34 chimera described above. Introducing these elements into RAD6-CDC34 resulted in a fusion protein that could not carry out CDC34 function. Thus, while these elements of CDC34's catalytic domain are important for its cell cycle function they are not the sole determinants within the catalytic domain responsible for this activity.

3.2. Materials and Methods

3.2.1. Yeast plasmids used in complementation experiments.
Various yeast overexpression plasmids carrying derivatives of *CDC34* and derivatives of the *RAD6-CDC34* chimera were constructed. All plasmids were high copy, carried the *TRP1* marker, and placed these coding sequences under control of the *CUP1* promoter and the *CYC1* terminator. All plasmids were also identical to the CDC34 plasmid described in Silver *et al.* (1992) except for the coding sequence changes described below.

One particular plasmid carried a derivative of *CDC34* in which nucleotides corresponding to codons 103-114 were deleted from the catalytic domain. The deleted codons define the polypeptide insert found in the catalytic domain of CDC34. This deletion derivative is referred to as *cdc34M*. The full coding sequence of *cdc34M* was generated in two fragments using PCR.

Synthesis of the first fragment employed a previously described primer that introduces an SstI site within the first three codons of *CDC34* (Silver *et al.*, 1992). The second primer used consisted of the following sequence 5'TCTGCCCGGGAGACCAACTTTG ATGTAAAATAGAAATAC3' corresponding to codons 95-120 minus the sequence to be deleted, namely codons 103-114. This primer introduces an A to C mutation (shown in bold face) producing a SmaI site (underlined) at the 3' end of this fragment, as well as a V118 to G118 substitution in the polypeptide sequence. The resulting conservative amino acid change had no effect on the ability of *CDC34* to function *in vivo* (T. Gwozd, pers.

comm.). Use of these primers along with a *CDC34* template produced the 5' fragment of *cdc34M* which included a 5' SstI and a 3' SmaI site used for cloning.

Synthesis of the second fragment also used a previously described primer that introduces a KpnI site 3' of the *CDC34* stop codon (Silver *et al.*, 1992). The second primer used consisted of the following sequence 5'TGGTCTCCCGGGCAGACCG TGG3' corresponding to codons 114-121 of CDC34 between nucleotides 343-364. This primer introduces a G to A substitution (shown in bold face) producing a SmaI site (underlined) as well as the same V118 to G118 amino acid substitution described above. Use of these primers along with a *CDC34* template produced a 3' fragment of *cdc34M* which included a 5' SmaI and a 3' KpnI site used for cloning.

A triple fragment ligation was used to clone the SstI/SmaI digested 5' fragment and the SmaI/KpnI digested 3' fragment of *cdc34M* into the SstI and KpnI sites of the previously constructed *CDC34* plasmid (Silver *et al.*, 1992). The *cdc34M* coding sequence was checked by sequencing using the double-stranded chain termination method on an Applied Biosystems automated sequencer. All oligonucleotide synthesis and sequencing described in this section were carried out by the DNA Synthesis and Sequencing Facility at the University of Alberta.

A set of plasmids bearing carboxy terminal deletion derivatives of *cdc34M* were also made. The carboxy terminal domains of previously constructed tail deletion derivatives of *CDC34* (Ptak *et al.*, 1994) were excised using the EcoRV and KpnI restriction enzymes and subsequently cloned into the same sites of a yeast overexpression plasmid carrying the *cdc34M* coding sequence. This placed the various tail deletions of *CDC34* within the context of the *cdc34M* catalytic domain. These derivatives included: $cdc34M\Delta_{265}$, $cdc34M\Delta_{244}$, $cdc34M\Delta_{231}$, $cdc34M\Delta_{218}$, $cdc34M\Delta_{209}$, $cdc34M\Delta_{200}$, and $cdc34M\Delta_{185}$ (see Figure 3.1). The numeric designations associated with each $cdc34M\Delta$ gene identifies an identical carboxy terminal deletion of the tail domain as was previously constructed for *CDC34* (see section 2.2.1) rather then to the actual length of the cdc34MΔ polypeptide encoded by these genes.

Plasmids were also constructed in which the glutathione S-transferase (*GST*) coding sequence was fused to the 5' end of *CDC34*, and various *cdc34M* derivatives. Two oligonucleotides were used to generate the *GST* coding sequence by PCR. The first of these consisted of the sequence 5'*CTGTAAC*GAATTCA**TA**TGTCCCCTATACTAGG TTATTGG3'. The *GST* start codon is shown in bold face. The nucleotides found 5' of the start codon (shown in italics) consist of the 3' end of the *CUP1* promoter. An EcoRI site (underlined) is also found within the *CUP1* sequence and was used here for cloning. The second oligonucleotide consisted of the sequence 5'*GCCATA*GAGCTCA**TT**CCC

CCGGGGATCCCACGACCTTCGAT3'. Nucleotides shown in italics comprise the initial codons found in *CDC34* as well as all of the *cdc34M* derivatives. Contained within this region is also an SstI site (underlined) used for cloning. The remaining nucleotides consist of the codons found at the 3' end of the *GST* coding sequence.

Use of these oligonucleotides along with a *GST* template produced the *GST* coding sequence flanked at its 5' end by a portion of the *CUP1* promoter and at its 3' end by codons 1-5 of *CDC34*, as well as the various *cdc34M* derivatives. This version of *GST* was digested with EcoRI and SstI and subsequently cloned into the same sites found in the *CDC34* plasmid as well the plasmids carrying the various *cdc34M* derivatives. Using this method, *GST* was cloned in frame with respect to the *CUP1* promoter as well as the specific coding sequences to which it was fused. The *GST* derivatives constructed in this fashion included: *GST-CDC34*, *GST-cdc34M*, *GST-cdc34MΔ_{265}*, *GST-cdc34MΔ_{244}*, *GST-cdc34MΔ_{231}*, *GST-cdc34MΔ_{218}*, *GST-cdc34MΔ_{209}*.

Plasmids carrying various tail deletion derivatives of the *RAD6-CDC34* chimera (referred to as *RC* here) were also constructed. *CDC34* tail segments were excised from previously constructed plasmids (Ptak *et al.*, 1994) using the EcoRV and KpnI restriction enzymes. These fragments were then cloned into the same sites of the previously constructed *RAD$_{CDC}$* plasmid which carries the *RC* coding sequence (Silver *et al.*, 1992). This placed the various CDC34 tail deletions within the context of the RAD6 catalytic domain. The *RC* derivatives constructed in this way included: *RCΔ_{265}*, *RCΔ_{244}*, *RCΔ_{231}*, *RCΔ_{218}*, *RCΔ_{209}*, *RCΔ_{200}*, *RCΔ_{185}*. The numeric designations associated with each *RCΔ* gene identifies an identical carboxy terminal deletion of the tail domain as was previously constructed for *CDC34* (see section 2.2.1) rather then to the actual length of the RCΔ polypeptide encoded by the gene.

Codons 103-114 which define the peptide insertion found in the catalytic domain of CDC34 were introduced into the corresponding positions of the *RC* coding sequence. This derivative will be referred to as *RP*. The *RP* coding sequence was generated in two fragments using PCR. Production of the 5' fragment employed a previously described primer that introduces an SstI site within the first three codons of the *RAD6* catalytic domain (Silver *et al.*, 1992). The second primer used consisted of the following sequence 5'CATA<u>CCCGGG</u>AGTCCA*CGTTTCAGCATCAGGTTCGTCGGTCATAGGATCCCC* TCTGTTCTGCAAAATATCCAAAC3' corresponding to the non-coding strand of the *RAD6* catalytic domain between codons 87-101 plus the nucleotides to be inserted (shown in italics). This primer alters three consecutive nucleotides from TGT to CCC (shown in bold face) generating a SmaI site (underlined) at the 3' end of this fragment and a T99 to G99 substitution in the polypeptide sequence of the RAD6 catalytic domain. This amino

acid change was previously shown to have no effect on the ability of *RAD6* to function *in vivo* (T. Gwozd, pers. comm.). Use of these primers along with a *RC* template produced the 5' fragment of *RP* which included a 5' SstI site and a 3' SmaI site used for cloning.

Synthesis of the 3' fragment of *RP* by PCR employed a previously described primer that introduces a KpnI site 3' to the stop codon found in the *CDC34* tail domain. The second primer used consisted of the following sequence 5'AGATGGACT<u>CCCGGG</u> TATGATGTCGC3' corresponding to the coding strand of the *RAD6* catalytic domain between codons 114-121. This primer alters three consecutive nucleotides from ACA to GGG (shown in bold face) producing both a SmaI site (underlined) as well as the same T99 to G99 amino acid substitution described above. This primer was used in combination with an *RC* template to produced the 3' fragment of *RP* which included a 5' SmaI site and a 3' KpnI site used for cloning.

Using a triple fragment ligation the SstI/SmaI digested 5' fragment and the SmaI/KpnI digested 3' fragment of *RP* were cloned into the SstI and KpnI sites of the previously constructed RAD$_{CDC}$ plasmid (Silver *et al.*, 1992).

Point mutants of *RC* and *RP* were also made and introduced into yeast overexpression plasmids. In both cases the mutation involved altering the codon corresponding to D90 found within the catalytic domain of *RAD6* from GAT to TCT. This results in the substitution of D90 with S90 generating the *RCS90* and *RPS90* derivatives.

All yeast overexpression plasmids were transformed into the yeast strain YL10 which carries the temperature sensitive *cdc34-2* allele. Plasmids carrying the various tail deletion derivatives of both *cdc34M* and *RC* were also transformed into the yeast strain YES71 in which the chromosomal copy of *CDC34* has been disrupted. For a more detailed description of these yeast strains see section 2.2.1. The ability each *CDC34* or *RC* derivative to complement for either the temperature sensitive allele or the disruption of *CDC34* was tested following the same procedures previously outlined (see section 2.2.1).

3.2.2. Construction of *E. coli* overexpression plasmids. *E. coli* overexpression plasmids carrying the coding sequences for *CDC34* and the tail deletion derivatives *CDC34*, *cdc34Δ$_{265}$*, *cdc34Δ$_{244}$*, *cdc34Δ$_{231}$*, *cdc34Δ$_{218}$*.*cdc34Δ$_{209}$*, and *cdc34Δ$_{185}$* have been previously described (Ptak *et al.*, 1994). Briefly, the coding sequences of *cdc34M*, *cdc34MΔ$_{265}$*, *cdc34MΔ$_{244}$*, *cdc34MΔ$_{231}$*, *cdc34MΔ$_{218}$*, *cdc34MΔ$_{209}$*, and *RC* were excised from the yeast overexpression plasmids described above using SstI and KpnI and inserted in frame between the SstI and KpnI sites of a previously described derivative of pET3a (see section 2.2.3). To increase the level at which transcripts of the *RC* gene were translated its first four R codons were altered from AGA to CGA or from AGG to CGG (see Figure 3.7; Chen and Inouye, 1994).

57

3.2.3. Protein overexpression. All *E. coli* overexpression plasmids were transformed into the E. coli strain BL21 along with the thermally induced T7 polymerase plasmid pGP1-2 (Tabor and Richardson, 1985). Protein overexpression and cell lysis follow the same procedures described for UBC1Δ and its various derivatives (see section 4.2). Similarly the procedures used to purify Ub labeled with ^{35}S-methionine and to prepare a crude lysate of recombinantly expressed wheat E1 are presented in sections 4.2.1 and 4.2.2 respectively.

Cell lysates from the overexpression of each CDC34 or RAD6 derivative were loaded onto a Mono Q HR 5/10 ion exchange column (Pharmacia) that had been equilibrated with buffer A (50 mM Tris (pH 7.5), 1 mM EDTA, 1 mM DTT). Each derivative was eluted from the column using a linear gradient in which the concentration of NaCl added to buffer A increased from 0 to 1 M over 50 min.

Peak fractions were pooled, and concentrated to 500 μl by filtration using centricon (Amicon) concentrators prior to loading onto a Superdex 75 HR 10/30 gel exclusion column (Pharmacia). Proteins were eluted from this column using a buffer consisting of 50 mM HEPES (pH 7.5), 150 mM NaCl, 1 mM EDTA, and 1 mM DTT. Peak fractions were again concentrated to 500 μl and subsequently frozen at -80 °C in the presence of 5% glycerol prior to further use.

3.2.4. *In vitro* ubiquitination assays. The activities of purified tail deletion derivatives of CDC34 and cdc34M as well as purified RC were tested using *in vitro* ubiquitination reactions. Concentrations of the various buffer components used in these reactions is outlined in section 4.2.3. Each purified derivative was added to a reaction at a final concentration of 1.2 μM along with purified ^{35}S-Ub also to a final concentration of 1.2 μM, and a crude lysate containing wheat E1 to an approximate final concentration of 8 nM. Final reaction volumes used were 100 μl and each reaction was incubated at 30 °C for 16 hr. Each reaction was terminated by the addition of 10 μl of 100% TCA and subsequently incubated on ice for 5 min. Once completed, the reactions were treated with a 1 in 10 volume of 100% TCA. Samples were then centrifuged and the TCA precipitated material retained and solubilized in SDS load mix (0.125 M Tris (pH 6.8), 20% glycerol, 2% SDS, 0.01 mg/ml bromphenol blue, 100 mM DTT). Reaction products containing ^{35}S-Ub were separated on an SDS-polyacrylamide gel (18% acrylamide, 0.1% bisacrylamide) and visualized by autoradiography.

3.3. Results

3.3.1. Cell cycle function of CDC34 depends upon residues 103-114 of the catalytic domain.

The functional role of CDC34's catalytic domain insertion was assessed by deleting the corresponding codons (103-114) from the *CDC34* coding sequence and testing the ability of this derivative (*cdc34M*) to functionally complement *cdc34* mutations. A yeast overexpression plasmid carrying the *cdc34M* coding sequence was transformed into the *cdc34-2* ts yeast strain or the *cdc34* disruption strain and complementation of either mutation tested. Cell viability of the ts mutant was measured at the non-permissive temperature of 37 °C. In the case of the disruption mutant, the ability of cells to survive the loss of the *CDC34* maintenance plasmid by FOA selection was used as a measure of cell viability (Silver *et al.*, 1992).

As seen in Figure 3.1 *cdc34M* complements the *cdc34* ts mutation but not the *cdc34* disruption mutation. This indicated that while residues 103-114 were dispensable for full CDC34 function within the ts strain they were essential for this function within the disruption strain. Therefore, under the conditions used here cdc34M could only function in the presence of the ts polypeptide.

Similar observations had previously been made for several CDC34 tail deletion derivatives including cdc34Δ185 (see section 2.3.1). It was concluded that the cdc34Δ185 and the cdc34 ts polypeptides interacted thereby restoring CDC34 function to the ts strain. Furthermore, the inability of cdc34Δ185 to complement the *cdc34* disruption strain resulted from its inability to self-associate; a conclusion supported by *in vitro* cross-linking (see section 2.3.2)

Like cdc34Δ185, cdc34M could only complement for the *cdc34* ts mutation indicating that it too must interact with the ts polypeptide to restore CDC34 function. Through such an interaction, the ts polypeptide would provide the interacting cdc34 ts/cdc34M complex with one copy of the catalytic domain insertion. Based on this premise, the inability of cdc34M to complement the *cdc34* disruption mutant would result from the absence of the catalytic domain insertion between interacting molecules of cdc34M. This suggests that CDC34 function requires that at least one copy of this insertion be present when molecules of CDC34 interact. As yet, such conclusions remain speculative and a definitive role for the catalytic domain insertion in defining CDC34 function remains to be determined.

As shown above and in Chapter 2, deletion of residues from the catalytic or the tail domain of CDC34 affects its cell cycle function. The experiments described below were carried out to identify if any additional affects could be observed when simultaneous deletions within the catalytic and tail domains were introduced into CDC34. To this end, a

set of plasmids carrying the coding sequences of various tail deletion derivatives of *cdc34M* were constructed (Figure 3.1). The ability of these derivatives to complement the *cdc34-2 ts* and the *cdc34* disruption mutants was assessed as described above for cdc34M.

Given that cdc34M could not complement a *cdc34* disruption mutation it was not surprising that the same observation was made for all of the cdc34M tail deletion derivatives (Figure 3.1). On the other hand, tail residues 171-218 of cdc34M were found to be required for complementation of the *cdc34-2* ts mutation (Figure 3.1) as compared to tail residues 171-185 which were required by CDC34 (Figure 2.1). Thus, deletion of residues 103-114 from the catalytic domain extended the tail length required for complementation of the ts mutant by 33 residues.

The Glutathione S-transferase polypeptide (GST) was also fused to the amino termini of CDC34 and various cdc34M tail deletion derivatives (Figure 3.2). Plasmids carrying the coding sequences for these fusions were tested for their ability to complement the *cdc34-2* ts mutation as described above. Work done in this lab showed that fusion of either the myc or flu epitopes to the amino terminus of CDC34 had no affect on CDC34 function (T. Arnason, pers. com.). As such, it was not expected that amino terminal fusion of GST to CDC34 and various cdc34M tail deletion derivatives would alter their relative abilities to carry out CDC34 function. Not surprisingly then, GST fusions of CDC34, cdc34MΔ_{244}, cdc34MΔ_{231}, and cdc34MΔ_{218}, restored full CDC34 function to the ts mutant while a GST fusion of cdc34MΔ_{209} was unable to so (Figure 3.2).

Remarkably, neither the GST-cdc34M nor the GST-cdc34MΔ_{265} fusions could complement for the ts mutation (Figure 3.2). Given that fusion of GST to cdc34MΔ_{244}, cdc34MΔ_{231}, and cdc34MΔ_{218}, had no affect on their *in vivo* function it is unlikely that self-association of GST or an unproductive interaction between GST and the ts polypeptide could explain the inability of GST-cdc34M and GST-cdc34MΔ_{265} to complement. Both GST-cdc34M and GST-cdc34MΔ_{265} differ from these other fusions in that they possess the polyacidic stretch of the tail domain. These observations identify a genetic interaction between GST and the polyacidic region of the tail which inhibits the ability of both GST-cdc34M and GST-cdc34MΔ_{265} to complement the ts mutation.

The GST-CDC34 fusion also possesses both GST and the polyacidic region of the tail domain. In contrast to GST-cdc34M though, GST-CDC34 retained its ability to complement the ts mutation. This indicated that the presence of the catalytic domain insertion within GST-CDC34 blocked the genetic interaction between GST and the polyacidic stretch of the tail. The manner in which the polypeptide insertion functions to block the inhibitory affect mediated by GST and the polyacidic region of the tail remains to be determined.

Taken together these complementation studies show that the catalytic domain insertion plays a key role in the *in vivo* function of CDC34. Deletion of this insert from CDC34 was also shown to alter properties associated with the tail domain. These alterations included the requirement of an additional 33 residues of the tail to restore CDC34 function to the *cdc34-2* ts mutant, and the inability of GST-cdc34M to functionally complement the ts mutant resulting from the genetic interaction between GST and the polyacidic region of the tail domain.

3.3.2. Deletion of residues 103-114 alters the *in vitro* activity of CDC34. Previous studies have shown that CDC34 is able to autoubiquitinate itself *in vitro* assembling K48 linked multiUb chains onto one or more of four K residues found within its tail domain (Banerjee *et al.*, 1993). Under the conditions used here (see section 3.2.4), CDC34 was also found to autoubiquitinate itself producing conjugates that included up to four Ubs (Figure 3.3, E2-Ub$_n$). These conjugates have been previously identified as consisting primarily of K48 linked multiUb chains rather than multiple Ubs conjugated to multiple K residues within CDC34 (Banerjee *et al.*, 1993). Also produced by CDC34 in these reactions were free di and triubiquitin chains (Figure 3.3, Ub$_2$ and Ub$_3$). *In vitro* reactions were used to determine how autoubiquitination and the synthesis of free Ub chains by CDC34 would be affected by deletion of the catalytic domain insertion, deletions of the tail domain, or simultaneous deletions within both domains.

An initial set of reactions was used to assess the affect of deleting successively larger portions of the CDC34 tail domain on these *in vitro* activities. The CDC34 tail deletion derivatives used were identical to those described in section 2.3.2. As seen in Figure 3.3, the autoubiquitination activity of CDC34 was virtually eliminated in reactions employing these derivatives. This result was not surprising as none of the CDC34 tail deletion derivatives contained the principal sites of CDC34 autoubiquitination. These sites reside at the carboxy terminus of the CDC34 tail domain and include lysine residues 273, 277, 293, and 294 (Banerjee *et al.*, 1993). In spite of this, a limited amount of autoubiquitination was observed identifying at least one minor site of ubiquitination within the first 265 residues of CDC34. Each of the tail deletion derivatives also synthesized free Ub$_2$ and Ub$_3$ to the same level as CDC34 (Figure 3.3). Thus, deletion of the tail from CDC34 had no affect on the synthesis of free chains.

The ability of cdc34M and its various tail deletion derivatives to carry out the autoubiquitination and free chain activities of CDC34 was also assessed. In these reactions each cdc34M derivative was present at an equivalent concentration to that employed for the various CDC34 derivatives. The *in vitro* activities of these derivatives showed that cdc34M differed from CDC34 in several interesting ways. First, cdc34M was able to conjugate at

least seven Ubs to itself as compared to four Ubs conjugated to CDC34 (Figure 3.4). The amount of Ub used by cdc34M in the autoubiquitination reaction was also six times greater then that observed for CDC34 (results not shown). Therefore, the autoubiquitination activity of cdc34M was found to be hyperactive in relation to that of CDC34.

Second, in spite of the fact that the cdc34M tail deletion derivatives lacked the principal sites of CDC34 autoubiquitination identified above, each derivative was able to at least auto-monoubiquitinate itself (Figure 3.4). Therefore, these derivatives must employ an alternate site(s) of ubiquitination from those found at the carboxy terminus of the tail .

Third, the autoubiquitination activity of cdc34MΔ_{265} also resulted in the conjugation of multiple Ubs to itself, albeit at a significantly lesser level than observed for cdc34M. As mentioned in the previous section, cdc34MΔ_{265} differs from the other cdc34M derivatives in that it possesses the polyacidic region of the tail. Thus, the auto-multiubiquitination activity of cdc34MΔ_{265} is dependent upon the polyacidic region of the tail domain.

Fourth, cdc34M also synthesized free Ub$_2$ and Ub$_3$ to similar levels as CDC34 (Figure 3.4). As seen in Figure 3.3 each of the CDC34 tail deletion derivatives also synthesized these free Ub chains to similar levels as CDC34. On the other hand, specific tail deletion derivatives of cdc34M showed reduced levels of Ub$_2$ and Ub$_3$ synthesis (Figure 3.4). In particular, the levels to which these chains were synthesized decreased as the tail was shortened from cdc34MΔ_{244} to cdc34MΔ_{209}. Thus, unlike CDC34, the synthesis of free multiUb chains by cdc34M was dependent upon the tail domain.

The results of these *in vitro* ubiquitination reactions demonstrated that deletion of residues 103-114 from CDC34's catalytic domain led to distinct *in vitro* activities. In particular, the activity of cdc34M differed from CDC34 in that: 1) cdc34M showed hyperactivity in the autoubiquitination reaction, 2) cdc34M tail deletions were found to use an alternate ubiquitination site(s) from those identified for CDC34, 3) multiubiquitination of cdc34MΔ_{265} at this alternate site(s) required the polyacidic region of the tail, and 4) synthesis of free multiUb chains by cdc34M was tail dependent. Points 3 and 4 also showed that deleting the catalytic domain insertion alters the *in vitro* properties associated with the tail domain.

3.3.3. The cell cycle function of the chimeric E2, RC requires a distinct region of the tail domain from that utilized by either CDC34 or cdc34M.

Deleting the catalytic domain insertion from CDC34 alters the *in vivo* properties associated with the tail domain. For example, an additional 33 residues of the tail domain was shown to be required for complementation of the ts mutation (Figure 3.1). Thus, the tail domain exhibited distinct functional properties depending upon whether it was fused to the CDC34 or the cdc34M catalytic domain.

In other studies, the ability of a fusion protein consisting of the RAD6 catalytic domain and the CDC34 tail domain (referred to as RC here) to carry out CDC34 function *in vivo* was assessed. It was found that RC could complement for both the *cdc34-2* ts and the *cdc34* disruption mutations (Kolman *et al.*, 1992; Silver *et al.*, 1992). To identify whether fusion of the tail to the RAD6 catalytic domain also altered the tail length required for complementation of these cdc34 mutations a set of plasmids carrying the coding sequences for various RC tail deletion derivatives was constructed (see section 3.2.1). The ability of the RC tail deletions to complement the *cdc34* ts and disruption mutations was tested as described in section 3.3.1 for cdc34M.

As seen in Figure 3.5, tail residues 171-209 were required by RC to restore full CDC34 function to the ts mutant, while an additional 9 residues of the tail (171-218) restored function to the disruption mutant. Comparing these results to those previously made for CDC34 showed that by replacing the CDC34 catalytic domain with that of RAD6 the tail length required for complementation of the ts mutant increased by 24 residues while an additional 9 residues were required for complementation of the disruption (Figure 3.5). On the other hand, RC was more effective at complementing *cdc34* mutations by comparison to cdc34M. While cdc34M could not complement for the disruption mutation RC readily did so. Furthermore, complementation of the ts mutant by RC required 9 fewer residues of the tail domain as compared to the tail length required by cdc34M (Figure 3.5). Thus, fusion of the CDC34 tail domain to the RAD6 catalytic domain resulted in distinct tail length requirements from those observed for both CDC34 and cdc34M with respect to their abilities to carry out CDC34 function.

3.3.4. RC's cell cycle function is dependent upon residue D88 of the RAD6 catalytic domain. The primary structure of the cdc34M catalytic domain is similar to that of other E2s in that it lacks the catalytic domain insertion found in CDC34. In this respect, cdc34M and RC show a greater degree of homology then do CDC34 and RC. As such, it was surprising to find that RC was more competent at carrying out CDC34 function *in vivo* then cdc34M (Figure 3.5). This indicated that some residue(s) present in the RAD6 catalytic domain, but absent in the cdc34M catalytic domain was responsible for the functional differences between RC and cdc34M.

By comparing primary E2 sequences, Liu *et al.* (1995) identified a number of unique amino acid residues within the catalytic domain of CDC34 other than the polypeptide insertion. In particular, residue S97 of CDC34 was shown to be an D at the corresponding position of most other E2s including RAD6 (D90 of RAD6). Liu *et al.* showed that the introduction of the amino acid substitution S97D into CDC34 disabled its ability to function *in vivo*. On the other hand, simultaneous deletion of the catalytic domain insertion and

63

introduction of the S97D substitution (cdc34MD97) generated a derivative shown to be fully competent in carrying out CDC34 function *in vivo*.

RC and cdc34MD97 are quite similar in that both lack the catalytic domain insertion of CDC34 and both carry the critical D97 residue at corresponding positions in their primary sequence. Therefore, it was possible that the cell cycle function of RC was dependent upon the presence of residue D90. To test this, the amino acid substitution D90S was introduced into the RAD6 catalytic domain of RC (RCS90). As seen in Figure 3.6 this amino acid substitution virtually eliminated the ability of RCS90 to functionally complement the *cdc34-2* ts mutant. Therefore, residue D90 does play a critical role in defining the cell cycle function of RC.

While the polypeptide insertion and residue S97 of CDC34 are critical for the cell cycle function associated with its catalytic domain, are these the sole functional determinants within this domain. If they were it would be expected that introducing these elements into the RC polypeptide would make it functionally equivalent to CDC34 in every respect. Instead, introduction of the CDC34 catalytic domain insertion into the corresponding position of RC generated the derivative RP which was unable to functionally complement the *cdc34-2* ts mutant (Figure 3.6). Furthermore, introduction of the amino acid substitution D90S into RP produced the derivative RPS90 which also could not functionally complement for the *cdc34-2* ts mutant (Figure 3.6). Therefore, additional residues are required in combination with residue S97 and the polypeptide insertion to define the cell cycle function provided by the catalytic domain of CDC34.

3.3.5. RC is able to autoubiquitinate itself *in vitro*. Attempts in our lab to express significant amounts of recombinant RAD6 or RC from *E. coli* proved to be unsuccessful. Given that other yeast E2s, including CDC34, UBC1, and UBC4 could be readily overexpressed in *E. coli* (section 2.3.2; Hodgins *et al.*, 1996; Gwozd *et al.*, 1994) it was surprising to find that no RAD6 derivative could be overexpressed using this system. The lack of purified RC also did not afford us the opportunity to compare its *in vitro* activity to that of CDC34 and cdc34M. A means by which this problem could be remedied was presented in a publication by Chen and Inouye (1994).

Chen and Inouye observed that in *E. coli* the presence of the arginine codons AGA and AGG within the first 25 codons of a transcript severely inhibited the level of protein translation from that transcript. Based on this study, it was likely that poor expression of RAD6 in *E. coli* resulted from the presence of three AGA codons and one AGG codon within its first eleven codons (Figure 3.7). When these sequences were altered to either the CGA or the CGG arginine codons recombinant RC was readily overexpressed (Figure 3.7) and purified.

Purified RC used in an ubiquitination reaction was shown to autoubiquitinate itself (Figure 8, E2-Ub_n) and could also synthesize free Ub_2. Like cdc34M, RC was found to autoubiquitinate itself to a greater degree then CDC34, and it was also found to generate free Ub_2 to a lesser degree then CDC34 (Figure 8). Unlike cdc34M, most of RC's autoubiquitination activity resulted in the formation of the monoubiquitinated conjugate. It remains to be determined how the introduction of various amino acid substitutions into CDC34 (e.g. CDC34D97), cdc34M (e.g. cdc34MD97), and RC (e.g. RCS90) affect these *in vitro* activities.

3.4. Discussion

Through the use of deletion analysis and amino acid substitutions key elements within the catalytic and tail domains of CDC34 which are responsible for its cell cycle function have been identified. Deletion analysis has shown that a small portion of the tail domain is required for this function. Furthermore, this same region of the tail is required for CDC34 self-association. These results indicated that in order for CDC34 to carry out its cell cycle function it must self-associate (Ptak *et. al.*, 1994).

Studies carried out on the catalytic domain have shown that the polypeptide insertion, as well as residues S97, and S139 are also important in defining the cell cycle function of CDC34 (Liu *et al.*, 1996; Pitluk *et al.*, 1995). The definitive role that these catalytic domain determinants play in defining CDC34 function remains to be elucidated. It is thought that these elements function to regulate CDC34 activity. This conclusion may be drawn based on the following evidence.

1) Using the RAD6 crystal structure (Cook *et al.*, 1992) as a model for the CDC34 catalytic domain, each of these elements is shown to reside near the active site cysteine (Figure 3.9). In particular, the side chains of both residues S97, and S139 line a groove in which the active site cysteine sits. The polypeptide insertion is also expected to sit near or possibly over this groove based on its location within the structure. As these elements reside near the active site cysteine they may function to limit access to this site by either, a CDC34 target, or a trans-acting factor such as an E3 (Pitluk *et al.*, 1995).

2) Deletion of the catalytic domain insertion or the simultaneous introduction of the amino acid substitutions E109A, D111A, and E113A into the catalytic domain insertion results in CDC34 hyper-autoubiquitination *in vitro* (Figure 3.4; Pitluk *et al.*, 1995). These modifications effectively remove a barrier to autoubiquitination increasing the degree to which Ub is utilized in this process. It is possible that the catalytic domain insertion limits the access of target lysines to the active site thereby limiting the transfer of Ub to the

carboxy terminus of the tail domain or to the growing multiUb chain. An alternate possibility is that the insertion limits the rate at which Ub is transferred from the active site to these target lysines.

It is interesting to note that Liu *et al.* (1995) showed that the simultaneous deletion of the catalytic domain insertion and introduction of the S97D (cdc34MD97), but not the S97A amino acid substitution restored full CDC34 function to a *cdc34* disruption mutant. On the other hand, the amino acid substitutions E109A, D111A, and E113A eliminated the ability of CDC34 to function *in vivo* (Pitluk *et al.*, 1995). The residues E109 within full length CDC34, and D97 within the catalytic domain deletion derivative are found at equivalent positions with respect to the carboxy terminus of CDC34's catalytic domain. This suggests that CDC34 function may be controlled by the presence of an acidic residue at this position.

Experiments are under way to provide some support for this hypothesis. First, introducing the single amino acid substitution E109A should be sufficient to elicit the same *in vivo* and *in vitro* affects observed for the CDC34 derivative carrying the three substitutions E109A, D111A, and E113A. Second, by reintroducing this acidic residue the derivative cdc34MD97 would be expected to autoubiquitinate itself at a level similar to that observed for CDC34, rather then that observed for cdc34M.

As CDC34 function is thought to be mediated through its self-association it is likely that the catalytic domain insertion also elicits its effect when molecules of CDC34 interact. The observation that cdc34M complements a *cdc34* ts mutant but not a *cdc34* disruption mutant suggests that it complements the ts mutation by interacting with the ts polypeptide. Through this complex, cdc34M may function to stabilize the ts polypeptide while the ts polypeptide provides one copy of the catalytic domain insert. Within the disruption strain though, interacting molecules of cdc34M provide no copies of the polypeptide insert perhaps accounting for the inability of cdc34M to function within this strain.

While the ability of cdc34M polypeptides to self-associate remains speculative such a model may explain some of the other affects associated with the deletion of the catalytic domain insertion. Included among these affects was the ability of cdc34M to use at least one alternate lysine residue as a target site for autoubiquitination (Figure 3.4). Preliminary studies have indicated that this alternate lysine(s) resides within the catalytic domain of CDC34 (results not shown). Two examples of E2 autoubiquitination have also shown that these processes may occur in either an intramolecular (Hodgins *et al.*, 1996), or an intermolecular fashion (Gwozd *et al.*, 1995). Based on the ability of CDC34 to self-associate and the positions of lysine residues within the CDC34 catalytic domain (Figure 3.10) it seems likely that the alternate site(s) will be ubiquitinated in an intermolecular

fashion. Verification of this hypothesis will require the determination of the exact lysine residue(s) which functions as this alternate autoubiquitination site.

The tail domain of cdc34M also exhibited some unique characteristics not observed in CDC34. By comparison to CDC34, cdc34M required significantly longer portions of the tail domain to complement the *cdc34* ts mutant (Figure 3.1) or to synthesize free Ub_2 and Ub_3 *in vitro* (Figure 3.4). In chapter 2 (Figure 2.7) a model was proposed to account for CDC34 self-association and how it may lead to the synthesis of multiUb chains. Another possible role for the catalytic domain insertion is that it, along with the tail domain function to stabilize CDC34 self-association. In the absence of the insertion a larger portion of the tail could be employed to make additional contacts thereby stabilizing cdc34M self-association leading to the synthesis of free multiUb chains or the interaction between the cdc34M and cdc34 ts polypeptides leading to complementation of the ts mutation. As yet, the affect of deleting the catalytic domain insertion on the self-associative properties of CDC34 has not been determined directly.

The first definitive function for the polyacidic stretch of the tail domain was also identified in this work. The multi-autoubiquitination of $cdc34M\Delta_{265}$ was found to be dependent upon this region of the tail domain. It remains to be seen whether or not this multiubiquitination reflects the assembly of a multiUb chain or simply the conjugation of multiple Ubs to distinct lysine residues. It also remains to be determined whether this portion of the tail is also involved in the multiubiquitination of CDC34 and cdc34M at lysine residue found at the carboxy terminus of the tail.

Within the GST-cdc34M fusion a genetic interaction between the polyacidic region of the tail and GST was observed to inhibit the ability of cdc34M to complement the ts mutant (Figure 3.2). As this affect is not observed for GST-CDC34 the presence of the catalytic domain insertion functions to block this genetic interaction The simplest explanation for these observations is that cdc34M function is inhibited through a direct interaction between GST and the polyacidic region. In such a model, the catalytic domain insertion would provide a steric block or alternatively would directly interact with the polyacidic region thereby blocking the interaction between GST and the polyacidic region. If true, it might be expected that the overexpression of the tail domain alone could compete for this interaction thereby restoring cdc34M function to the ts mutant.

Previous studies have shown that the RC chimera can carry out CDC34 function *in vivo* (Kolman *et al.*, 1992; Silver *et al.*, 1992). Like cdc34M, RC lacks the catalytic domain insertion found in CDC34. Furthermore, introduction of the amino acid substitution S97D into cdc34M restored full CDC34 function to this derivative. This suggested that the presence of residue D90 was key in allowing RC to carry out CDC34

function. This was shown to be correct as the D90S amino acid substitution introduced into RC virtually eliminated its ability to complement the *cdc34* ts mutant (Figure 3.6).

The presence of the RAD6 catalytic domain within the RC chimera does allow it to carry out CDC34 function but not to the same degree as CDC34 itself or as cdc34MD97. In particular, RC must be expressed at high levels to fully complement *cdc34* mutations. It was also shown that by comparison to CDC34, RC complementation requires a greater portion of the tail domain (Figure 3.5). Furthermore, introduction of the catalytic domain insertion along with residue S97 into the RAD6 catalytic domain of RC (RPS90) generated an E2 unable to complement the *cdc34* ts mutation (Figure 3.6). These observation show that additional elements apart from the insertion and S97 are required for full CDC34 function.

| | Viability | |
Derivatives	ts	disruption
CDC34	+	+
cdc34M	+	—
cdc34MΔ₂₆₅	+	—
cdc34MΔ₂₄₄	+	—
cdc34MΔ₂₃₁	+	—
cdc34MΔ₂₁₈	+	—
cdc34MΔ₂₀₉	—	—
cdc34MΔ₂₀₀	—	—
cdc34MΔ₁₈₅	—	—

Figure 3.1. **Functional complementation of** cdc34 **mutants by various CDC34 deletion derivatives.** The catalytic domain of CDC34 (shown in gray) includes a polypeptide insertion (residues 103-114, shown in black) not found in most E2s. The tail domain is shown in white and contains a highly acidic polypeptide stretch (residues 244-265, shown in black with white lines). Each derivative was tested for its ability to complement either a cdc34 ts or disruption mutation under selective conditions (see results section). Viability was scored based on colony size and plating efficiency by comparison to full length CDC34. A positive score indicates identical growth while a negative score indicates the absence of growth.
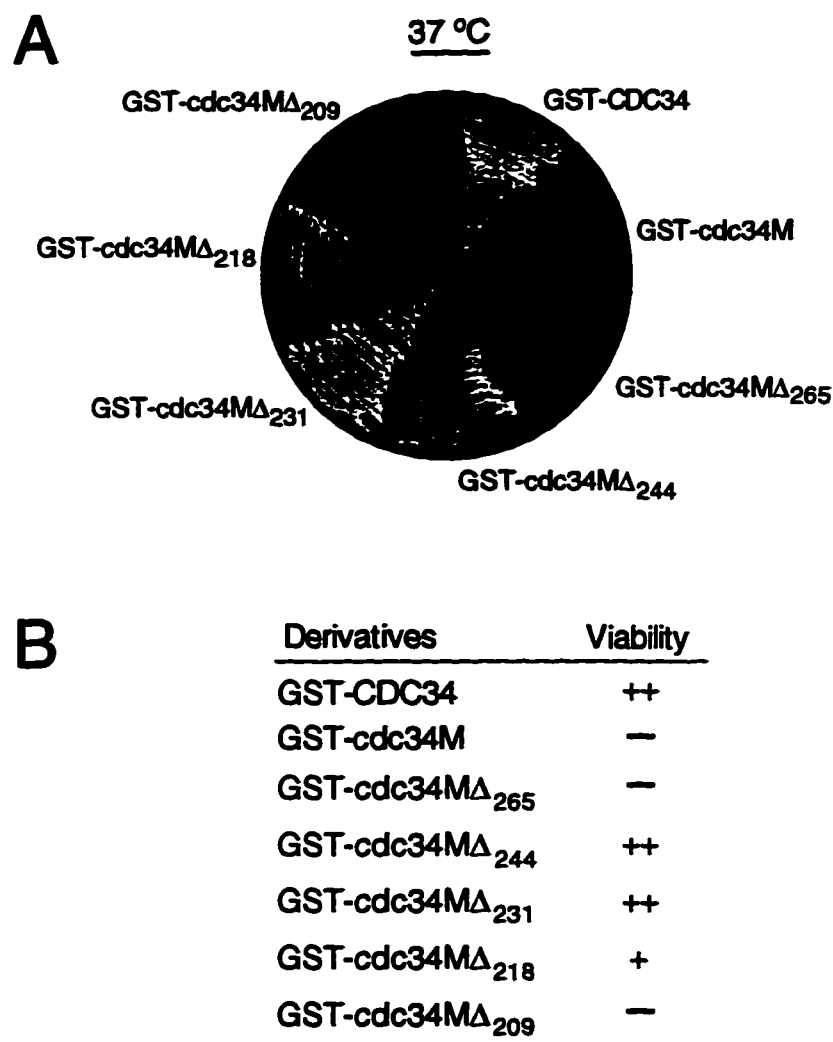
Figure 3.2. **Functional complementation of the** *cdc34* **ts mutant by various GST-CDC34 fusion derivatives.** *5' GST* fusions of *CDC34* and various tail deletion derivatives of *cdc34M* were tested for their ability to complement a *cdc34* ts mutant at the non-permissive temperature of 37 °C (Part A). Viability was scored based on colony size and plating efficiency by comparison to full length *GST-CDC34*. A score of ++ indicates identical growth while scores of + and - indicate the presence of fewer and smaller colonies or the absence of growth respectively (Part B).
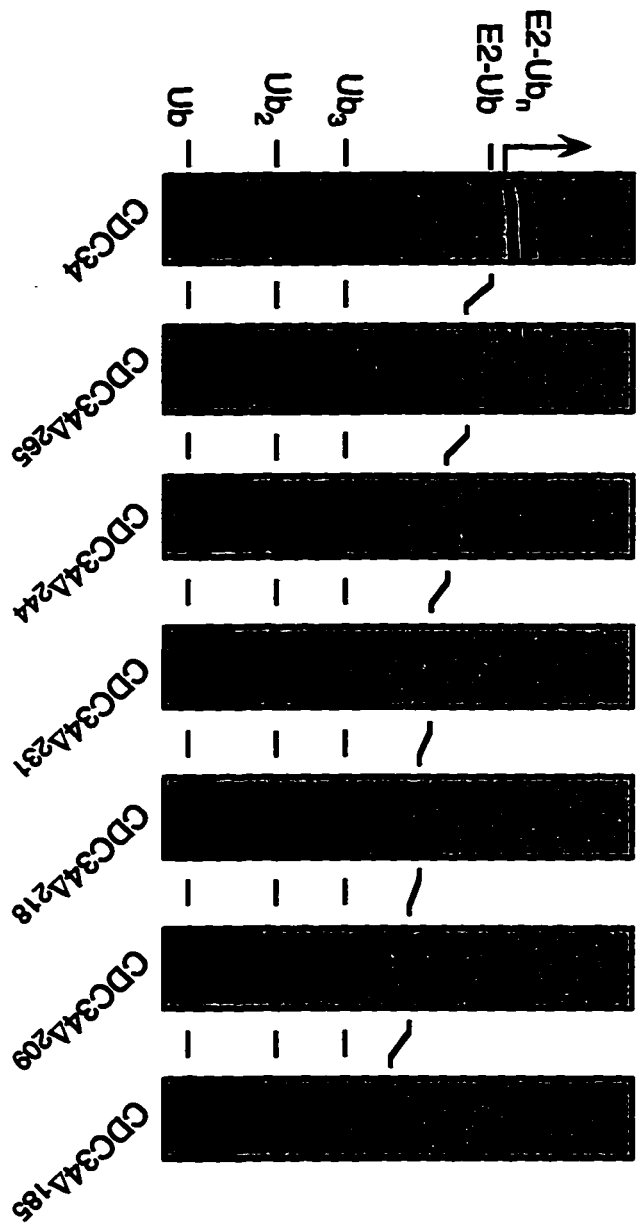
Figure 3.3. *In vitro* **ubiquitination reactions employing various CDC34 tail deletion derivatives.** Purified 35S-Ub was incubated along with E1 and either CDC34 or one of the CDC34 tail deletion derivatives. Reactions were analyzed using SDS-PAGE followed by autoradiography. Bands corresponding to free Ub, free multiUb chains (Ub_2, Ub_3), and the monoUb conjugate of each derivative (E2-Ub) are indicated. Also indicated are the multiUb conjugates of CDC34 (E2-Ub_n, arrow).
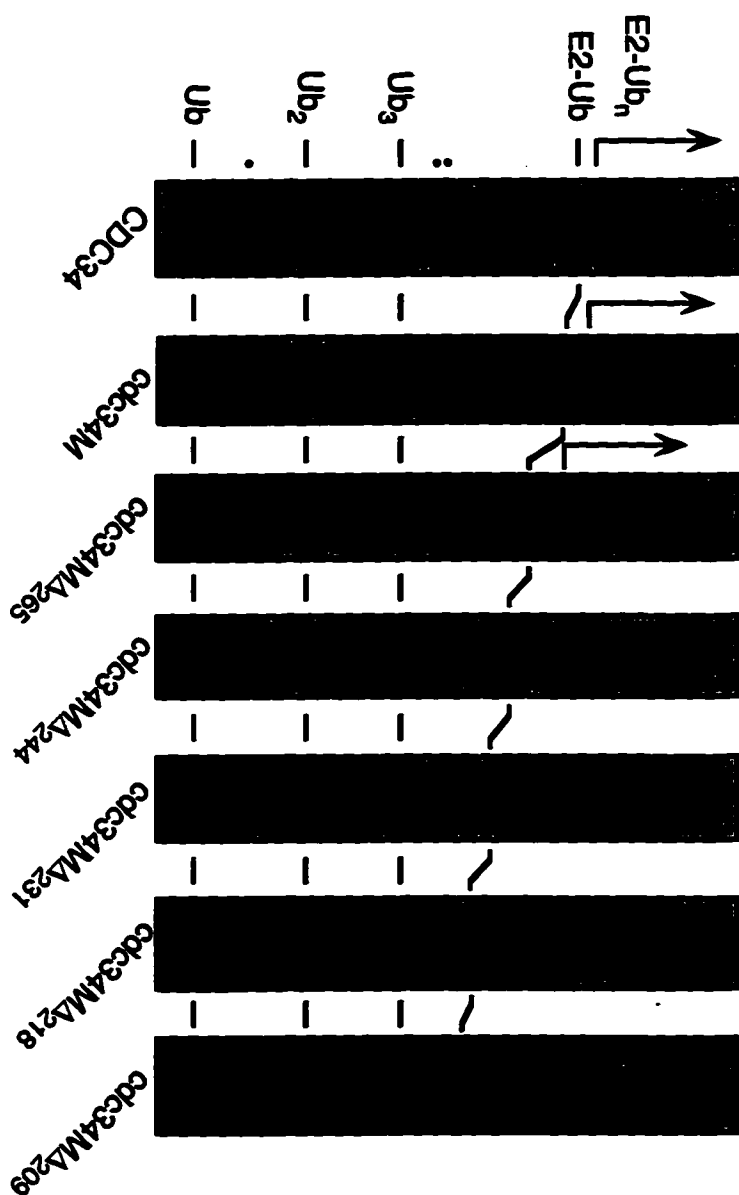
Figure 3.4. *In vitro* **ubiquitination reactions employing various cdc34M tail deletion derivatives.** Purified ^{35}S-Ub was incubated along with E1 and either CDC34, cdc34M, or one of the cdc34M tail deletion derivatives. Reactions were analyzed using SDS-PAGE followed by autoradiography. Bands corresponding to free Ub, free multiUb chains (Ub_2, Ub_3), and monoUb conjugate of each derivative (E2-Ub) are identified. Also identified are the multiUb conjugates of CDC34, cdc34M, and cdc34MΔ_{265} (E2-Ub$_n$, arrow). Dots identify contaminants present in the particular ^{35}S-Ub preparation employed for these reactions.

Derivative	Tail residues required for viability	
	ts	disruption
CDC34	171-185	171-209
cdc34M	171-218	—
RC	171-209	171-218

Figure 3.5. **Tail length required for complementaion of** *cdc34* **mutations is dependent upon the catalytic domain.** Portions of CDC34's tail domain required to complement the *cdc34* ts and disruption mutants when found in the context of either the wild type (Ptak et al., 1994) or the cdc34M (Figure 3.1) catalytic domains have been determined and are summarized here. An analogous set of tail deletions were made within the context of the RAD6 catlytic domain (RC). Residue boundaries represent the minimum tail length required to functionally complement the *cdc34* ts and disruption mutants.
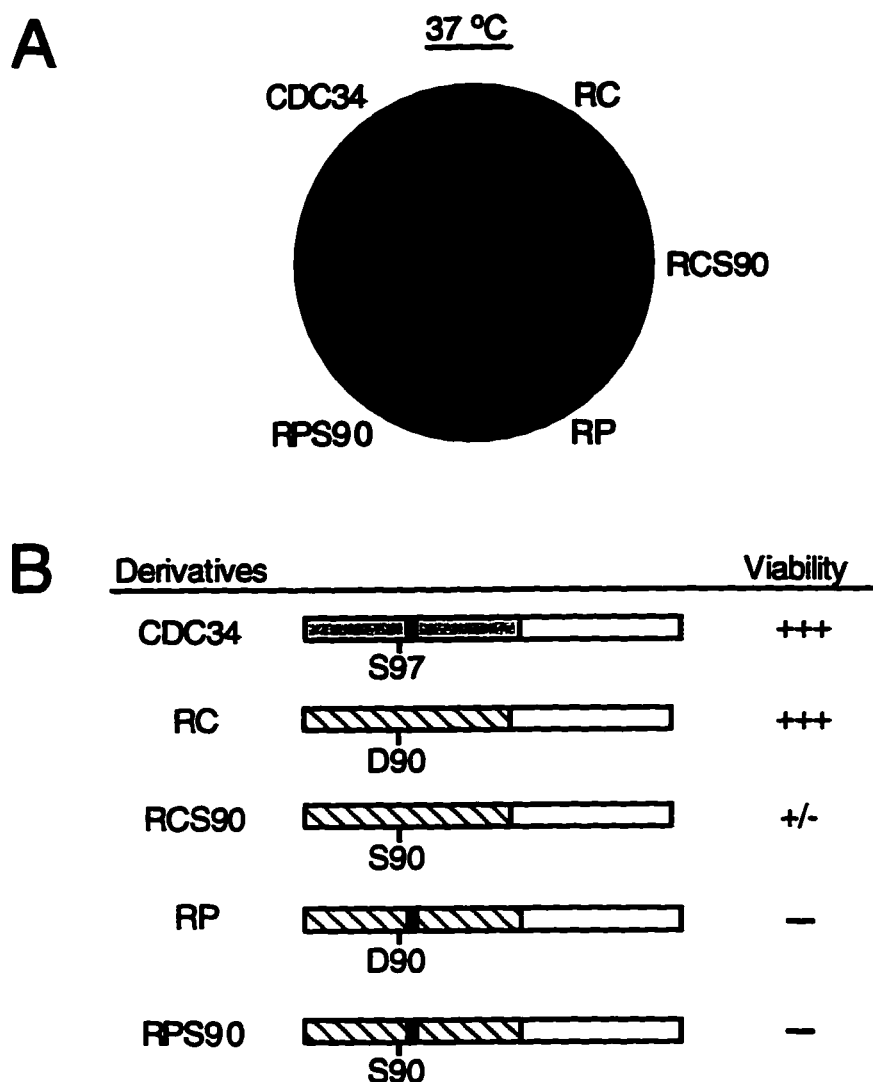
Figure 3.6. **Residue D90 of RAD6 is required for complementation of the** *cdc34* **ts mutant by RC.** Primary structures of CDC34 and various RAD6-CDC34 chimeras are shown (PartB). The catalytic domains of CDC34 and RAD6 are shown as gray and striped respectively. The CDC34 catalytic domain insertion is shown in black while CDC34's tail domain is shown in white. The amino acid substitution D90S was intoduced into the RAD6 catalytic domain of specific derivatives. The analogous position S97 in the catalytic domain of CDC34 has also been identified. The ability of each derivative to complement the *cdc34-2* ts mutant at the non-permissive temperature of 37 °C was tested (Part A). Viability was scored based on colony size and plating efficiency relative to that seen for CDC34. A score of +++ indicates identical growth while scores of +/- and - indicated the presence of fewer and smaller colonies or the absence of growth respectively (Part B).

74

R codons: **AGA**   **CGA**
                  AGG   **CGG**

Figure 3.7. Overexpression of the RC polypeptide. The coding sequence of the RAD6-CDC34 chimera *RC* was altered such that four of the first five R codons were altered from either AGA or AGG to either CGA or CGG. The ability of plasmids carrying these two *RC* coding sequences to support the overexpression of RC in *E. coli* was tested. Shown is a coomassie stained gel over which crude lysates of *E. coli* harboring these plasmids were run. The band corresponding to RC is indicated.
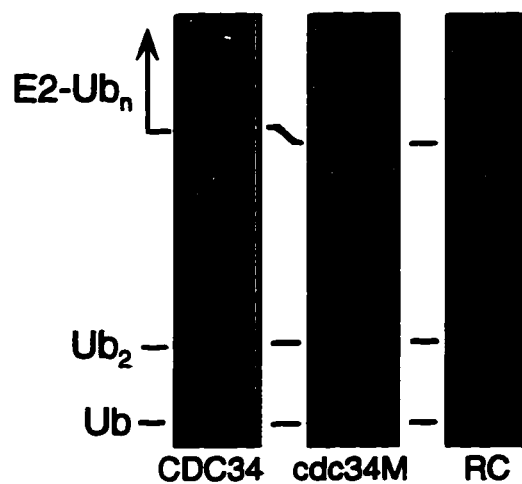
Figure 3.8. **RC is capable of multi-autoubiquitination** *in vitro*. Purified ^{35}S-Ub was incubated with E1 and either CDC34, cdc34M, or RC. Reactions were analyzed using SDS-PAGE followed by autoradiography. Bands corresponding to free Ub, and Ub_2 as well as the monoUb and multiUb conjugates of CDC34, cdc34M, and RC ($E2\text{-}Ub_n$, arrow) are indicated.
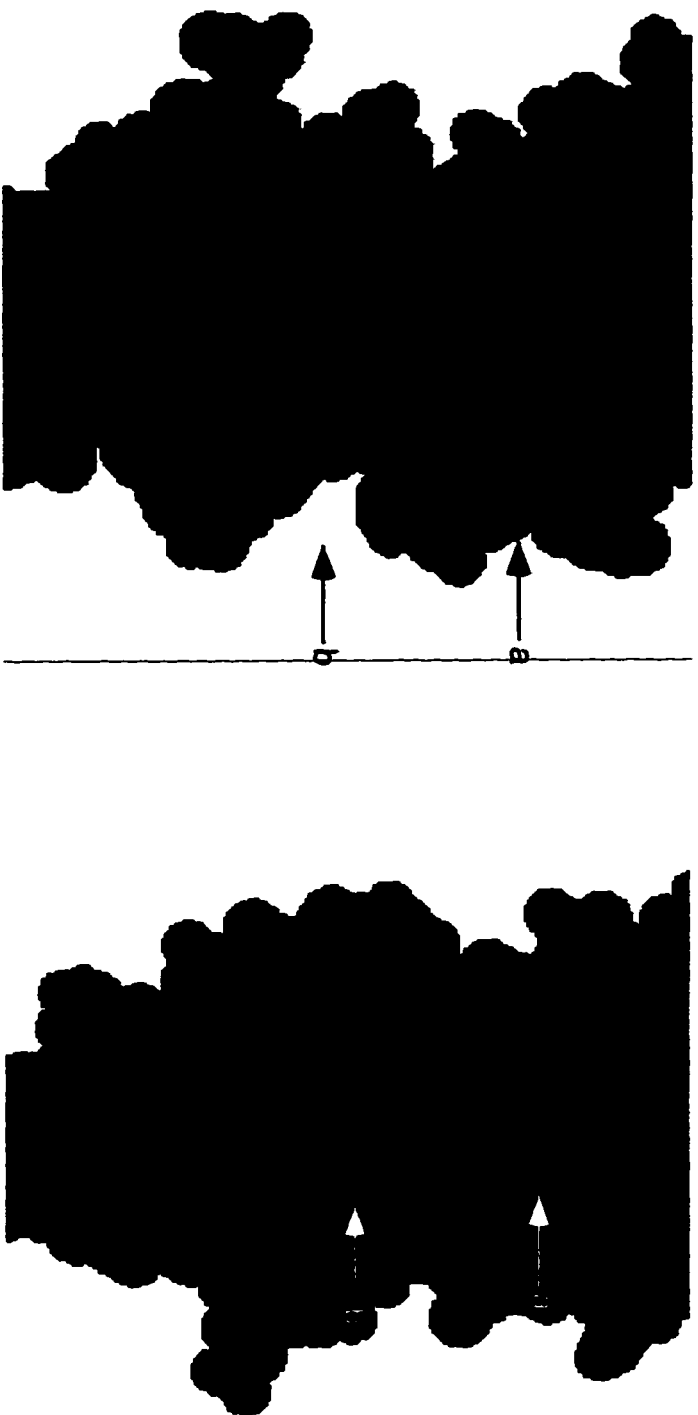
Figure 3.9. **Key residues within the catalytic domain of CDC34.** The crystal structure of the *Arabidopsis thaliana* RAD6 homolog (Cook *et al.*, 1993) is used here as a structural model for the CDC34 catalytic domain. Two distinct views of this structure are shown. Highlighted are residues within the CDC34 catalytic domain that play a key role in CDC34 function. Included are the active site cysteine (yellow), S97 (purple), and S139 (green) which is the first residue of the SPANVEAA loop (red). The two residues (pink) between which the CDC34 catalytic domain insertion resides (arrow a) are also indicated. Arrow b identifies the apparent active site cleft.
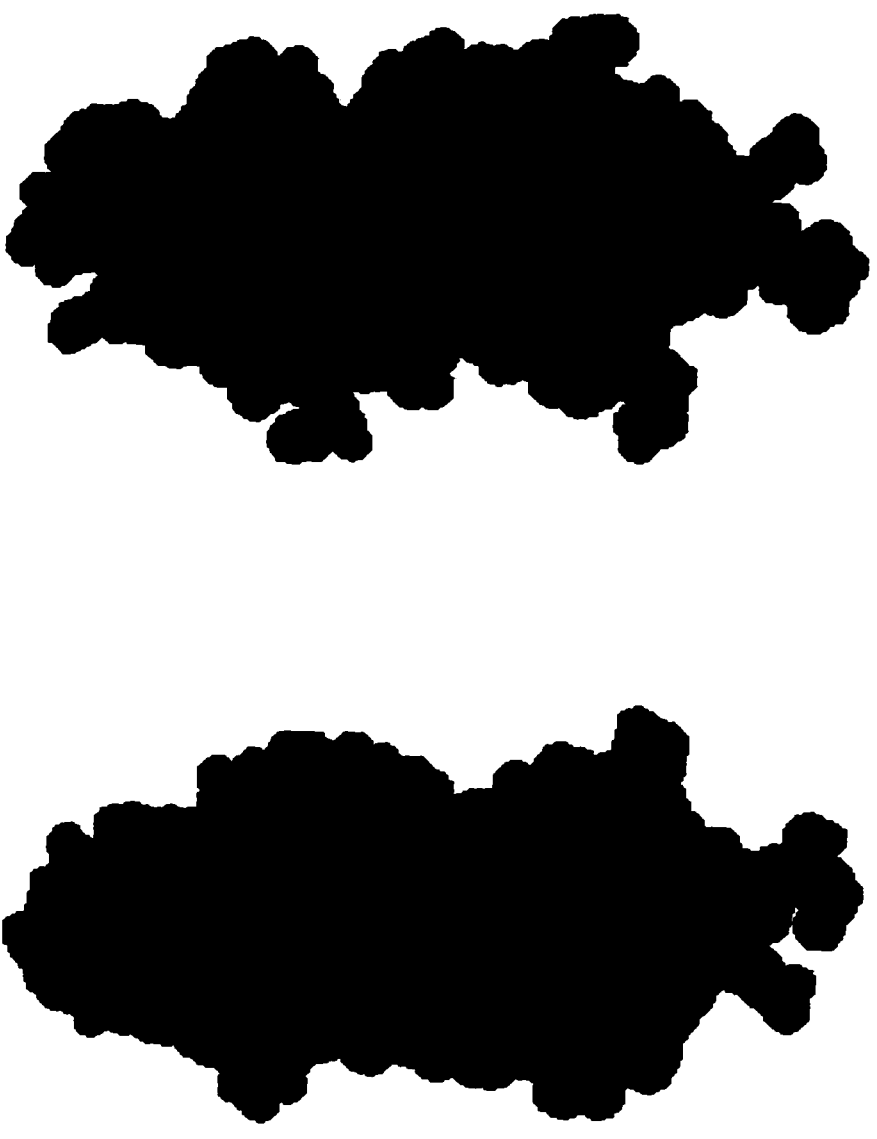
Figure 3.10. **Lysine residues within the catalytic domain of CDC34.** The crystal structure of the *Arabidopsis thaliana* RAD6 homolog (Cook *et al.*, 1993) is used here as a structural model for the CDC34 catalytic domain. Two distinct views of this structure related by a 180° rotation are shown. Highlighted are the positions corresponding to lysine residues within the CDC34 catalytic domain (red). Also shown is the active site cysteine (yellow).

3.5 Bibliography

Banerjee, A., Gregori, L., Xu, Y., and Chau, V. (1993). The bacterially expressed yeast CDC34 geneproduct can undergo autoubiquitination to form a multiubiquitin chain-linked protein. *J. Biol. Chem.* **268**, 1993.

Chen, G-F. T., and Inouye, M. (1994). Role of the AGA/AGG codons, the rarest codons in global gene expression in *Escherichia coli. Genes & Dev.* **8**, 2641-2652.

Cook, W. J., Jeffery, L. C., Sullivan, M.L., and Vierstra, R. D. (1992). Three-dimensional strycture of a ubiquitin-conjugating enzyme (E2). *J. Biol. Chem.* **21**, 15116-15121.

Gwozd, C. S., Arnason, T. G., Cook, W. J., Chau, V., and Ellison, M. J. (1994). The yeast UBC4 ubiquitin conjugating enzyme monoubiquitinates itself in vivo: evidence for an E2-E2 homointeraction. *Biochemistry* **34**, 6296-6302.

Hodgins, R., Gwozd, C., Arnason, T., Cummings, M., and Ellison, M.J. (1996). The tail of a ubiquitin conjugating enzyme redirects multi-ubiquitin chain synthesis from the lysine 48-linked configuration to a novel nonlysine-linked form. *J. Biol. Chem.* **46**, 28766-28771.

Jungmann, J., Reins, H. A., Schobert, C., and Jentsch, S. (1993). Resistence to cadmium mediated by ubqiutin-dependent proteolysis. *Nature* **361**, 369-371.

Kolman, C. J., Toth, J., and Gonda, D. K. (1992). Identification of a portable determinant of cell cycle function within the carboxy-terminal domain of the yeast CDC34 (UBC3) ubiquitin conjugating enzyme. *EMBO J.* **11**, 3081-3090.

Liu, Y., Mathias, N., Steussy, N., and Goebl, M. G. (1995). Intragenic suppression among *CDC34 (UBC3)* mutations defines a class of ubiquitin-conjugating catalytic domains. *Mol. Cell. Biol.* **15**, 5635-5644.

Pitluk, Z. W., McDonough, M., Sangan, P., and Gonda, D.K. (1995). Novel *CDC34 (UBC3)* ubiquitin-conjugating enzyme mutants obtained by charge to alanine scanning mutagenesis. *Mol. Cell. Biol.* **15**, 1210-1219.

Ptak, C., Prendergast, J. A., Hodgins, R., Kay, C. M., Chau, V., and Ellison, M. J. (1994). Functional and physical characterization of the cell cycle ubqiutin-conjugating enzyme CDC34 (UBC3): Identification of a functional determinant within the tail that facilitates CDC34 self-association. *J. Biol. Chem.* **42**, 26539-26545.

Seufert, W., and Jentsch, S., (1990). Ubiquitin-conjuagting enzymes UBC4 and UBC5 mediate selective degradation of of short-lived and abnormal proteins. *EMBO J.* **9**, 543-550.

Seufert, W., McGrath J. P., and Jentsch, S. (1990). *UBC1* encodes a novel member of an essential subfamily of yeast ubiquitin-conjugating enzymes involved in protein degradation. *EMBO J.* **9**, 4535-4541.

Silver, E. T., Gwozd, T. J., Ptak, C., Goebl, M., and Ellison M. J. (1992). A chimeric ubiquitin conjugating enzyme that combines the cell cycle properties of CDC34 (UBC3) and the DNA repair properties of RAD6 (UBC2): implications for the structure, function, and evolution of the E2s. *EMBO J.* **11**, 3091-3098.

Tabor, S., and Richardson, C. C. (1985). A bacteriophage T7 RNA poymerase/promoter system for controlled exclusive expression of specific genes. *Proc. Natl. Acad. Sci. USA* **82**, 1074-1078.

Vassal, A., Boulet, A., Decoster, E., and Faye, G. (1992). QR18, a novel ubiquitin-conjugating enzyme in *Saccharomyces cerevisiae. Biochem. Biophys. Acta* **1132**, 211-213.

Chapter 4

The role of ubiquitin activating enzyme, E1 in the assembly of multiubiquitin chains conjugated to UBC1Δ.

4.1. Introduction

Protein ubiquitination proceeds through the linear transfer of Ub from E1 to E2 through a transthiolation reaction and then from E2 to the protein target. It is generally thought that *in vivo* an E3 is also required to facilitate the interaction between E2 and its target (Hershko *et al.*, 1983).

Ub itself is included among the known ubiquitination targets. *In vitro* studies have shown that the reiterative conjugation of Ub to Ub can lead to the synthesis of free multiUb chains (van Nocker and Vierstra, 1991; Chen and Pickart, 1990). Furthermore, these chains are competent substrates for E1 activation and as such may be transferred to an E2 (Chen and Pickart, 1990). Once linked to an E2 the chain may then be transferred either to Ub thereby extending the free multiUb chain or to another protein target. Free multiUb chains do occur *in vivo* suggesting that this manner of generating multiUb chains conjugated to a protein target is biologically relevant (Haldeman *et al.*, 1995; Spence *et al.*, 1995; van Nocker and Vierstra, 1993).

An alternative mechanism for the conjugation of a multiUb chain to a protein target involves two steps. In the first step, Ub becomes singly conjugated to the protein target. In the second step, the multiUb chain is assembled on the first Ub through subsequent conjugations of Ub to Ub. These processes have also been shown to require E3s (Johnson *et al.*, 1995; Johnson *et al.*, 1992; Chau *et al.*, 1989; Hough and Rechsteiner, 1986).

Previous *in vitro* studies have shown that UBC1Δ; a carboxy terminal deletion derivative of the yeast E2 UBC1, is able to autoubiquitinate itself generating a multiUb chain linked to its own K93 residue (Hodgins *et al.*, 1996). The work presented in this chapter shows that the assembly of multiUb chains conjugated to UBC1Δ also proceeds through two distinct steps in an E3 independent fashion.

Initially, the first Ub becomes conjugated to K93 of UBC1Δ through an intramolecular transfer from the active site cysteine to the ε-amino side chain of the lysine residue (Hodgins *et al.*, 1996). This monoubiquitinated version of UBC1Δ then becomes the substrate for the relatively rapid addition of subsequent Ubs to the growing conjugated chain (this work).

It has also been shown here that in order for chain elongation to proceed monoubiquitinated UBC1Δ must also function as a competent substrate for Ub transfer

from E1 to its own active site cysteine. As such, monoubiquitinated UBC1Δ also functions as the E2 responsible for chain elongation. Finally, the formation of a thiolester between monoubiquitinated UBC1Δ and Ub is also shown to be dependent upon the specific E1 used in the reaction.

4.2 Materials and Methods

4.2.1. Overexpression and purification of Ub and UBC1Δ from *E. coli*.

Gene cassettes coding for ubiquitin (Ub), the ubiquitin mutant UbR48, and UBC1Δ were previously cloned into a derivative of the *E. coli* overexpression plasmid pET3a (Hodgins *et al.*, 1996). The overexpression and purification protocols described are identical for Ub, UbR48 and UBC1Δ. Overexpression plasmids were co-transformed with the thermally induced T7 polymerase plasmid pGP1-2 into the *E. coli* strain BL21 (Tabor and Richardson, 1985). Single colonies from each transformation were used to inoculate LB liquid media supplemented with the antibiotics ampicillin (50 μg/ml) and kanamycin (75 μg/ml). Cultures were initially incubated overnight at 30 °C and subsequently diluted forty fold using fresh LB supplemented with ampicillin and kanamycin to a final volume of 100 ml. The diluted culture was then incubated at 30 °C to a final absorbance of 0.4 at 590 nm. Cells were then shifted to 42 °C for 1 hr followed by a final incubation at 37 °C for an additional 2 hr. Cells were then harvested by centrifugation, resuspended in 500 μl of lysis buffer (25% sucrose, 50 mM Tris-Cl (pH 8.0), 1 mM DTT), and lysed by the lysozyme method described previously (Gonda *et al.*, 1989). Cell lysates were then centrifuged at 40 000 rpm for 45 min. using a Beckman Ti70 rotor and the supernatants collected and frozen at -80 °C prior to further processing.

Overexpression of ^{35}S-labeled Ub and UbR48 follows the same basic protocol just described with the following changes. Once a culture reached an OD_{590} of 0.4 the cells were harvested by centrifugation and washed twice using M9 media supplemented with 1 mM MgSO$_4$, 0.1 mM CaCl$_2$, 12 mM glucose, and 18 μg/ml thiamine. After washing, the cells were resuspended in 100 ml of supplemented M9 that also contained ampicillin, kanamycin, and all amino acids (40 μg/ml) except for cysteine and methionine. The culture was then incubated an additional 1 hr at 30 °C, after which cells were induced at 42 °C for 20 min. Following induction, rifampicin was added to a final concentration of 200 μg/ml. and cultures incubated an additional 10 min at 42 °C. Cultures were then shifted to 37 °C for 1 hr after which *trans* -[^{35}S] methionine (ICN) was added (25 μCi) and the cultures incubated at 37 °C for an additional 10 min.

Upon completion of protein overexpression and labeling, cells were harvested, washed twice using lysis buffer, and then lysed using the lysozyme method. Cell lysates were then clarified using centrifugation at 14 000 rpm using an eppendorf tabletop centrifuge. The supernatant was separated from the loose pellet and stored at -80 °C prior to further processing.

Labeled or unlabeled protein present in the clarified cell lysate was purified using an FPLC system (Pharmacia Biotech Inc.). Initially, 2 ml of cell lysate was passed over a MonoQ HR 5/10 ion exchange column using a buffer consisting of 50 mM Tris (pH 7.5), 1 mM EDTA, and 1 mM DTT. As Ub, UbR48, and UBC1Δ elute in the flow through fractions, these were collected, pooled, and concentrated to 2 ml by centricon (Amicon) filtration. Concentrated samples were then run over a MonoS HR 5/10 ion exchange column using a buffer consisting of 50 mM HEPES (pH 7.5), 1 mM EDTA, and 1 mM DTT. This step was used to separate the desired protein away from lysozyme which was added during cell lysis. Again, Ub, UbR48, and UBC1Δ elute in the flow through fractions and so these fractions were collected, pooled, and concentrated to 500 μl. Concentrated samples were then passed over a Superdex 75 HR 10/30 gel exclusion column using a buffer consisting of 50 mM HEPES (pH 7.5), 150 mM NaCl, 1 mM EDTA, and 1 mM DTT. Peak fractions were collected, pooled, and concentrated to 500 μl after which glycerol was added to a final concentration of 5% v/v and the protein solutions stored at -80 °C in 50 μl aliquots.

Purity of the protein preparations was determined visually using SDS-PAGE, followed by Coomassie Blue staining. For ^{35}S-labeled Ub and UbR48 purity was also checked by autoradiography. Ub, UbR48, and UBC1Δ were found to be the principal proteins observed in their respective preparations making up greater than 90% of the total protein present. Protein concentrations were determined using the BCA protein assay kit (Pierce).

4.2.2. Overexpression and preparation of a crude lysate containing wheat E1. A wheat E1 overexpression plasmid (Hatfield *et al.*, 1990) was co-transformed with the thermally induced T7 polymerase plasmid pGP1-2 into the *E. coli* strain BL21 (Tabor and Richardson, 1985). Overexpression of wheat E1 followed the same basic protocol described with the following changes. First, overnight cultures were diluted forty fold to a final volume of 200 rather than 100 ml. Second, to the clarified cell lysates were added the protease inhibitors (all from Sigma), antipain, aprotinin, chymostatin, leupeptin, and pepstatin A (10 μg/ml) as well as PMSF (100 μg/ml). Third, the clarified cell lysate was dialyzed overnight against 4 L of buffer consisting of 10 mM HEPES (pH 7.5) and 1 mM DTT. After dialysis, the sample was retained and centrifuged at 17 000 rpm for 10 min. The supernatant was collected and added to it were the protease

inhibitors at the same concentrations given above as well as glycerol to a final concentration of 5% v/v. The crude preparation of wheat E1 was then stored at -80 °C in 200 μl aliquots. Activity of wheat E1 within this preparation was tested using an *in vitro* ubiquitination assay (see below).

4.2.3 *In vitro* ubiquitination reactions. All ubiquitination reactions were carried out in a buffer consisting of 10 mM HEPES (pH 7.5), 5 mM $MgCl_2$, 40 mM NaCl, and 5 mM ATP unless stated otherwise. The buffer also contained the protease inhibitors antipain, aprotinin, chymostatin, leupeptin, pepstatin A (all at 20 μg/ml), and PMSF (180 μg/ml). Also added were phosphocreatine (3.3 mg/ml), creatine kinase (5 μg/ml), and inorganic pyrophosphatase (0.6 units/ml) in order to maintain ATP levels over the course of the reaction.

In general, equimolar amounts of UBC1Δ and either purified ^{35}S-labeled Ub, or ^{35}S-labeled UbR48 were added to the reactions along with either a crude preparation of wheat E1, or purified bovine E1 (generously provided by C. Pickart). Alternatively, purified UBC1Δ~(^{35}S-Ub) thiolester or UBC1Δ-(^{35}S-UbR48) conjugate was added to the reaction in place of UBC1Δ, or both UBC1Δ, and Ub. Final concentrations of these reaction components as well as the final reaction volumes varied and are specified for each experiment.

4.2.4 Comparison of wheat E1 and bovine E1 activities. *In vitro* ubiquitination reactions which included UBC1Δ (1.2 μM), and ^{35}S-Ub (1.2 μM) together with either wheat (8 nM) or bovine E1 (27 nM) were set up at a final volume of 100 μl. The reactions were incubated at 30 °C for 16 hr after which reaction products were precipitated out of solution using a 1 in 10 volume of 100% TCA. After the addition of TCA, the samples were incubated on ice for 5 min. and then pelleted by centrifugation at 14 000 rpm for a further 5 min. The resulting pellets were air dried and solubilized in SDS load mix (0.125 M Tris (pH 6.8), 20% glycerol, 2% SDS, 0.01 mg/ml bromphenol blue, 100 mM DTT). Reaction products were separated by running the solubilized pellet over an SDS-polyacrylamide gel (18% acrylamide, 0.1% bisacrylamide) and visualized using autoradiography. Assignment of reaction products was made based on their molecular masses as determined by their migration on the gel relative to the migration of proteins of known molecular mass.

4.2.5 Purification and stability of the UBC1Δ~Ub thiolester. Purified UBC1Δ (1.2 μM), ^{35}S-Ub (1.2 μM) and wheat E1 (8 nM) were added to a ubiquitination reaction to a final reaction volume of 1 ml. The reaction was incubated at 30 °C for 5 hr after which it was immediately loaded onto a Superdex 75 16/30 gel exclusion column equilibrated with a buffer consisting of 50 mM HEPES (pH 7.5), 150 mM NaCl, 1 mM

EDTA and 50 µg/ml BSA (Fraction V, Boehringer Mannheim). Using the same buffer, 1 ml fractions were collected as the reaction products were eluted from the column. An elution profile of the reaction products containing ^{35}S-Ub was generated by taking a 50 µl aliquot from each collected fraction and determining the CPM present in each using a Beckman LS 6800 scintillation counter. The CPM observed in each fraction was then summed to give the total CPM eluted from the column. Using this value, the percentage of total CPM found in each fraction was determined and used to produce an elution profile for reaction products containing ^{35}S-Ub.

The apparent molecular mass of each peak observed in the elution profile was determined by comparison to the elution position of protein standards with known molecular masses. These included: BSA (66 kDa), carbonic anhydrase (29 kDa), and cytochrome C (12 kDa). The void volume of the column was determined using blue dextran.

The contents of specific peak fractions were verified using SDS-PAGE followed by autoradiography. In this case 50 µl aliquots were taken from fractions 64-71 and to each was added 25 µl of SDS load mix containing 100 mM DTT. These samples were incubated at 37 °C for 0.5 hr prior to loading onto an SDS-polyacrylamide gel (18% acrylamide, 0.1% bisacrylamide). Reaction products present in each fraction were visualized by autoradiography and assignments for each was made based on their molecular masses as determined by their migration through the gel relative to that of protein standards. Any UBC1Δ-(^{35}S-Ub) thiolester present in these fractions would be cleaved by the DTT present in the SDS load mix. As a result, the free ^{35}S-Ub observed in fractions 64-71 represents the amount of ^{35}S-Ub originally linked to UBC1Δ through a thiolester bond.

Stability of the thiolester present in the remaining eluent of fractions 65-69 was tested by first pooling these fractions, and then concentrating this solution to 1 ml using centricon (Amicon) filtration. The concentrated sample was then frozen at -80 °C prior to further use. This sample was thawed the next day and a 50 µl aliquot of this concentrate retained for analysis by SDS-PAGE and autoradiography. The remaining concentrate was loaded onto a gel filtration column and an elution profile of those components of the concentrate containing ^{35}S-Ub generated as described above.

Purified UBC1Δ-(^{35}S-Ub) thiolester used in the time course experiment (section 4.2.6) was synthesized in essentially the same manner as described above with some differences. To maximize product yield the final concentrations of UBC1Δ and ^{35}S-Ub were raised to 4.8 µM, while that of wheat E1 was raised to approximately 12 nM. To minimize the amount of the UBC1Δ-Ub conjugate produced the reaction time was decreased from 5 to 2

85

hr By generating an elution profile for this reaction as described above the principal fraction (fraction 66) containing thiolester was determined and retained. Of the total CPM eluted from the column 12% was found in fraction 66 corresponding to an [^{35}S-Ub] of 0.57 μM. As fraction 66 contained both thiolester and conjugate, this concentration corresponds to the sum of the concentrations of these two reaction products.

4.2.6. Time course. *In vitro* ubiquitination reactions were set up in which one or more of the following components were included at the given final concentrations: purified UBC1Δ~(^{35}S-Ub) thiolester (0.28 μM); UBC1Δ (0.27 μM); ^{35}S-Ub, (0.27 μM); and bovine E1 (27 nM). See Figure 4.4A for the specific components found in each reaction. Final reaction volumes used were 300 μl and the reaction was incubated at 30 °C for 8 hr. 50 μl aliquots were taken at 0, 1, 2, 4 and 8 hr time points and immediately placed in 50 μl of SDS load mix containing 100 mM DTT. Samples were then immediately frozen using liquid nitrogen. Each sample was then thawed and incubated at 37 °C for 15 min. prior to loading onto an SDS-polyacrylamide gel. Reaction products present in each sample were visualized by autoradiography.

The amount of each reaction product found at each time point was determined. This required that the amount of ^{35}S-Ub found in each reaction product be quantified. Each reaction product corresponds to a band observed on the SDS polyacrylamide gels. Quantitation of these bands was carried out using a Fujix phosphorimager. The amount of ^{35}S-Ub found in each band was then expressed as percentage of the total amount of ^{35}S-Ub present in all the bands observed for a particular time point. In Figure 4.5A the percentage of ^{35}S-Ub present in free Ub$_2$ and both the E2-Ub and the E2-Ub$_2$ conjugates at each time point was plotted. Similarly, in Figures 4.5B, and D the amount of ^{35}S-Ub present in the conjugate species containing two or more Ubs (i.e. E2-Ub$_n$; n ≥ 2) was determined and summed for each time point. In the case of Figure 4.5C values for the percentage E2 conjugate were determined as follows. The moles of ^{35}S-Ub found in the E2-Ub conjugate is equivalent to the moles of E2 found in this conjugate. For conjugates containing two or more Ubs, the moles of ^{35}S-Ub present must be first divided by the number of Ubs present in the chain in order to define the moles of E2 present in these chains. As the amount of E2 added to the reaction was known, using these values the percentage of E2 found in the E2-Ub or the E2-Ub$_n$ (n ≥ 2) conjugates was determined and expressed as the percentage E2 conjugate observed at each time point.

4.2.7. Purification of the UBC1Δ-(^{35}S-UbR48) conjugate. Purification of the monoubiquitinated conjugate UBC1Δ-(^{35}S-UbR48) was identical to the protocol used in thiolester purification with the following changes. First, ^{35}S-UbR48 was added to the reaction in place of ^{35}S-Ub. Second, the reaction was incubated at 30 °C for 16 hr rather

than 2 hr. Third, once completed, DTT was added to the reaction at a final concentration of 100 mM in order to cleave any thiolester present. The reaction was then incubated an additional 1 hr after the addition of DTT and loaded onto the gel filtration column. Fourth, once the peak fractions containing the UBC1Δ-(^{35}S-UbR48) conjugate were identified (fractions 64-67) 50 μl aliquots were retained and analyzed by SDS-PAGE followed by autoradiography. The remainder of these fractions were pooled and concentrated by centricon filtration to 1 mL. Marginal loss of conjugate was observed during concentration as determined by the number of counts found prior to and after concentration. Furthermore, negligible counts were observed in the filtrate indicating little if any of the conjugate passed through the Centricon membrane during concentration. Based on the number of ^{35}S-Ub counts found the concentration of UBC1Δ-(^{35}S-UbR48) in the concentrated sample was 140 nM.

4.2.8. Formation of a thiolester between UbR48 and the UBC1Δ-UbR48 conjugate.

Three *in vitro* ubiquitination reactions were set up as follows and are identified as reactions 5-7 in Figure 4.7. Reaction 5 included purified UBC1Δ-(^{35}S-UbR48) conjugate at a final concentration of 70 nM, and free ^{35}S-UbR48 at a concentration of 120 nM. Reaction 7 was identical to reaction 6 except that bovine E1 was added to a final concentration of 6 nM. Reaction 6 included free UBC1Δ (120 nM), free ^{35}S-UbR48 (120 nM), and bovine E1 (5 nM). All final reaction volumes were 1 ml and all reactions were incubated at 30 °C for 2 hr. Reactions 8-10 of Figure 4.9 are identical to these three reactions except that bovine E1 used in reactions 6 and 7 was replaced with wheat E1 (8 nM) for reactions 9 and 10.

Once completed, the reactions were initially frozen using liquid nitrogen and then thawed just prior to loading onto the column. Elution profiles were determined as described above using 200 μl aliquots from each fraction for scintillation counting. The remaining eluent found in specified peak fractions (59-69 in Figure 4.7, 60-68 in Figure 4.9) was subjected to TCA precipitation. The pellets were solubilized in SDS load mix and their contents analyzed by SDS-PAGE followed by autoradiography. Quantitation of bands observed in the autoradiographs as shown in Figure 4.7 employed the Fujix phosphorimager following the basic procedure outlined above.

4.3 Results

4.3.1. Dependence of multiUb chain assembly on the source of E1.

The ubiquitin conjugating enzyme UBC1Δ has been shown to support the assembly of both free multiUb chains (this work) and multiUb chains conjugated to itself at residue K93 (Hodgins et. al., 1996). This activity has been observed using in vitro ubiquitination reactions that include ^{35}S-Ub, UBC1Δ and a source of E1. For example, a reaction employing bovine E1 generates free and conjugated chains consisting of up to five and eight Ubs respectively (Figure 4.1). It has been suggested that in the absence of an E3, chain assembly depends solely upon the activity of the E2~Ub thiolester, or in this case UBC1Δ~Ub. If this were true then the function of E1 in this process would be relegated only to the synthesis of the UBC1Δ~Ub thiolester. Thus, the ability of UBC1Δ to support multiUb chain assembly in these reactions should not be dependent upon the source of E1 used so long as the E1 supported UBC1Δ~Ub production.

Unexpectedly, the use of wheat rather than bovine E1 caused the synthesis of both free and conjugated multiUb chains to become drastically retarded with respect to the number of Ubs incorporated into the chain (Figure 4.1). The reduction in chain extension resulting from the use of wheat E1 may have reflected an inability of wheat E1 to support UBC1Δ~Ub thiolester formation.

The abilities of these two E1s to carry out this reaction was tested directly using two reactions. Each reaction contained both UBC1Δ, ^{35}S-UbR48, as well as either wheat or bovine E1. The multiUb chains generated in these reactions are linked to one another primarily through an isopeptide bond involving the Ub residue K48 (Hodgins et al., 1996). Therefore, substituting Ub with UbR48 in these reactions eliminates synthesis of most multiUb chains. This ensures that the UBC1Δ~UbR48 thiolester is the principal reaction product.

Upon completion, the products of these two reactions were identified using gel exclusion chromatography. An elution profile was generated by measuring the ^{35}S-UbR48 counts of each fraction coming off of the column (Figure 4.2). Three peaks were observed in this profile which were subsequently shown to consist of UbR48 linked to E1 (Figure 4.2, E1-UbR48), the UBC1Δ~UbR48 thiolester, and free UbR48. As seen in Figure 4.2, the similar sizes of the UBC1Δ~UbR48 peaks show that wheat and bovine E1 are equivalent with respect to their abilities to synthesize the UBC1Δ~UbR48 thiolester. Therefore, the inability of multiUb chains to be fully extended in reactions containing wheat E1 could not have resulted from a defect in UBC1Δ~Ub thiolester formation.

Based on these observations, complete extension of the multiUb chains required some novel activity of bovine E1 which the wheat E1 lacked. Furthermore, this E1 requirement also suggested that the UBC1Δ~Ub thiolester could not support this process alone.

4.3.2. Purification and stability of the UBC1Δ~Ub thiolester. In order to verify these conclusions, the degree to which the UBC1Δ~Ub thiolester could assemble multiUb chains alone and its dependence on bovine E1 for this process was tested directly. The first requirement of such an experiment was a source of purified UBC1Δ~Ub thiolester.

Thiolester was generated using an *in vitro* ubiquitination reaction containing UBC1Δ, ^{35}S-Ub, and wheat E1 that was scaled up ten fold by comparison to the reaction shown in Figure 4.1 (Figure 4.3B, lane R). Wheat rather than bovine E1 was used here as it primarily catalyzes UBC1Δ~Ub thiolester formation with only limited amounts of free Ub chains and the UBC1Δ-Ub conjugates formed to contaminate the preparation. Upon completion, the thiolester was separated from the other reaction components using gel exclusion chromatography. An elution profile was generated by measuring the ^{35}S-Ub counts of each fraction coming off of the column that gave rise to two peaks (Figure 4.3, reaction). These peaks centered on fractions 66 and 84 corresponding to apparent molecular masses of 23 kDa and 7 kDa respectively.

The 7 kDa peak was found to contain free Ub (results not shown) while the 23 kDa peak was close to the expected elution position of Ub linked to UBC1Δ (25 kDa) representing either the UBC1Δ~Ub thiolester, the UBC1Δ-Ub conjugate or both. Using SDS-PAGE followed by autoradiography the contents of the 23 kDa peak fractions were identified (Figure 4.3B, fractions 64-71). Prior to loading the gel, each fraction was treated with DTT reducing any UBC1Δ~Ub thiolester present to free UBC1Δ and free Ub. Thus, any free Ub observed in these fractions corresponded to the presence of thiolester. From this analysis, the 23 kDa peak was found to contain both the UBC1Δ~Ub thiolester (free Ub), and the UBC1Δ-Ub conjugate. These results showed that the UBC1Δ~Ub thiolester could be purified away from all of the reaction components except for the UBC1Δ-Ub conjugate.

If purified thiolester readily broke down into free UBC1Δ and free Ub its inability to assemble multiUb chains could be attributed to this inherent instability. For this reason the stability of the thiolester was tested over an extended period of time and under relatively harsh conditions. Initially, fractions 65-69 from the 23 kDa peak (Figure 4.3A, reaction) were pooled and then concentrated by filtration, a process requiring centrifugation for approximately 6 hr at 5000 rpm. Once concentrated, the sample was frozen overnight at

-80 °C, thawed the next day, and run over a gel exclusion column to see if any thiolester remained.

In spite of these treatments, the elution profile of the concentrated sample revealed only a single peak that was coincident with the 23 kDa peak (Figure 4.3A, concentrate). The lack of a Ub peak verified that none of the thiolester present was broken down into free UBC1Δ and Ub. Furthermore, SDS-PAGE identified the principal products in the concentrated sample to be thiolester (free Ub), and the E2-Ub conjugate (Figure 4.3B, lane C). As such, the thiolester remained stable over a 24 hr period under a variety of conditions.

Although the thiolester did not break down into free UBC1Δ and Ub over the course of 24 hr a small proportion was converted to UBC1Δ-Ub, Ub$_2$, and UBC1Δ-Ub$_2$ (Figure 4.3B, lane C). This observation was reproduced in subsequent experiments (see Figure 4.5A). The presence of both Ub$_2$, and UBC1Δ-Ub$_2$ in these preparations indicated that the UBC1Δ~Ub thiolester possessed a weak multiubiquitination activity.

To limit the yield of these contaminants some changes to the initial reaction conditions were made. First, the rate of UBC1Δ~Ub thiolester formation is significantly faster than that of the UBC1Δ-Ub conjugate (results not shown). As a result, the total reaction time was reduced from 5 to 2 hr to minimize the amount of conjugate formed. Second, as concentration of peak fractions containing the thiolester resulted in the further synthesis of these products this step was not employed. Instead, the principal fraction from the 23 kDa peak was used directly as a source of purified thiolester immediately after elution from the column thereby minimizing the quantities of these contaminants (see Figure 4.4B). Third, by increasing the initial reaction concentrations of UBC1Δ, ^{35}S-Ub, and wheat E1 the amount of thiolester produced and present in this fraction was increased to a level sufficient for use in subsequent experiments (see Figure 4.4B). By introducing these changes into the purification scheme a ready source of stable UBC1Δ~Ub thiolester was prepared and used to study the role of E1 in multiUb chain assembly.

4.3.3. The assembly of multiUb chains onto UBC1Δ requires E1. With the purified UBC1Δ~Ub thiolester in hand several experiments were designed to test mechanistic questions relating to the synthesis of multiUb chains. The specific components of each reaction used in this study have been outlined in Figure 4.4A. The ability of each reaction to support multiUb chain assembly was measured at various times using SDS-PAGE followed by autoradiography (Figure 4.4B-D). The amount of ^{35}S-Ub incorporated into these chains was also followed using phosphorimaging analysis and these values plotted as a function of time (Figure 4.5A-D).

90

Of the four reactions outlined in Figure 4.4A one through three employed purified thiolester. Figure 4.3B showed that the thiolester preparation used in these reactions contained some E2-Ub conjugate representing only 7% of the total ^{35}S-Ub added to each reaction. The remaining 93% represented ^{35}S-Ub linked to UBC1Δ through a thiolester bond.

Using this system, the ability of purified UBC1Δ~Ub thiolester to support multiUb chain assembly alone was tested (Figure 4.4A, reaction 1). The principal product produced from this reaction was the UBC1Δ-Ub conjugate (Figure 4.4C-D, lane 1). The amount of Ub found conjugated to UBC1Δ increased linearly from 7% to 21% over an 8 hr period (Figure 4.5A). This observation was not surprising as synthesis of the UBC1Δ-Ub conjugate has been shown to involve an intramolecular transfer of thiolester linked Ub from the active site cysteine to residue K93 of UBC1Δ (Hodgins *et al.*, 1996). The fact that this intramolecular transfer continued at the same rate over 8 hr also supports the conclusion that the UBC1Δ~Ub thiolester is not hydrolyzed to free Ub and UBC1Δ over the course of the reaction. With respect to multiUb chain assembly though, UBC1Δ~Ub only supported minimal free Ub$_2$ and E2-Ub$_2$ conjugate synthesis (Figure 4.5A). This verified the conclusions drawn earlier that the UBC1Δ~Ub thiolester was able to support only marginal multiUb chain assembly.

Although minimal multiUb chain assembly was observed in this reaction it still provided some insight into how the thiolester might be involved in chain assembly. In order to synthesize free Ub$_2$ an interaction between at least two thiolester molecules such that one thiolester linked Ub could be transferred to the other was required. This would result in the UBC1Δ~Ub$_2$ thiolester. In fact, this thiolester has been previously observed (results not shown). Free Ub$_2$ is then released from the thiolester by the action of DTT resulting in free Ub$_2$. Also, the UBC1Δ-Ub$_2$ conjugate may be generated by the intramolecular transfer of thiolester linked Ub$_2$ to K93 of UBC1Δ. Alternatively, synthesis of the UBC1Δ-Ub$_2$ conjugate could require an interaction between the thiolester and the E2-Ub conjugate. Through this interaction, thiolester linked Ub could be transferred to the singly conjugated Ub resulting in the UBC1Δ-Ub$_2$ product. Therefore, it is reasonable to conclude that an interaction between two molecules of UBC1Δ~Ub is responsible for the assembly of free and conjugated multiUb chains, but the full effectiveness of this complex requires another factor(s).

The results from Figure 4.1 suggested that bovine E1 may constitute such a factor. In this scenario E1 would support multiUb chain assembly by stabilizing the interactions between two UBC1Δ~Ub thiolesters. Through this stabilization the thiolester complex would become fully active with respect to its chain building activity. Alternatively, E1 may

play a direct catalytic role using its own ability to form a thiolester with Ub to support multiUb chain assembly.

It should be noted here that the synthesis of free multiUb chains is significantly enhanced by the activity of a thiol containing compound such as DTT (R. Hodgins, pers. comm.). Given that the amount of DTT present in these reactions was negligible, the results pertaining to the synthesis of free chains are in no way conclusive. This fact and that no free chains consisting of more than two Ubs were observed for any reaction (Figure 4.4C-D) limits the conclusions drawn from these experiments to multiUb chains that are linked to K93 of UBC1Δ.

When bovine E1 and an excess amount of ATP are added to a reaction containing purified UBC1Δ~Ub thiolester (Figure 4.4A, reaction 3) conjugated multiUb chains become fully extended, and include up to eight Ubs in the chain (Figure 4.4D, lane 3). Therefore, the presence of bovine E1 in this reaction stimulates the assembly and elongation of conjugated multiUb chains by comparison to the marginal amount of chain assembly supported by UBC1Δ~Ub alone (compare lanes 1 and 3, Figure 4.4D).

To determine whether the role of bovine E1 in stimulating multiUb chain assembly required its ATPase activity a reaction which included only E1 and purified UBC1Δ~Ub thiolester was set up (Figure 4.4A, reaction 2). It should be noted that a reaction employing bovine E1 and Ub to which no ATP was added still resulted in the synthesis of the E1~Ub thiolester (results not shown). As E1~Ub thiolester formation is ATP dependent, one of the reaction components added must have been contaminated with ATP. It is likely that ATP bound to bovine E1 during its purification is the source of this contamination. Therefore, reactions to which ATP has not been added in excess still contain residual ATP and so represent reactions carried out at a low ATP concentration.

Based on these observations, reaction 2 (Figure 4.4A) consists of bovine E1, UBC1Δ~Ub, and ATP at a low concentration. This reaction supports the assembly of conjugated chains which include up to five Ubs. Thus, under these conditions the presence of bovine E1 still stimulated multiUb chain assembly by comparison to UBC1Δ~Ub (compare lanes 1 and 2, Figure 4.4D). On the other hand, a low ATP concentration did not allow the chains to become fully extended as seen at a high ATP concentration (compare lanes 2 and 3, Figure 4.4D). Therefore, stimulation of multiUb chain assembly and elongation requires both E1 and ATP, identifying a catalytic role for bovine E1 in this process.

4.3.4. The UBC1Δ-Ub conjugate is the initial substrate for multiUb chain assembly. Further comparison of the chain building activities seen at low and high ATP concentrations provided some insight into the mechanism used to assemble multiUb chains conjugated to UBC1Δ.

At a low ATP concentration (reaction 2) thiolester linked Ub was incorporated into conjugated multiUb chains during the first 2 hr of the reaction accounting for just over 20% of the total Ub present (Figure 4.5B). At this time, chains consisting primarily of two or three Ubs were observed (Figure 4.4C, lane 2). After this initial burst, the chain building activity eventually plateaus with slow incorporation of Ub up to five Ubs in the chain (Figure 4.4D lane 2). By contrast, at a high ATP concentration (Figure 4.4A, reaction 3) thiolester linked Ub was rapidly incorporated into chains (Figure 4.5B) with 30% incorporation observed after 1 hr. It was only after 8 hr that this activity began to plateau, at which point some 70% of the Ub was found to be incorporated into conjugated chains.

While the abilities of these two reactions to support the assembly of conjugated chains were quite different, the percentage of UBC1Δ to which multiUb chains had been attached was determined to be virtually equivalent for both (Figure 4.5C, E2-Ub$_n$). As such, the increased chain building activity seen in the presence of ATP does not result from an increased synthesis of UBC1Δ-Ub$_n$ conjugates, but from an increased addition of Ub to pre-existing molecules of UBC1Δ-Ub$_n$.

The increasing amount of UBC1Δ-Ub$_n$ seen in Figure 4.5C was also found to be in counterpoint to the depletion of the monoubiquitinated conjugate both at low and at high ATP concentration (Figure 4.5C E2-Ub). Based on this observation a product-precursor relationship was established between UBC1Δ-Ub$_n$ and UBC1Δ-Ub identifying UBC1Δ-Ub as the initial substrate in the assembly of conjugated multiUb chains.

As mentioned, the UBC1Δ-Ub conjugate is synthesized from the UBC1Δ~Ub thiolester through an intramolecular transfer of Ub. This transfer results in the contamination of thiolester preparations with the conjugate (Figure 4.4B). As a result, addition of the thiolester preparation to a ubiquitination reaction provides a source of preformed substrate. On the other hand, no preformed substrate was present in a reaction where the thiolester preparation was replaced with free UBC1Δ and Ub requiring that it first be made prior to chain assembly (Figure 4.4A, reaction 4). A comparison of reactions 3 and 4 showed that the rate of Ub incorporation into chains at a high ATP concentration is initially considerably faster when the thiolester preparation is used (Figure 4.5B). Also, the rate of Ub incorporation into chains proceeds at a linear rate when the thiolester preparation is not used (Figure 4.5B).

These observations should be considered in light of the following: first, the rate of thiolester formation is considerably faster in these reactions than the rate at which the conjugate forms (results not shown); second, in the presence of preformed substrate and thiolester the incorporation of Ub into chains proceeds rapidly; third, the linear rate of UBC1Δ~Ub thiolester conversion into UBC1Δ-Ub conjugate parallels the linear rate at which Ub incorporation into chains occurs in the absence of preformed thiolester and substrate. Based on these points, the rate at which the UBC1Δ-Ub conjugate formed controlled the rate at which conjugated multiUb chains were assembled. Thus, UBC1Δ-Ub not only comprised the initial substrate for the assembly of conjugated multiUb chains, its synthesis defined the rate limiting step of this process.

4.3.5. Purification of the UBC1Δ-Ub conjugate. The intramolecular transfer of Ub from the active site cysteine (C88) to K93 implied that within the UBC1Δ structure the side chains of these two residues are spatially close together (Hodgins *et al.*, 1996). This conclusion was subsequently supported by molecular modeling (M. Cummings, pers. comm.). As a result, it was reasonable to expect that Ub linked either to C88 through a thiolester link or to K93 through an isopeptide would occupy the same surface of UBC1Δ. As a consequence, it seemed likely that Ub linked to K93 would block access to the active site. Therefore, it was expected that the UBC1Δ-Ub conjugate would not be able to form a thiolester with a second molecule of Ub.

To test this hypothesis a source of purified conjugate had to be obtained. Conjugate purification employed the basic protocol described earlier for thiolester purification with the following changes. First, the reaction was allowed to incubate for 16 rather than 2 hr as the formation of the conjugate was found to be slow. Second, once the reaction was completed DTT was added at a high concentration disrupting any thiolester present. Third, since the conjugate is essentially inert when present in solution on its own fractions containing the conjugate were concentrated prior to further use.

Shown in Figure 4.6A is the elution profile for this reaction. Two peaks were observed, one corresponding in molecular mass to either conjugate or thiolester (E2-Ub peak) and the other to Ub. Samples from the E2-Ub peak fractions (64-67) were separated on an SDS-polyacrylamide gel and analyzed by autoradiography. As Figure 4.6B shows the E2-Ub conjugate was the only reaction product detected indicating it may be purified to near homogeneity using this methodology.

4.3.6. Bovine E1 is able to catalyze the formation of a thiolester between the purified UBC1Δ-UbR48 conjugate and free UbR48. With purified UBC1Δ-Ub conjugate in hand its ability to form a thiolester with free Ub ((UBC1Δ-Ub)~Ub) was tested. To simplify the interpretation of reactions used in this

94

experiment Ub was replaced with UbR48 in the synthesis and purification of the E2-Ub conjugate as well as a source of free Ub in subsequent reactions. As most conjugated multiUb chains are formed through a linkage between K48 of one Ub and the carboxy terminus of the successive Ub in the chain the use of UbR48 results in the elimination of most multiUb chains. The di- and triubiquitinated chains formed in the presence of UbR48 likely employ the amino terminus of Ub rather than K48 to extend the chain (Hodgins *et al.*, 1996). By limiting the degree to which conjugated chains may be formed it was expected that if (UBC1Δ-UbR48)~UbR48 thiolester synthesis occurred it would be the major product of the reaction.

A reaction which included purified UBC1Δ-(^{35}S-UbR48) conjugate , free ^{35}S-UbR48, and bovine E1 was set up and after a sufficient incubation time for thiolester formation the reaction was loaded onto a gel exclusion column. An elution profile of reaction products containing ^{35}S-UbR48 was generated and the components of peak fractions identified by SDS-PAGE and autoradiography as described earlier. The elution profile for this reaction (Figure 4.7A, reaction 7) revealed two peaks centered at fractions 45, and 84, corresponding to E1 charged with UbR48 and free UbR48 respectively. A third peak was also observed centered around fraction 62. This peak corresponded to an apparent molecular mass of 31 kDa close to the 33 kDa predicted for a compound consisting of the UBC1Δ-UbR48 conjugate and a second molecule of UbR48.

It was possible that this compound formed through a non covalent interaction between the conjugate and free UbR48. When these two molecules were incubated together in the absence of E1 the elution profile did not reveal a 31 kDa peak, rather two peaks corresponding to the UBC1Δ-UbR48 conjugate and free UbR48 were observed (Figure 4.6A, reaction 5). Therefore, the 31 kDa peak must have consisted of UbR48 covalently linked in some form to the UBC1Δ-UbR48 conjugate. Furthermore, synthesis of this compound was dependent upon bovine E1.

To determine which compounds were contained in the 31 kDa peak, fractions (59-69) were treated with DTT, and then analyzed using SDS-PAGE followed by autoradiography (Figure 4.7B, right panel). As seen in Figure 4.7B (right panel) free UbR48 and UBC1Δ-UbR48 comprise the principal components of these fractions. Quantitation showed that in fractions 61-63 these two compounds are present in equivalent amounts (Figure 4.8). This indicated that all of the conjugate and free UbR48 present in fractions 61-63 were linked together via a thiolester bond. Thus, in the presence of bovine E1 the (UBC1Δ-UbR48)~UbR48 thiolester was synthesized.

Quantitation also showed that in fractions 64-68 the amount of UBC1Δ-UbR48 conjugate exceeds that of free UbR48. This indicates that not all of the conjugate was used

up in forming the (UBC1Δ-UbR48)~UbR48 thiolester. Using these quantitation results it was determined that by the end of this reaction (Figure 7A, reaction 7) of the total UBC1Δ-UbR48 conjugate added twice as much was converted into the (UBC1Δ-UbR48)~UbR48 thiolester as remained free; i.e. the ratio of (UBC1Δ-UbR48)~UbR48 thiolester to UBC1Δ-UbR48 at the end of the reaction was two. Therefore, formation of the (UBC1Δ-UbR48)~UbR48 thiolester was favored in this reaction.

Similar analysis of a reaction which included UBC1Δ, UbR48, and bovine E1 (Figure 7.A, reaction 6) revealed that at the end of the reaction of the total UBC1Δ added one and a half times as much free UBC1Δ remained as compared to the amount of UBC1Δ~UbR48 formed. Therefore, the conversion of UBC1Δ into the UBC1Δ~UbR48 thiolester was not favored in this reaction.

Reaction 6 also generated the UBC1Δ-UbR48 conjugate, which was identified using SDS-PAGE followed by autoradiography (Figure 7.A, left panel). The amount of conjugate generated was found to be thirty fold less than the amount of free UBC1Δ present in the reaction. Both UBC1Δ and UBC1Δ-UbR48 may function as a bovine E1 substrate during thiolester formation. In this reaction UBC1Δ might be expected to inhibit the use of UBC1Δ-UbR48 as a substrate during thiolester formation given that it is present in such excess. Instead, most of the UBC1Δ-UbR48 conjugate generated in reaction 6 eluted from the gel filtration column at a position corresponding to the (UBC1Δ-UbR48)~UbR48 thiolester such that the ratio of (UBC1Δ-UbR48)~UbR48 thiolester to UBC1Δ-UbR48 was 1.5.

These results showed that in reactions employing bovine E1 and UbR48: 1) the UBC1Δ-UbR48 conjugate may be converted into the (UBC1Δ-UbR48)~UbR48 thiolester, 2) when UBC1Δ-UbR48 is used as a substrate its conversion into the (UBC1Δ-UbR48)~UbR48 thiolester is favored, 3) synthesis of the (UBC1Δ-UbR48)~UbR48 thiolester is not inhibited by the presence of excess UBC1Δ in the reaction, and 4) when UBC1Δ is used as a substrate its conversion into the UBC1Δ~UbR48 thiolester occurs, but is not favored. These observations strongly indicate that bovine E1 favors the UBC1Δ-UbR48 conjugate over UBC1Δ as a substrate during thiolester formation

4.3.8. Wheat E1 is unable to facilitate thiolester formation between the UBC1Δ-UbR48 conjugate and free UbR48. The fact that the UBC1Δ-Ub conjugate can serve both as a substrate for multiUb chain assembly and thiolester formation strongly suggests that the (UBC1Δ-UbR48)~UbR48 thiolester functions as a key intermediate in chain assembly. As both of these processes are E1 dependent it may be that the inability of wheat E1 to support multiUb chain assembly stems from its inability to support the synthesis of this intermediate. This was tested by determining whether or not

wheat E1 could catalyze (UBC1Δ-UbR48)~UbR48 thiolester formation in an experiment identical to that depicted in Figure 4.7.

The elution profile of a reaction that contained UBC1Δ-UbR48, free UbR48 and wheat E1 (Figure 4.9A, reaction 10) revealed a 23 kDa peak corresponding to UBC1Δ-UbR48, a 7 kDa peak corresponding to UbR48, but the 31 kDa peak corresponding to the (UBC1Δ-UbR48)~UbR48 thiolester was absent. The lack of any (UBC1Δ-UbR48)~UbR48 thiolester was verified by analyzing fractions 60-68 using SDS-PAGE followed by autoradiography (Figure 4.9B, right panel). The principal component of these fractions was shown to be UBC1Δ-UbR48. What free Ub is observed in these fractions likely corresponds to the presence of contaminating free E2 in the original conjugate preparation that was able to form thiolester with UbR48 added to the reaction.

This result is in contrast to that seen in Figure 4.7 (reaction 7) where the inclusion of bovine E1 to the reaction leads to a shift in the elution position of reaction products from monoubiquitinated to diubiquitinated forms of UBC1Δ corresponding to the synthesis of the (UBC1Δ-UbR48)~UbR48 thiolester. The inability of wheat E1 to carry out this reaction cannot be accounted for by a defect in the synthesis of the UBC1Δ~Ub thiolester as a reaction in which free UBC1Δ and UbR48 are incubated with wheat E1 results in the synthesis of the UBC1Δ~UbR48 thiolester (see Figure 4.8A, reaction 10 and Figure 4.8B, left panel). Based on these results, wheat E1 was unable to utilize the UBC1Δ-Ub conjugate as a substrate for thiolester formation. The inability to form what is likely a key intermediate in multiUb chain assembly probably accounts for the inability of wheat E1 to facilitate the assembly of conjugated multiUb chains.

4.4. Discussion

A generally accepted mechanism of protein ubiquitination is outlined by the following pathway:

$$\text{E2} \xrightarrow[\quad a \quad]{\text{E1-Ub} \quad \text{E1}} \text{E2-Ub} \xrightarrow[b]{\text{T} \quad \text{T-Ub} \quad \text{E2}} \quad \xrightarrow[\text{T-Ub}_n]{c} \text{E2} \quad \text{T-Ub}_{n+1}$$
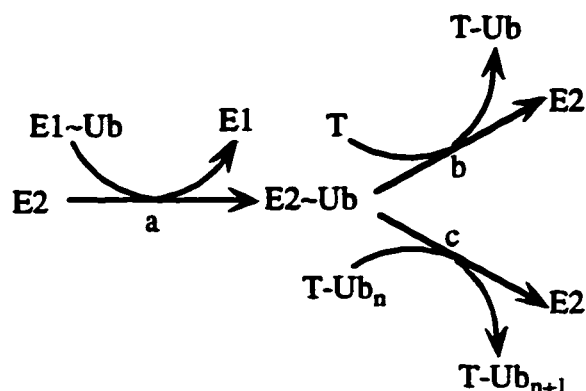
In this simplified scheme Ub is activated by E1 through the formation of an E1~Ub thiolester which is then transferred to the E2 through a transthiolation reaction generating the E2~Ub thiolester (reaction a). In a reaction that may be facilitated by E3, the E2~Ub serves as the immediate donor of Ub to a protein target (T). The initial transfer of Ub from the E2 functions to generate the monoubiquitinated form of the target (reaction b). In subsequent transfers Ub is conjugated to Ub already linked to the target (reaction c). This last stage functions to extend the multiUb chain linked to the target by one Ub, i.e. from T-Ub_n to T-Ub_{n+1}.

From the various *in vitro* ubiquitination reactions carried out in this study, UBC1Δ autoubiquitination conforms to some aspects of this reaction scheme. In particular, UBC1Δ readily forms a thiolester with Ub in an E1 dependent manner as depicted in reaction a. The UBC1Δ~Ub thiolester then carries out an intramolecular transfer of Ub to one of its own lysine residues. As such, this reaction represents a special case of reaction b where the E2 and the protein target T are both UBC1Δ. Furthermore, monoubiquitinated UBC1Δ (UBC1Δ-Ub) functions as the initial substrate for chain elongation (Figure 4.5C). The rate at which Ub is incorporated into these conjugated chains (Figure 4B, E2+(Ub, E1, ATP)) paralleled the linear rate at which the UBC1Δ-Ub substrate was formed (Figures 4.5A, E2-Ub). This indicated that the initial conjugation reaction (i.e. reaction b) defined the rate limiting step in multiUb chain assembly. From these observations then, the first stage in the assembly of multiUb chains conjugated to UBC1Δ can be depicted by the following pathway:

$$\text{UBC1}\Delta \xrightarrow{\quad \overset{\text{E1~Ub} \qquad \text{E1}}{\searrow \qquad \nearrow}\quad} \text{UBC1}\Delta\text{~Ub} \xrightarrow{\quad \text{limiting} \quad} \text{UBC1}\Delta\text{-Ub} \qquad \text{(d)}$$
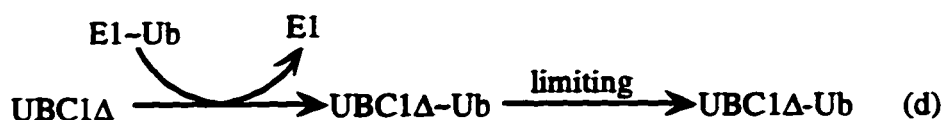
Once the UBC1Δ-Ub substrate has formed its Ub moiety functions as a site for chain elongation. Under the conditions used in this study up to eight Ubs could be incorporated into this chain under certain conditions.

In pathway c the E2~Ub thiolester, in this case UBC1Δ~Ub is depicted as the immediate donor of Ub to the growing chain. If this were true then purified UBC1Δ~Ub should have been able to support chain assembly alone. Instead, a reaction containing UBC1Δ~Ub alone was ineffective at chain elongation (Figure 4.4D, lane 1). Thus, pathway c as depicted above, is either incomplete or incorrect as a mechanistic step in the extension of multiUb chains onto the UBC1Δ-Ub substrate.

Other experiments illustrated that the number of Ubs incorporated into these conjugated chains was sensitive to the E1 used. The use of bovine E1 allowed for chain elongation up to eight Ubs while the use of wheat E1 severely limited chain elongation to at most three Ubs (Figure 4.1). This indicated that some function of bovine E1 which the wheat E1 lacked was responsible for this process.

Both of these E1s readily supported the transthiolation of Ub to UBC1Δ as depicted in reaction a. However, when UBC1Δ was replaced by the UBC1Δ-Ub conjugate as a substrate in this reaction

$$\text{UBC1}\Delta\text{-Ub} \xrightarrow{\quad \overset{\text{E1~Ub} \qquad \text{E1}}{\searrow \qquad \nearrow}\quad} \text{(UBC1}\Delta\text{-Ub)~Ub} \qquad \text{(e)}$$
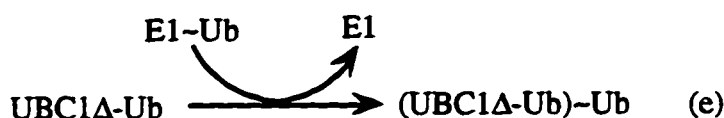
bovine E1, but not wheat E1 could catalyze the formation of (UBC1Δ-Ub)~Ub (Figures 4.7 and 4.9) as illustrated in pathway e. Furthermore, the UBC1Δ-Ub conjugate was a better substrate then UBC1Δ for thiolester formation in reactions catalyzed by bovine E1. The inability of wheat E1 to use the UBC1Δ-Ub conjugate as a substrate in the transthiolation reaction suggests that the (UBC1Δ-Ub)~Ub thiolester is an intermediate in the assembly of multiUb chains conjugated to UBC1Δ. As such, (UBC1Δ-Ub)~Ub would function as the immediate donor of Ub to the growing chain.

From the discussion presented above it has been concluded that the immediate donor of Ub to the growing chain conjugated to UBC1Δ is the (UBC1Δ-Ub)~Ub thiolester intermediate rather than the UBC1Δ~Ub thiolester. This raises a particular problem for

reactions in which purified thiolester was used as the sole source of both Ub and UBC1Δ; how does the UBC1Δ~Ub thiolester get converted into (UBC1Δ-Ub)~Ub.

The (UBC1Δ-Ub)~Ub thiolester preparation used in these reactions was shown to be contaminated by the UBC1Δ-Ub conjugate (Figure 4.4B). Thus, in order for (UBC1Δ-Ub)~Ub to be generated in these reactions Ub must be transferred from the thiolester to the conjugate as depicted in pathway f.

$$UBC1\Delta\text{~}Ub + UBC1\Delta\text{-}Ub \longrightarrow UBC1\Delta + (UBC1\Delta\text{-}Ub)\text{~}Ub \quad (f)$$

Furthermore, a direct transfer of Ub as depicted in pathway f does not occur given that the presence of UBC1Δ~Ub and UBC1Δ-Ub in a reaction is not sufficient for (UBC1Δ-Ub)~Ub synthesis. This suggested that if this transfer does occur it must be mediated by some other component in the reaction. The most likely candidate for this role would be bovine E1. A possible way by which bovine E1 could mediate this transfer is depicted by pathway g.

$$UBC1\Delta\text{-}Ub + E1 \xrightarrow{\quad\overset{UBC1\Delta}{}\quad} E1\text{~}Ub \xrightarrow{\quad\overset{UBC1\Delta\text{-}Ub}{}\quad} E1 + (UBC1\Delta\text{-}Ub)\text{~}Ub \quad (g)$$

In the first step of this pathway Ub is back transferred from the UBC1Δ~Ub thiolester to E1 in a transthiolation reaction. Such a back transfer has been observed in a reaction which included the UBC1Δ~Ub thiolester and bovine E1 (results not shown). It has already been determined that the second step in which Ub is transferred from E1~Ub to the UBC1Δ-Ub conjugate occurs (section 4.3.6).

The conclusions drawn from this study bring us back to the same pathway depicted at the start of this discussion with one difference, the E2~Ub thiolester is replaced by the (UBC1Δ-Ub)~Ub thiolester as the immediate donor of Ub to the growing chain. This presents the same questions raised at the outset, does the (UBC1Δ-Ub)~Ub thiolester catalyze chain assembly alone or does it require bovine E1. Furthermore, as this thiolester also consists of the UBC1Δ-Ub substrate does chain assembly proceed through the intramolecular transfer of Ub from (UBC1Δ-Ub)~Ub to form UBC1Δ-Ub$_2$ or is this an intermolecular process.

Although this study appears to have moved in full circle it also identified some novel functions for bovine E1. In particular, it was found that this E1 likely takes part in the back transfer of Ub from an E2~Ub thiolester to itself, and subsequently transfers it once again

to an E2. Experiments are underway to definitively show that this process occurs and address whether it is ATP dependent. Furthermore, if it is ATP dependent is it dependent upon ATP hydrolysis or simply upon ATP binding. In a previous study it was shown that the transfer of Ub from the E1-Ub thiolester to an E2 was stimulated by the binding of either ATP or AMP-Ub to E1 (Pickart *et al.*, 1994). It will be of interest to see if pathway g is stimulated in a similar fashion.

It has also been shown that the UBC1Δ-Ub conjugate functions as a better substrate then UBC1Δ in the thiolester reaction catalyzed by bovine E1 (reaction a). This identified a level of discrimination within bovine E1 with respect to the choice of substrate. The most likely explanation for this affect is that bovine E1 may utilize one of its Ub binding sites to favorably interact with the conjugate. This raises the possibility that upon formation of the thiolester both E1 and (UBC1Δ-Ub)-Ub remain in a complex in which the thiolester linked Ub is transferred to the growing chain and the conjugate active site once again becomes free for another round of thiolester formation. Such a complex may explain the relatively rapid and possibly processive transfer of Ub into chains upon formation of the UBC1Δ-Ub conjugate.
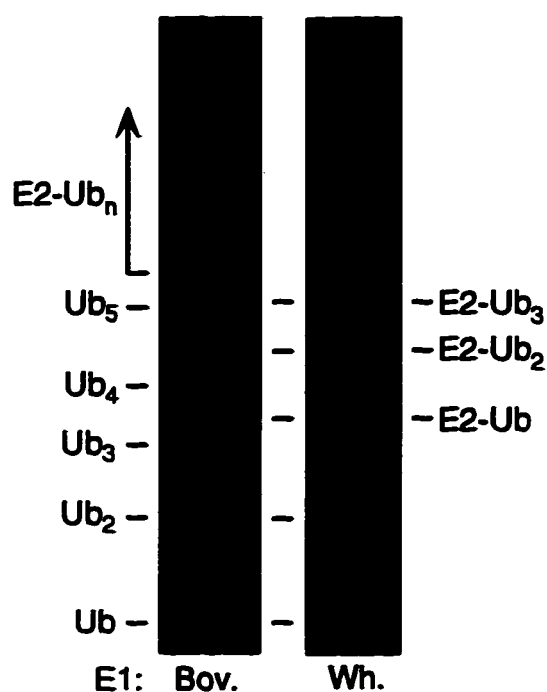
Figure 4.1. *In vitro* **ubiquitination reactions using two sources of E1.** *In vitro* ubiquitination reactions that included equimolar amounts of purified UBC1Δ and ^{35}S-Ub as well as either bovine E1 (Bov.) or wheat E1 (Wh.) were incubated at 30 °C for 16 hr. Reaction products were separated on an SDS-polyacrylamide gel and visualized by autoradiography. Identified are free multiUb chains (Ub_n) as well as multiUb chains conjugated to UBC1Δ ($E2\text{-}Ub_n$, arrow).
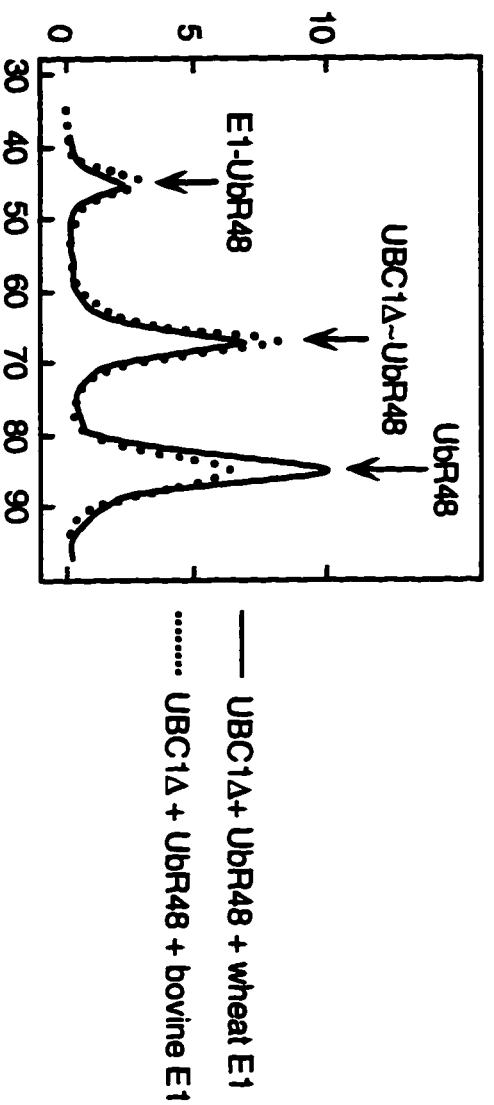
Figure 4.2. Comparison of UBC1Δ~UbR48 thiolester formation by wheat and bovine E1. Shown are the elution profiles of 35S-UbR48 from two *in vitro* ubiquitination reactions which used either wheat E1 (solid line) or bovine E1 (dotted line). These reactions contained UBC1Δ (120 nM), and 35S-UbR48 (120 nM) as well as either wheat (8 nM) or bovine E1 (6 nM) at final concentrations shown in brackets. Using SDS-PAGE followed by autoradiography (results not shown) the contents of each peak was found to consist of UbR48 bound to E1 (E1-UbR48), the UBC1Δ~UbR48 thiolester, and free UbR48 respectively.

A

B

Figure 4.3. **Purification of the UBC1Δ~Ub thiolester.** Part A shows the elution profile of 35S-Ub from an *in vitro* ubiquitination reaction that included UBC1Δ, 35S-Ub and wheat E1. The reaction was incubated at 30 °C for 5 hr. prior to loading onto a gel exclusion column (solid line). Also shown is the elution profile of 35S-Ub found in peak fractions 65-69 that were pooled, concentrated, and frozen overnight prior to loading onto the gel exclusion column (dotted line). Elution profiles were generated by plotting the 35S-Ub counts (cpm) observed in fractions 35-95. Apparent molecular masses for each peak was determined based on comparison to the elution position of protein standards of known molecular mass (not shown). In Part B samples from the reaction (R), from aliquots of peak fractions 64-71 (Part A, solid line), and from concentrated peak fractions (C) were run over an SDS-polyacrylamide gel and the reaction products containing 35S-Ub present in each were visualized by autoradiography (Part B).

104
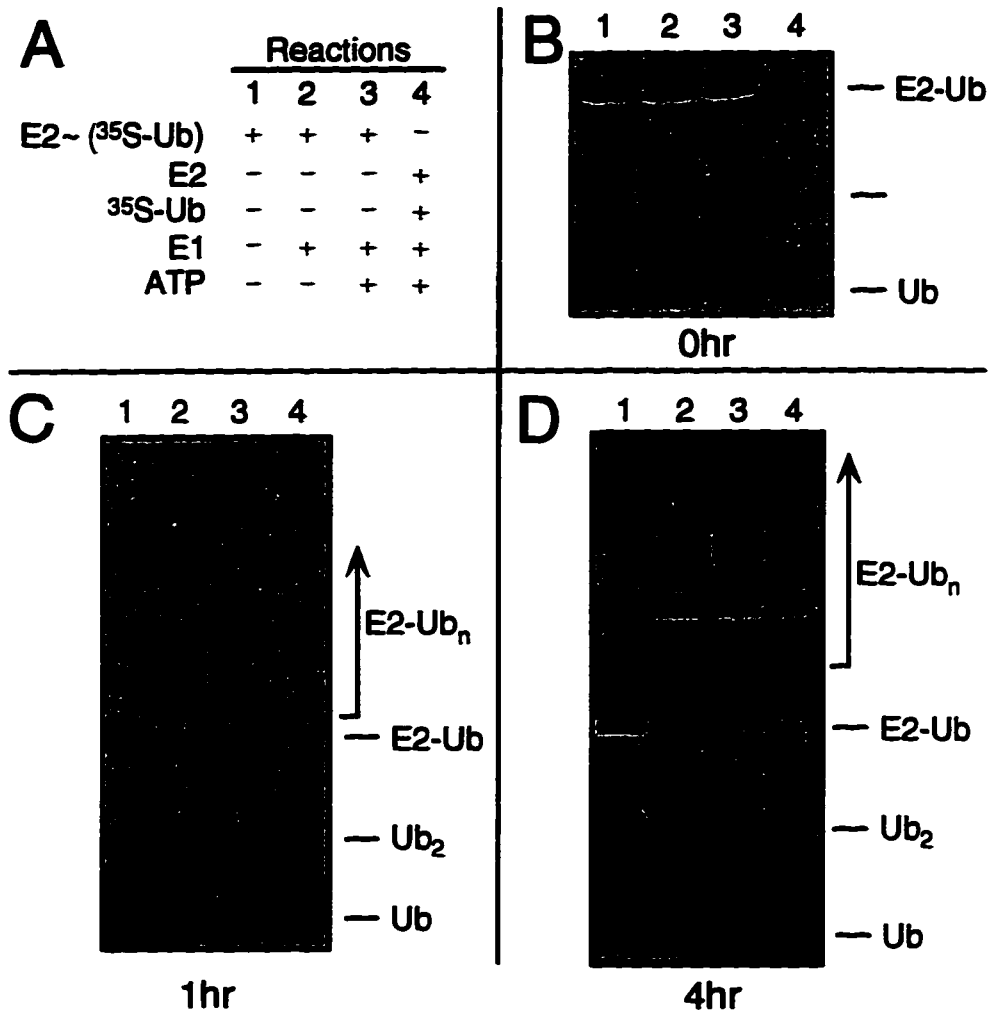
Figure 4.4. **Time course of various *in vitro* ubiquitination reactions.** Part A illustrates the various components present in four different *in vitro* ubiquitination reactions. These components include E2~(^{35}S-Ub) (purified UBC1Δ~(^{35}S-Ub) thiolester), E2 (purified UBC1Δ), E1 (purified bovine E1) as well as purified ^{35}S-Ub and ATP. Aliquots were taken from each reaction at various time points, run out on SDS polyacrylamide gels and the reaction products visualized by autoradiography. Autoradiographs for the 0 hr (Part B), 1 hr (Part C), and 4 hr (Part D) timepoints are shown.

105
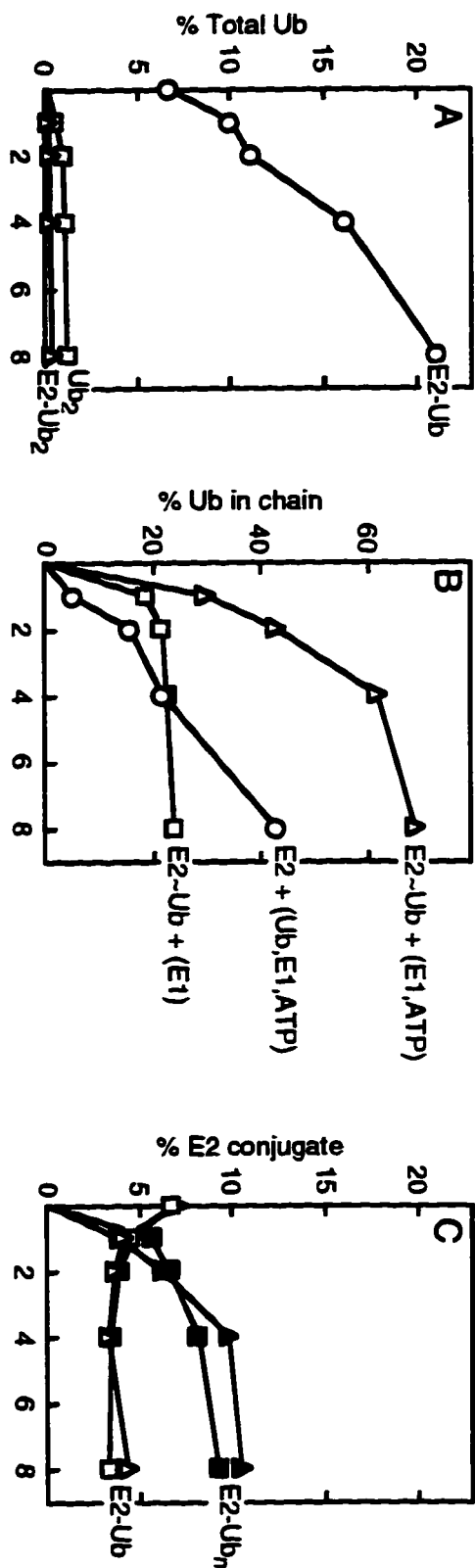
Figure 4.5. Synthesis of UBC1Δ-Ub conjugates as a function of time. Products generated in reactions 1-4 as shown in Figure 4.4 were quantitated and plotted as a function of time. Part A shows the curve generated from reaction 1 in which purified thiolester was incubated alone. Values for the amounts of monoubiquitinated conjugate (E2-Ub, circles), diubiquitinated conjugate (E2-Ub$_2$, triangles), and free diubiquitin (Ub$_2$, squares) observed at each time point are given as a percentage of the total ^{35}S-Ub added to the reaction. Part B shows the curve generated for reactions in which the E2~Ub thiolester was incubated with bovine E1 without the addition of ATP (reaction 2, squares) or with the addition of ATP (reaction 3, triangles). Also shown is the curve generated for the reaction in which free E2 and Ub are incubated with bovine E1, and ATP (reaction 4, circles). Values for the percentage of Ub in chain represent the percentage of total ^{35}S-Ub found in the multiUb conjugates, i.e. for E2-Ub$_n$ where n > 2. Part C shows curves generated for reactions 2, and 3 where the percentage of E2 conjugate was determined as a percentage of the total UBC1Δ (E2) that was converted into either the monoUb conjugate (E2-Ub; reaction 2, open squares; reaction 4, open triangles), or into multiUb conjugates (E2-Ub$_n$ where n > 2; reaction 2, closed squares; reaction 4, closed triangles).

106

A

% Total CPM

(graph with y-axis labeled 0, 5, 10, 15 and x-axis labeled 30 40 50 60 70 80 90 100, peaks labeled E2-UbR48 and UbR48)
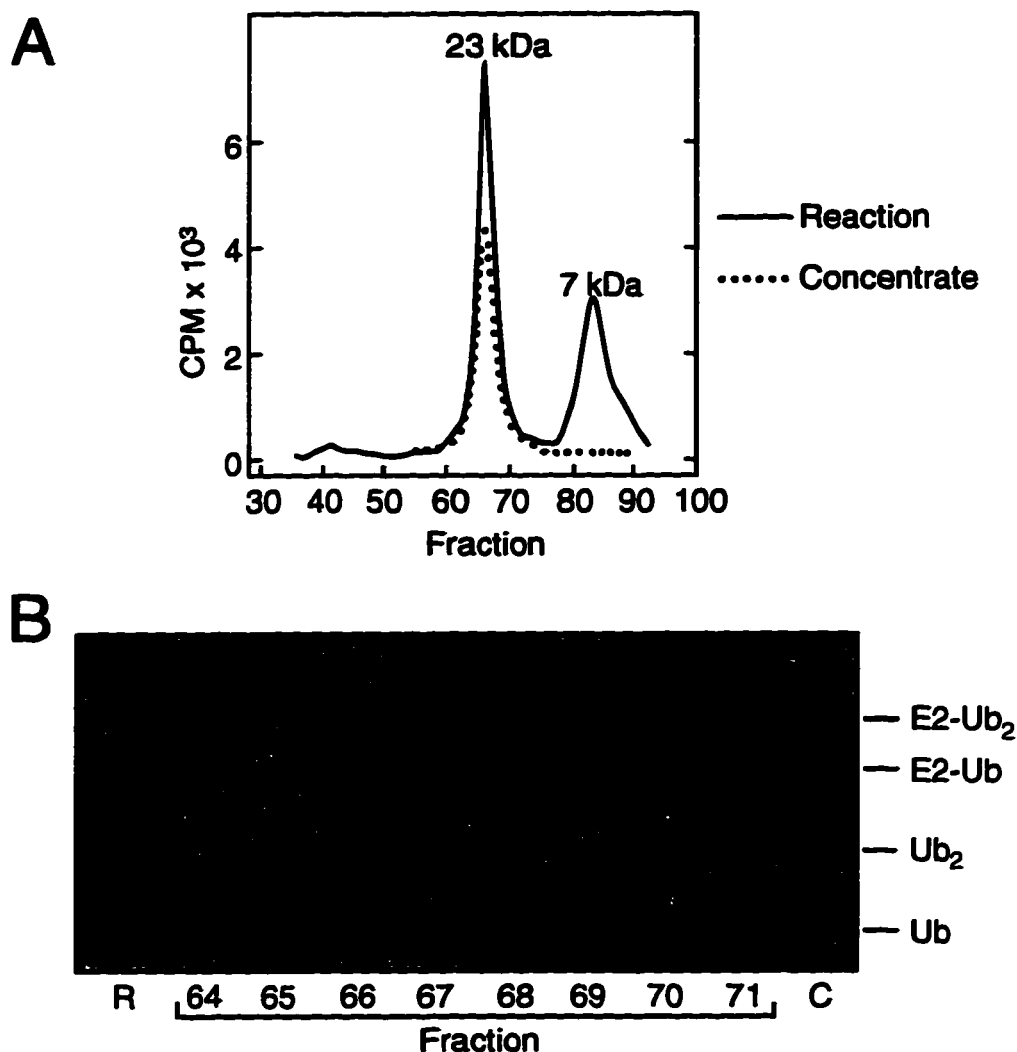
B

Fraction: 64 65 66 67

— E2-Ub

— Ub
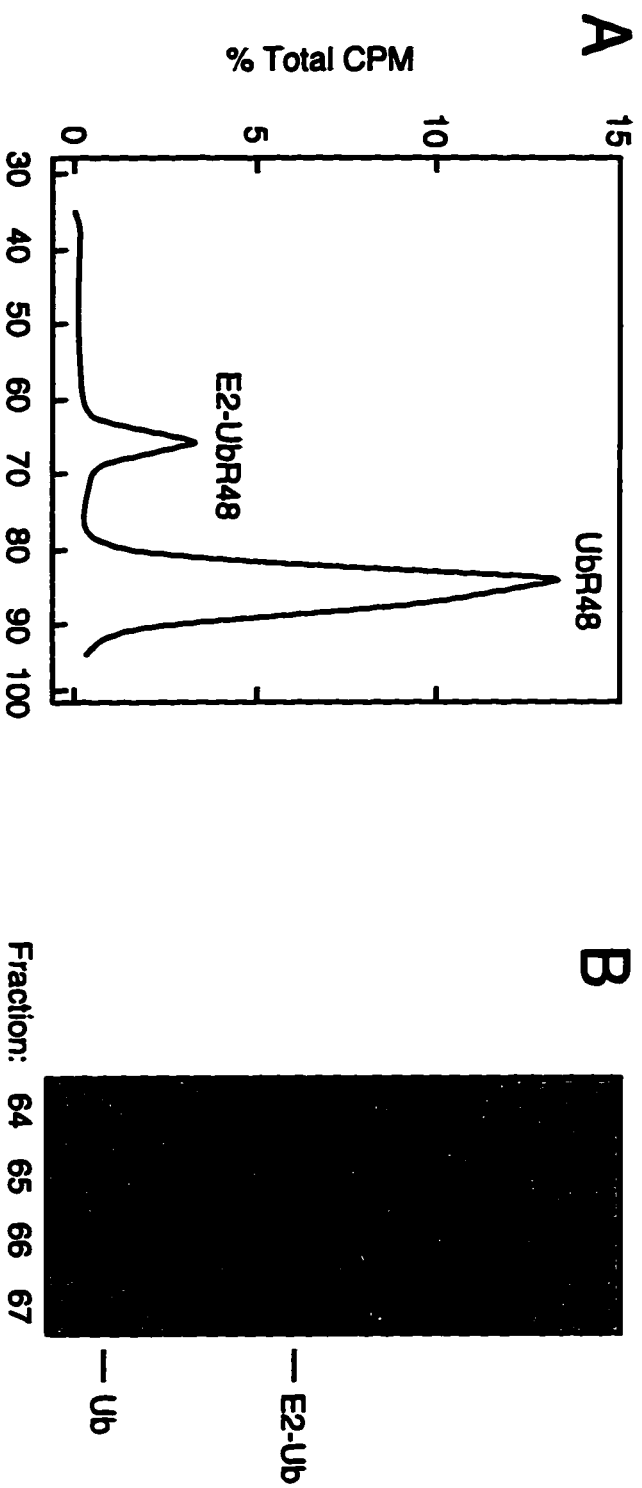
Figure 4.6. **Purification of the UBC1Δ-UbR48 conjugate.** Part A shows the elution profile of ^{35}S-R48Ub from an *in vitro* ubiquitination reaction which included UBC1Δ, ^{35}S-R48Ub and wheat E1. The reaction was incubated at 30 °C for 16 hr. Prior to loading the reaction onto a gel exclusion column it was incubated for an additional hour in the presence of DTT to cleave any thiolester present. In Part B, peak fractions (64-67) corresponding to the UBC1Δ-(^{35}S-R48Ub) conjugate were loaded onto an SDS-polyacrylamide gel and the components of each fraction visualized by autoradiography.

107

Figure 4.7. *In vitro* ubiquitination reactions employing bovine E1 and the UBC1Δ-(^{35}S-UbR48) conjugate. Shown in part A are the elution profiles of ^{35}S-UbR48 from *in vitro* ubiquitination reactions in which purified UBC1Δ-(^{35}S-UbR48) conjugate (E2-UbR48), and free ^{35}S-UbR48 were incubated in the absence (reaction 5, solid line) or presence (reaction 7, dotted line) of bovine E1. A third elution profile was also generated for a reaction that included UBC1Δ (E2), ^{35}S-UbR48, and bovine E1 (reaction 6, dashed line). In part B, peak fractions (59-69) from reactions 6 (right panel) and 7 (left panel) were loaded onto an SDS-polyacrylamide gel and the components of each fraction visualized by autoradiography.

A

% Total CPM

Fraction

31 kDa

23 kDa

7 kDa

—— E2-UbR48 + UbR48 (5)

– – E2 + UbR48 + E1 (6)

•••••• E2-UbR48 + UbR48 + E1 (7)

B

Fraction: 59 60 61 62 63 64 65 66 67 68 69

E2 + UbR48 + E1

59 60 61 62 63 64 65 66 67 68 69

E2-UbR48 + UbR48 + E1

— E2-Ub₃
— E2-Ub₂
— E2-Ub

— Ub

Figure 4.8. **Quantitation of components found in the 31 kDa peak.** Components of fractions 59-69 which comprise the 31 kDa peak observed in Figure 4.7A were identified by SDS-PAGE followed by autoradiography (Figure 4.7B, right panel). This treatment identified bands corresponding to ^{35}S-UbR48 and UBC1Δ-(^{35}S-UbR48). The CPM present in the bands corresponding to ^{35}S-UbR48 and the UBC1Δ-(^{35}S-UbR48) was determined. Shown here is a plot of the CPM found in these bands for each of fractions 59-69.

Figure 4.9. *In vitro* ubiquitination reactions employing wheat E1 and the UBC1Δ-(^{35}S-UbR48) conjugate. Shown in part A are the elution profiles of ^{35}S-UbR48 from *in vitro* ubiquitination reactions in which purified UBC1Δ-(^{35}S-UbR48) conjugate (E2-UbR48), and free ^{35}S-UbR48 were incubated in the absence (reaction 8, solid line) or presence (reaction 10, dotted line) of bovine E1. A third elution profile was also generated for a reaction that included UBC1Δ (E2), ^{35}S-UbR48, and bovine E1 (reaction 9, dashed line). In part B, peak fractions (60-68) from reactions 9 (left panel) and 10 (right panel) were loaded onto an SDS-polyacrylamide gel and the components of each fraction visualized by autoradiography.
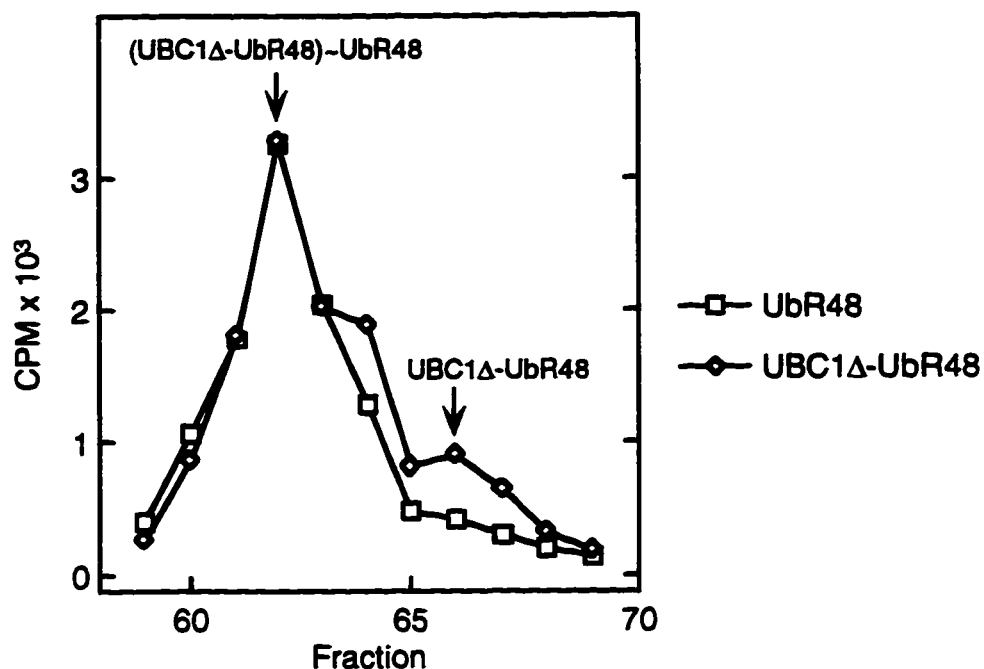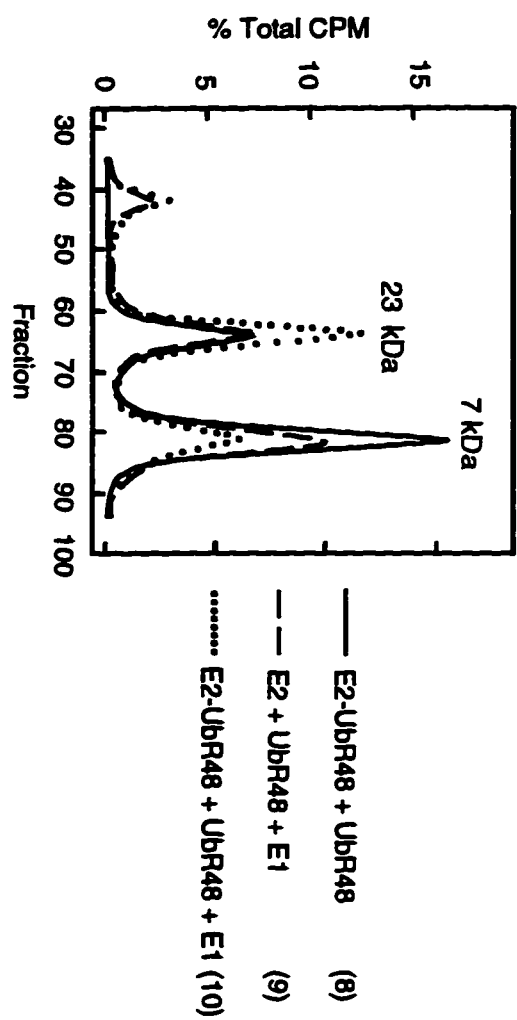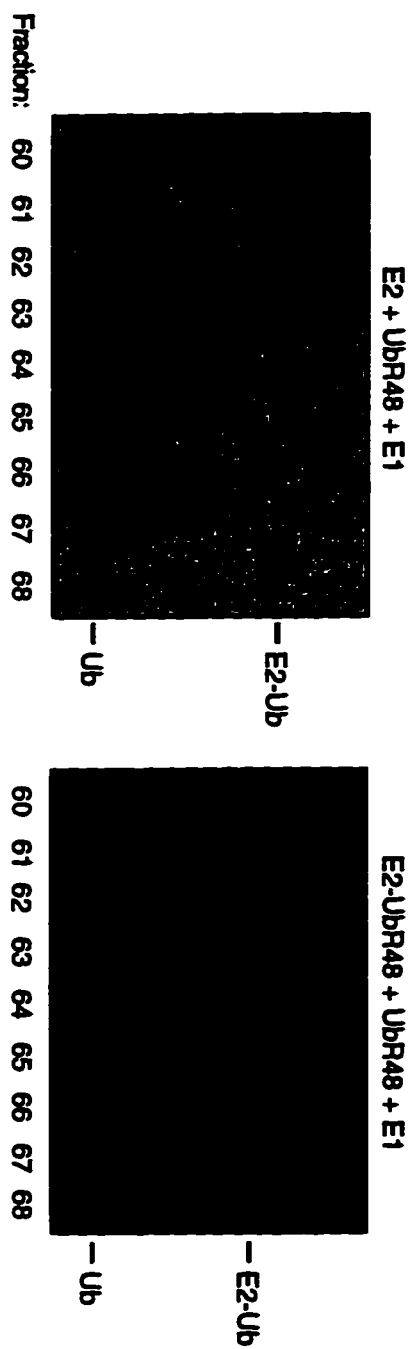
A

B

4.5. Bibliography

Chau, V., Tobias, J. W., Bachamir, A., Marriot, D., Ecker, D. J., Gonda, D. K., and Varshavsky, A. (1989). A multiubiquitin chain is confined to specific lysine in a targeted short-lived protein. *Science* **243**, 1576-1583.

Chen, Z., and Pickart, C., M. (1990). A 25 kilodalton ubiquitin carrier protein (E2) catalyzes multi-ubiquitin chain synthesis via lysine 48 of ubiquitin. *J. Biol. Chem.* **265**, 21835-21842.

Gonda, D. K., Bachmair, A., Wunning, I., Tobias, J. W., Lane, S. W., and Varshavsky, A. (1989). Universality and structure of the N-end rule. *J. Biol. Chem.* **264**, 16700-16712.

Haldeman, M. T., Finley, D., and Pickart, C. M. (1995). Dynamics of ubiquitin conjugationduring erythroid differentiation *in vitro*. *J. Biol. Chem.* **270**, 9507-9516.

Hatfield, P. M., Callis, J., and Vierstra, R. D. (1990). Cloning of ubiquitin activating enzyme from wheat and expression of a functional protein in Escerichia coli. *J. Biol. Chem.* **26**, 15813-15817.

Hershko, A., Heller, H., Elias, S., and Ciechanover, A. (1983). Components of ubiquitin-protein ligase system: resolution, affinity purification, and role in protein breakdown. *J. Biol. Chem.* **258**, 8206-8214.

Hodgins, R., Gwozd, C., Arnason, T., Cummings, M., and Ellison, M. J. (1996). The tail of ubiquitin-conjugating enzyme redirects multi-ubiquitin chain synthesis from the lysine 48-linked configuration to a novel nonlysine-linked form. *J. Biol. Chem.* **271**, 28766-28771.

Hough, R., and Rechsteiner, M. (1986). Ubiquitin-lysozyme conjugates: Purification and suseptibility to proteolysis. *J. Biol. Chem.* **261**, 2391-2399.

Johnson, E. S., Bartel, B., Seufert, W., and Varshavsky, A. (1992). Ubiquitin as a degradation signal. *EMBO J.* **11**, 497-505.

Johnson, S. J., Ma, P. C. M., Ota, I. M., and Varshavsky, A. (1995). A proteolytic pathway that recognizes ubiquitin as a degradation signal. *J. Biol. Chem.* **270**, 17442-17456.

Pickart, C. M., Kasperek, E. M., Beal, R., and Kim, A. (1994). Substrate properties of site-specific mutant ubiquitin protein (G76A) reveal unexpected mechanistic features of ubiquitin-activating enzyme (E1). *J. Biol. Chem.* **269**, 7115-7123.

Spence, J., Sadis, S., Haas, A. L., and Finley, D. (1995). A ubiquitin mutant with specific defects in DNA repair and multiubiquitination. *Mol. Cell. Biol.* **15**, 1265-1273.

Tabor, S., and Richardson, C. C. (1985). A bacteriophage T7 RNA poymerase/promoter system for controlled exclusive expression of specific genes. *Proc. Natl. Acad. Sci. USA* **82**, 1074-1078.

van Nocker, S., and Vierstra, R. D. (1991). Cloning and characterization of a 20-kDa ubiquitin carrier protein from wheat that catalyzes multiubiquitin chain formation *in vitro*. *Proc. Natl. Acad. Sci. USA* **88**, 10297-10301.

van Nocker, S., and Vierstra, R. D. (1993). Multiubquitin chains linked through lysine 48 are abundant in vivo and are competent intermediates in the ubiquitin proteolytic pathway. *J. Biol. Chem.* **268**, 24766-24773.

Chapter 5

The introduction of specific amino acid substitutions into the ubiquitin conjugating enzyme UBC1Δ affects its autoubiquitination activity.

5.1. Introduction

At the primary sequence level yeast E2s can range in similarity between thirty-three and ninety-three percent identity (Seufert *et al.*, 1990). The lack of sequence conservation may reflect differences in function or inessential positions that are subject to genetic drift. Sequence similarities however likely reflect structural regions which carry out functions that are common to all E2s. These commons functions would include the ability of E2s to interact with E1, Ub and possibly themselves. The fact that for many E2s the catalytic domain is sufficient for its function indicates that this domain contains the information required for common and unique E2 functions. Comparing the crystal structures of two E2s consisting solely of the catalytic domain shows these structures may be superimposed (Cook *et al.*, 1993). This indicates that the catalytic domains of all E2s are structurally similar. Therefore, the structural features which determine functional specificity or similarity are defined by the distribution of amino acids on a common E2 structure. In this study we wanted to determine which of these surface features were responsible for common E2 functions.

As a model E2 the carboxy terminal deletion derivative of UBC1, namely UBC1Δ was chosen for a number of reasons. First, as UBC1Δ consists solely of the E2 catalytic domain it is expected to be structurally equivalent to other E2s of known structure. This conclusion is based on the fact that while the primary sequence of RAD6 and UBC4 are forty-two percent identical their crystal structures may be superimposed (Cook *et al.*, 1993). As UBC1Δ and UBC4 show forty-six percent identity (Seufert *et al.*, 1990), it is highly likely that UBC1Δ will also have an equivalent structure. Second, UBC1Δ shows some interesting *in vitro* characteristics. Included among these is the ability to: form an E2~Ub thiolester; synthesize free multiUb chains; transfer thiolester linked Ub to one of its own lysine residues to form an E2-Ub conjugate making UBC1Δ itself a target for ubiquitination; extend a multiUb chain from the initial Ub conjugate.

To identify the function of common surface features found in E2s, amino acid substitutions were introduced at conserved, surface residues in UBC1Δ. Of the substitutions introduced, two were found to render UBC1Δ null with respect to its *in vivo*

function and showed distinct *in vitro* activities with respect to the conjugation of Ub to UBC1Δ, and the elongation of multiUb chains from this Ub. These observations indicate that the surface features defined by these residues function in the conjugation of Ub to a protein target and in the assembly of multiUb chains, but do not affect the formation of the E2~Ub thiolester.

5.2. Materials and Methods

5.2.1. *UBC1Δ* derivatives. Point mutations in *UBC1Δ* were introduced using the Promega Altered Sites Mutagenesis System. Initially, the *UBC1Δ* coding sequence was cut out of a previously constructed *E. coli* overexpression plasmid (Hodgins *et al.*, 1996) using the restriction enzymes SstI and HindIII and cloned into the pSELECT vector (Promega). Using synthetic oligonucleotides, mutations were introduced into *UBC1Δ* that replaced the S97 and A111 codons with the R codon AGG. These mutations were introduced both singly and in combination generating the three UBC1Δ derivatives R97, R111, and R97/R111. One other UBC1Δ derivative named A125 was generated by simultaneously replacing the E125, H129, L131, R132, and E135 codons with the A codons GAA, CAC, TTA, CGC, and GAA respectively. The coding sequence of each derivative was verified by DNA sequencing using the double stranded chain termination method on an Applied Biosystems automated sequencer. Oligonucleotide synthesis and sequencing were carried out by the DNA Synthesis and Sequencing Facility at the University of Alberta.

5.2.2. Yeast Plasmids and Strains. All high copy expression plasmids carrying the *UBC1Δ* mutants also carried the *TRP1* marker and were identical in sequence to each other except for the altered codons identified above. Construction of these plasmids involved cutting the mutated *UBC1Δ* coding sequences out of the pSELECT vector using SstI and KpnI and cloning them into the previously constructed *CDC34* yeast overexpression plasmid (Silver *et al.*, 1992) using the identical sites. A previously constructed control plasmid, pES12 lacking the coding sequence of any ubiquitin conjugating enzyme, but equivalent to the above plasmids in all other respects was also used as a null control (Silver *et al.*, 1992). Each plasmid was subsequently transformed into the yeast strain MHY508 (*Mata his-Δ200 leu2-3,112 ura3-52 lys2-801 trp1-1 ubc4Δ1::HIS3 ubc5-Δ1::Leu2 ref.*), using the same procedure described elsewhere (Gietz *et al.*, 1992).

5.2.3. Complementation Experiments. MHY508 cells transformed with the various yeast plasmids were grown at room temperature on synthetic defined plates (SD)

supplemented with all amino acids (Sherman *et al.*, 1981) except tryptophan. Two individual colonies from each transformation were inoculated into liquid dropout media and grown to early exponential phase (1×10^7 cells/ml) prior to replating. In all cases 1×10^5 cells were first spotted and then streaked out onto SD plates supplemented as described above or on similar SD plates containing 2 µg/ml of the amino acid analog canavanine. Cells grown on SD plates lacking tryptophan were incubated at 25 °C, 30 °C, 34 °C, and 37 °C for three days. Plates grown at 37 °C were incubated for an additional three days at room temperature to allow for colony development. Cells grown on SD plates lacking tryptophan and containing canavanine were grown at room temperature for three days.

5.2.4. Protein overexpression and purification. Construction of mutated *UBC1Δ E. coli* overexpression plasmids involved cutting the mutated *UBC1Δ* coding sequences out of the pSELECT vector using SstI and KpnI and cloning them into a modified version of pET3a (Ptak *et al.*, 1994). These plasmids were transformed into the *E. coli* strain BL21 carrying the pGP1-2 plasmid (Tabor and Richardson, 1985) which bears a heat inducible version of the T7 polymerase.

Overexpression and purification of ^{35}S-labeled and unlabeled versions of WT and mutated UBC1Δ, as well as Ub followed the same procedures described in section 4.2.1.

5.2.5. Ubiquitination Assays. Purified UBC1Δ and its derivatives were employed in ubiquitination assays using the same conditions described in the materials and methods section of chapter 4. These proteins were added along with ^{35}S-Ub to a final concentration of 1.2 µM. Also added was either a lysate containing recombinant wheat E1 (Figure 5.4) or purified bovine E1 (Figure 5.8). Wheat E1 was expressed from an *E. coli* overexpression plasmid (Hatfield *et al.*, 1990) and prepared as described in the materials and methods section of chapter 4. Bovine E1 was kindly supplied by C. Pickart. Each reaction had a final volume of 100 µl and was incubated at 30 °C for 16 hr. Upon completion, reaction components were precipitated by the addition of a 1 in 10 volume of 100% TCA followed by centrifugation. The resulting pellets were air dried and solubilized in SDS load mix (0.125 M Tris (pH 6.8), 20% glycerol, 2% SDS, 0.01 mg/ml bromphenol blue, 100 mM DTT). Samples were then loaded onto an SDS-polyacrylamide gel (18% acrylamide, 0.1% bisacrylamide) followed by autoradiography. In the case of Figure 5.8 the amount of ^{35}S-Ub found in bands corresponding to Ub as well as the various free and conjugated multiUb chains were determined using phosphorimage analysis using a Fujix phosphorimager. Quantitative analysis of the phosphorimage was done using the MacBAS 2.0 program.

5.2.6. Gel Exclusion Chromatography. Reactions containing ^{35}S-Ub, wheat E1 along with one of the various UBC1Δ derivatives were set up at a final volume of 500

μl. Reaction products were analyzed by gel exclusion chromatography using a Superdex 75 HR 16/30 column (Pharmacia) as described in section 4.2. 1 ml fractions were collected over the course of each column run. 300 μl aliquots were taken from fractions 35-95 and counted using a Beckman LS 6800 scintillation counter. These values were summed to provide a measure of the total amount of ^{35}S-Ub eluted from the column. Using this value the percentage of total ^{35}S-Ub counts found in each of fractions 35-95 was determined. By plotting these values an elution profile of reaction products containing ^{35}S-Ub was generated (see Figure 5.5, part A). Molecular masses corresponding to each peak containing ^{35}S-Ub was determined by comparison to the elution volume of known standards. Standards used included: Blue Dextran (used to determine the void volume of the column), BSA (66 kDa), Carbonic Anhydrase (32.5 kDa) and Cytochrome C (12.4 kDa). Peak fractions were then TCA precipitated and analyzed by SDS-PAGE followed by autoradiography. Quantitation of bands corresponding to Ub as well as the various free and conjugated multiUb chains was carried out by phosphorimaging analysis as described above.

5.2.7. Protein Crosslinking. Two sets of cross-linking reactions were carried out employing ^{35}S-labeled versions of UBC1Δ and its derivatives mixed with their unlabeled counterparts giving a final E2 concentration of 15 μM in each reaction. To one set unlabeled ubiquitin was also added to a final concentration of 60 μM. All reactions were carried out in a buffer consisting of 50 mM HEPES (pH 7.5), 150 mM NaCl, and 1 mM DTT. Prior to the addition of crosslinker the other reaction components were mixed together and preincubated on ice for 15 min. Following this, the crosslinker BS^3 was added to a final concentration of 1 mM and the reaction incubated on ice for an additional 1 hour. Cross-linked species were detected by SDS-PAGE followed by autoradiography. Molecular mass estimates for each crosslinked species was made based on a comparison of its mobility through the gel relative to that of protein standards. These standards (Bio Rad) included: Phosphorylase B (106 kDa), BSA (80 kDa), Ovalbumin (49.5 kDa), Carbonic anhydrase (32.5 kDa), Soybean trypsin inhibitor (27.5 kDa), Lysozyme (18.5 kDa).

5.3. Results

5.3.1. Introduction of amino acid substitutions within UBC1Δ. In order to function within the ubiquitin pathway E2s must interact with a variety of proteins. Some of these interacting partners such as E1 and Ub are shared by E2s reflecting conserved functions. The finding that conserved amino acid residues cluster on the surface of an E2, close to the active site cysteine, and within invariant structures identified potential sites of

interaction between E2s and proteins with which they commonly interact (Cook *et al.*, 1993). In an attempt to disrupt such interactions specific amino acid substitutions were introduced at surface residues of UBC1Δ within these conserved E2 structures.

Using the available E2 crystal structures (Cook *et al.*, 1992; 1993) as models for the structure of UBC1Δ, amino acid substitutions were made at the conserved surface residues S97 and A111. Each residue was altered to an arginine both singly and in combination generating derivatives of UBC1Δ that will be referred to as R97, R111, and R97/R111 (Figure 5.1). These alterations were chosen as they replace the small negatively charged hydroxyl group of S97 or the small side chain of A111 with the large, positively charged side chain of arginine. We reasoned that the introduction of arginine's bulky and charged side chain onto the surface of UBC1Δ would disrupt its ability to take part in conserved interactions. A likely consequence of such a disruption would be the loss of some UBC1Δ function.

In another study by Pitluk *et al.*, (1995) involving CDC34, five charged surface residues found in the conserved carboxy terminal region of its catalytic domain were simultaneously changed to alanine residues. These alterations eliminated the ability of CDC34 to assemble multiUb chains onto itself. Although a specific functional defect resulted from these substitutions the cell cycle function of CDC34 was not affected as this derivative was able to complement for a *cdc34* disruption mutation (Pitluk *et al.*, 1995). These results showed that while amino acid substitutions introduced into conserved structures may lead to the loss of an E2 function, the function lost may not necessarily be an essential one.

In light of this observation, a similar derivative of UBC1Δ (referred to as A125) was made in which the analogous five residues were substituted for alanine with the expectation that it too would exhibit a defect in multiUb chain assembly.

5.3.2. Complementation of a *UBC4/5* disruption by *UBC1Δ* mutants. A potential consequence of introducing amino acid substitutions at conserved positions would be the loss of an essential E2 function. To see if the alterations made to UBC1Δ resulted in the loss of an essential activity the *in vivo* function of the various UBC1Δ derivatives was tested.

Disruption of the yeast E2 genes *UBC4* and *UBC5* results in a number of phenotypes including slow growth, temperature sensitivity, and sensitivity to the amino acid analog canavanine (Seufert and Jentsch, 1990). UBC1Δ has been shown to complement for these defects (R. Hodgins, pers. comm.) therefore plasmids carrying no E2 sequence or the UBC1Δ coding sequence (WT) were transformed into a UBC4/5 disruption strain and their abilities to rescue the phenotypes described was tested. Figures 5.2 and 5.3 show that in

comparison to the null control, the presence of UBC1Δ increases the growth rate of these cells, and allows them to survive at both the non-permissive temperature of 34 °C and in the presence of the amino acid analog canavanine. UBC1Δ was also found to partially complement the disruption mutations at 37 °C.

These results verify that UBC1Δ may functionally replace UBC4 and UBC5 *in vivo*. Thus, within the context of the *UBC4/5* disruptions UBC1Δ activity was essential for cell viability under selective conditions. Using similar complementation experiments the affect of the various amino acid substitutions on UBC1Δ activity was also tested.

Plasmids carrying the *R97, R111*, and *R97/R111* coding sequences when transformed into the *UBC4/UBC5* disruption strain were unable to complement for any of the phenotypes (Figure 5.2 and 5.3) showing growth characteristics equivalent to that of cells carrying the null control plasmid. Thus, the substitutions made to generate the derivatives R97, R111 and R97/R111 were found to render UBC1Δ null with respect to its *in vivo* function. Thus, substitution of these conserved positions played an essential role in the *in vivo* function of UBC1Δ.

In contrast, a plasmid carrying the *A125* coding sequence was shown to complement for the slow growth, temperature sensitivity, and canavanine sensitivity phenotypes to almost the same degree as WT *UBC1Δ* (Figure 5.2 and 5.3). *A125* did show a greater temperature sensitivity at 37 °C relative to WT, but this effect was minimal given that the ability of WT *UBC1Δ* to complement at this temperature was itself severely compromised.

As discussed above, amino acid substitutions of A125 when made to CDC34 also were shown to have minimal affects on its ability to function *in vivo*. These results show that while structures and amino acid residues within the carboxy terminus are conserved, their contributions to E2 function are not essential. Furthermore, comparison of the *in vivo* activities of R97, R111, and R97/R11 to that of A125 delineates the functions of two structural regions within UBC1Δ as being essential and non-essential respectively.

5.3.3. *In vitro* ubiquitination reactions using wheat E1. The *in vivo* studies illustrated that amino acid positions 97 and 111 play an essential role in UBC1Δ function, while positions 125, 129, 131, 132, and 135 did not. To ascertain the mechanistic consequences of these substitutions, the activity of UBC1Δ and its various derivatives was tested *in vitro*.

Purified UBC1Δ, ^{35}S-Ub, and a crude lysate of recombinantly expressed wheat E1 when used in an *in vitro* ubiquitination reaction generate a number of products containing ^{35}S-Ub (Figure 5.4). These products were separated using SDS-PAGE and visualized using autoradiography. Several criteria were used to identify the various bands observed. First, DTT was added to each reaction prior to loading them onto the gel reducing any

UBC1Δ~Ub thiolester present to free UBC1Δ and free Ub. As such, only monoUb and multiUb conjugates as well as free multiUb chains could be observed. Second, the molecular mass of each species was determined based on its migration trough the gel relative to that of various molecular mass standards. Third, conjugated multiUb chains differ from free multiUb chains of equal length in that they migrate through the gel more slowly owing to the presence of UBC1Δ. Fourth, Ub is conjugated to UBC1Δ at residue K93 such that the R93 derivative is unable to conjugate Ub to itself. As a result R93 can only synthesize free multiUb chains and so was used here to positively identify those bands corresponding to these chains.

Using these criteria, Figure 5.4 showed that UBC1Δ (WT) supported the synthesis of free diubiquitin (Ub_2), the monoUb conjugate (E2-Ub), as well as conjugated multiUb chains of up to three Ubs in length ($E2-Ub_n$). In contrast, the derivative A125 synthesized predominantly E2-Ub and to some extent Ub_2. Thus, the amino acid substitutions made to A125 affect its ability to support the assembly of both free and conjugated multiUb chains. Not surprisingly, these results parallel the *in vitro* effects associated with the analogous substitutions made in CDC34 supporting the idea that the particular region in which the A125 substitutions were made is responsible for conserved, but non-essential E2 functions.

By comparison, R97 was found to synthesize Ub_2 and $E2-Ub_n$ to the same degree as wild type whereas R111 or R97/R111 exhibited the same multiUb chain assembly defect as A125.

Thus, the various UBC1Δ derivatives could be classified into two groups based on their *in vitro* activities. One group synthesized free and conjugated multiUb chains (WT and R97) while the other group was defective in this respect (A125, R111, and R97/R111). As each of these groups contained at least one member which showed an ability to function *in vivo* (WT or A125), and at least one member that could not function *in vivo* (R97, or R111 and R97/R111) there is no correlation between their *in vitro* abilities to synthesize multiUb chains and their ability to function *in vivo*.

5.3.4. Analysis of thiolester and conjugate forms of UBC1Δ and its derivatives using gel exclusion chromatography. Altering conserved residues on the surface of UBC1Δ was initially expected to affect conservative interactions between either Ub, E1 or itself. We examined directly the interaction between Ub and UBC1Δ within either the UBC1Δ-Ub conjugate or the UBC1Δ~Ub thiolester by comparing the hydrodynamic properties of these species formed with each UBC1Δ derivative using gel exclusion chromatography. As the *in vivo* and *in vitro* activities of R97/R111 was shown to be equivalent to R111 it was not included in these and subsequent experiments. The

elution of proteins through a gel exclusion column is dependent upon its stoke's radius which for a spherical protein is dependent upon its molecular mass. The actual molecular mass of UBC1Δ is 16 kDa but it elutes from the column at a molecular mass of 20 kDa (results not shown). This is a consequence of the structural asymmetry of E2s (Ptak et al., 1994; Cook et al., 1993) which leads to a greater apparent stoke's radius and hence elution at a higher apparent molecular mass. A tight association between Ub and UBC1Δ was expected to negate the asymmetry observed in UBC1Δ allowing the complex to elute at the expected molecular mass of 25 kDa. A loose interaction on the other hand was expected to add to the asymmetry of UBC1Δ resulting in a complex which eluted at a molecular mass greater than 25 kDa.

Using an *in vitro* ubiquitination reaction employing UBC1Δ, ^{35}S-Ub, and wheat E1, Ub thiolester and conjugate forms of UBC1Δ were produced. Upon completion, the reaction was loaded onto a gel exclusion column and the elution position of the thiolester and conjugate identified.

An elution profile was generated by determining the percentage of total counts found in each collected fraction (Figure 5.5A). This elution profile gave rise to two peaks corresponding to molecular masses of 23 kDa and 7 kDa respectively. The 7 kDa peak was found to contain free Ub (results not shown). The 23 kDa peak was close to the expected elution position of Ub linked to UBC1Δ (25 kDa) representing either the UBC1Δ~Ub thiolester, the UBC1Δ-Ub conjugate or both. Using SDS-PAGE followed by autoradiography the contents of the 23 kDa peak fractions were identified (Figure 5.5B). Prior to loading onto the gel, each fraction was treated with DTT reducing any E2~Ub thiolester present to free UBC1Δ and free Ub. Thus, any free Ub observed in these fractions corresponded to the presence of thiolester.

Analysis of the 23 kDa peak indicated that the UBC1Δ~Ub thiolester (free Ub), and the UBC1Δ-Ub conjugate coeluted from the column and were the principal components of this peak. The elution of these complexes at a position close to the expected molecular mass indicated that covalently linked Ub tightly associated with UBC1Δ.

Repeating these procedures using the derivatives R97, R111, A125 generated elution profiles that were identical to that produced by WT UBC1Δ (results not shown). SDS-polyacrylamide gels also showed that in each case the 23 kDa peak contained both thiolester and conjugate. As such, Ub and UBC1Δ linked as either thiolester or conjugate remained closely associated in spite of the UBC1Δ amino acid substitutions.

Further analysis showed that of the total Ub added to each of these reactions approximately 50% was utilized in the synthesis of thiolester and conjugate (Figure 5.6, % Thiolester + Conjugate). As the UBC1Δ~Ub thiolester must be formed prior to the

generation of the UBC1Δ-Ub$_n$ conjugates the sum of thiolester and conjugate reflects the total amount of thiolester synthesized over the course of the reaction. As a result, the equivalent abilities of each derivative to utilize Ub also indicated equivalent abilities to synthesize thiolester.

Breaking these totals down identified that for both WT and A125 a greater amount of Ub remained linked to UBC1Δ as thiolester (31% and 29% respectively) then was used to form conjugate (18% in each case) giving thiolester to conjugate ratios of 1.7 and 1.6 respectively. Reactions employing R97 and R111 on the other hand favored the conversion of thiolester linked Ub (21% for both) into Ub conjugates (26% and 31% respectively) giving thiolester to conjugate ratios of 0.8 and 0.7 respectively.

While each of these reactions showed equivalent abilities to generate thiolester the subsequent utilization of the thiolester in conjugate formation was shown to vary. Furthermore, a greater propensity towards the synthesis of conjugated species was observed for R97 and R111 the same UBC1Δ derivatives unable to function *in vivo*. This suggests that the structures in which the R97 and R111 amino acid substitutions were introduced are involved in essential UBC1Δ activities downstream of thiolester formation.

5.3.5. Detection of both the UBC1Δ homodimer and the UBC1Δ-Ub heterodimer by *in vitro* crosslinking. E2s have also been shown to self-associate (Pickart and Rose, 1985; Haas and Bright, 1988; Girod and Vierstra, 1993; Chen *et al.* 1993, Ptak *et al.*, 1994, Gwozd *et al.*, 1995) and to weakly interact with free Ub (Prendergast *et al.*, 1995). Using crosslinking reactions the ability of UBC1Δ and its various derivatives to take part in these interactions was tested.

In the presence of the lysine cross-linker BS^3 each UBC1Δ derivative readily produced a crosslinked dimer, (Figure 5.7, (E2)$_2$). The addition of Ub to these reactions also identified the ability of each derivative to readily form a crosslinked heterodimer with Ub, (Figure 5.7, E2-Ub). Furthermore, the percentage of total UBC1Δ incorporated into these dimer species was found to be equivalent to the amount of incorporation observed for each derivative. As such, these crosslinking reactions showed that UBC1Δ is capable of self-association and interacts with free Ub. Furthermore, the amino acid substitutions introduced into UBC1Δ had no obvious affect on either interaction.

5.3.6. *In vitro* ubiquitination reactions using bovine E1. In the previous chapter, the activity of UBC1Δ with respect to the assembly of free and conjugated multiUb chains was shown to be dependent upon E1. In these reactions the use of wheat E1 resulted in minimal chain building activity (Figure 5.4) compared to reactions that employed bovine E1 (Figure 5.8). Furthermore, these differences stem from the ability (in the case of bovine E1) or the inability (in the case of wheat E1) of the E1 to catalyze the

formation of a thiolester between Ub and the UBC1Δ-Ub conjugate. Based on these differences it was of interest to examine chain synthesis using the various UBC1Δ derivatives in the presence of bovine E1.

A set of *in vitro* reactions was set up employing the various UBC1Δ derivatives, ^{35}S-Ub, and bovine E1. Reaction products were analyzed using SDS-PAGE followed by autoradiography and band assignments were made as described above (Figure 5.8). The reaction which employed WT UBC1Δ synthesized free and conjugated multiUb chains consisting of up to four and eight Ubs respectively. Conjugated chains extended beyond eight Ubs but the exact extent could not be assessed as the bands begin to smear at higher molecular masses. It should be noted that in comparison to the free multiUb chains observed in a reaction employing R93 a considerably smaller amount of these chains was observed in the WT UBC1Δ reaction. Presumably, this results from competition between the synthesis of free and conjugated multiUb chains in which the latter reaction is favored. As a result the higher molecular weight species seen in the WT reaction have been designated as multiUb conjugates of UBC1Δ (E2-Ub$_n$).

When the percentage of total Ub incorporated into free and conjugated multiUb chains was determined for each UBC1Δ derivative it was shown that WT, R111, and A125 shared similar activities (51%, 53%, 54% respectively). Interestingly, the activity of R97 (64% incorporation) was found to be greater than these other three derivatives by at least 10%.

The difference between R97 and the others becomes more pronounced when the length of the conjugated chains synthesized are examined. For R97, 57% of the Ub was incorporated into conjugated chains consisting of five or more Ubs, whereas only 39% incorporation to this length was observed for WT. A125 exhibited a similar activity to WT UBC1Δ for chains of five Ubs or greater (32%), whereas the corresponding activity for R111 was considerably reduced (15%). Thus, while A125 and WT UBC1Δ show similar activities with respect to the elongation of conjugated chains, R97 was more effective, while R111 showed a defect in this activity.

When these derivatives were examined for free chain synthesis WT and R97 exhibited similar activities for the synthesis of free chains up to four Ubs in length. By comparison R111 and A125 were severely impaired in this activity synthesizing only Ub$_2$.

Comparison of the *in vitro* reactions employing wheat E1 (Figure 5.4) to those employing bovine E1 (Figure 5.8) identified some similarities and differences in the activities of each UBC1Δ derivative. Overall, the use of bovine E1 allowed for an increased incorporation of Ub into multiUb chains and the increased elongation of these chains. Even so, some parallels in the activities of these derivatives are observed when

either E1 is used. For example, both WT and R97 UBC1Δ were observed to have equivalent activities in free chain synthesis, whereas both R111 and A125 showed equivalent, and impaired activities in this respect.

Parallel activities are also observed in these reactions with respect to the synthesis of conjugated multiUb chains for WT and R97. In each case WT and R97 UBC1Δ can elongate chains to the same length, and in each case R97 shows an increased ability to incorporate Ub into these conjugated chains. Similarly, R111 shows a defect in the elongation of conjugated chains by comparison to WT and R97 for both sets of reactions.

Interestingly, the elongation of conjugated chains by A125 while impaired in reactions employing wheat E1 was observed to be similar to that of WT UBC1Δ in reactions employing bovine. This indicates that the defect exhibited by A125 in chain elongation may be suppressed by bovine E1, but not wheat E1.

5.4. Discussion

The clustering of conserved residues on an E2 surface suggested that such a region plays an essential role in activities common to all E2s (Cook et al., 1993). One possibility was that this E2 surface comprised a conservative interaction site with Ub, E1, or itself. Amino acid substitutions were initially introduced into UBC1Δ with the intent of disrupting such interactions. These substitutions were made within a highly conserved region of UBC1Δ at sites just carboxy terminal to its active site cysteine (R97, R111).

A third derivative of UBC1Δ was also made in which amino acid substitutions were introduced within conserved structures found at the carboxy terminus (A125). Analogous substitutions had previously been introduced into the same region of CDC34. Although this CDC34 derivative exhibited a defect in the assembly of conjugated multiUb chains *in vitro*, it was still able to carry out the cell cycle function of CDC34 *in vivo* (Pitluk et al., 1995). It was expected that A125 would exhibit analogous *in vivo* and *in vitro* properties.

The inability of both R97 and R111 to complement a *UBC4/5* disruption identified the region just on the carboxy terminal side of the active site as being essential for the *in vivo* activity of UBC1Δ. In contrast, the mutant A125 was found to be virtually identical to WT with respect to its ability to complement for the *UBC4/5* disruption. Thus, as observed for CDC34, the *in vivo* activity of UBC1Δ was not affected by substitutions introduced at its carboxy terminus.

In spite of the fact that R97 and R111 rendered UBC1Δ null with respect to its *in vivo* function both derivatives were found to be active *in vitro* . From *in vitro* ubiquitination reactions both derivatives readily supported thiolester formation in the presence of either

wheat or bovine E1. Furthermore, gel exclusion chromatography and crosslinking studies could not identify any obvious defects in the ability of these mutants to self-associate, to interact with free Ub, or to interact with covalently linked Ub (i.e. as thiolester or conjugate). In these respects, R97 and R111 were identical to both WT and A125 UBC1Δ.

Rather than affecting interactions and activities resulting in the formation of an E2~Ub thiolester, in vitro ubiquitination reactions identified distinct activities for each derivative downstream of this event. Specifically, differences were observed in the formation of the monoubiquitinated conjugate of UBC1Δ as well as the formation of both free and conjugated multiUb chains.

Use of wheat E1 in these reactions led primarily to the synthesis of both E2~Ub thiolester and the monoubiquitinated conjugate of UBC1Δ (UBC1Δ-Ub). Synthesis of UBC1Δ-Ub has been shown to proceed via an intramolecular reaction in which thiolester linked Ub is transferred from the active site cysteine (C88) of UBC1Δ to the amino side chain of its K93 residue (Hodgins et al., 1996). As such, the amount of conjugate formed reflects the transfer rate of Ub from C88 to K93. In this respect the R97 and R111 derivatives were found to have an increased rate of conjugate formation by comparison to WT and A125 UBC1Δ (Figure 5.6).

In chapter 4 it was shown that synthesis of the monoubiquitinated conjugate is a property of the UBC1Δ~Ub thiolester in that the transfer was not dependent upon E1. As such, only interactions between Ub and UBC1Δ function to define this intramolecular transfer. It is possible that the structures in which the R97 and R111 substitutions were introduced define a Ub binding pocket. These structures include a loop-helix-loop motif that would allow ubiquitin to sit on the surface of UBC1Δ like a ball in a cup (see Figure 5.1, the region highlighted in red). Introduction of the bulky, positively charged side chain of arginine into this region may sufficiently perturb an interaction between UBC1Δ and Ub leading to an increase in the rate at which the intramolecular transfer occurs. While these observations are suggestive, structural studies are currently being carried out to definitively identify the surfaces of Ub and UBC1Δ that interact.

In vitro reactions employing bovine E1 allowed each UBC1Δ derivative to increase both the amount of Ub that could be incorporated into multiUb chains and the extent to which the chains were elongated by comparison to reactions employing wheat E1. Even so, the differences in activity of R97 and R111 when compared to WT UBC1Δ were similar for both sets of reactions. Given that the synthesis of multiUb is favored in reactions employing bovine E1, its use simply exacerbated the affects observed in the wheat E1 reactions.

In the case of A125 though distinct differences were observed in these two reactions sets. When wheat E1 was used A125 showed a defect in the extension of multiUb chains that was equivalent to that of R111. On the other hand, in the presence of bovine E1 A125 showed a similar ability to WT in the elongation of conjugated multiUb chains. Thus, bovine E1 functioned to stabilize the A125 defect restoring its ability to elongate multiUb chains. This suggests that A125 interacts with bovine E1 in the process of multiUb chain assembly. The normalization of A125's chain building activity to that of WT in the presence of bovine E1 suggests that such a process may also occur *in vivo*. Such an affect may account for the equivalent abilities of A125 and WT UBC1Δ to complement for the *UBC4/5* disruption mutant. Although the experiments presented in chapter 4 showed that the assembly of multiUb chains conjugated to UBC1Δ requires bovine E1, this work did not definitively identify the need for an E1-UBC1Δ complex during this process. Experiments are currently being carried out to address this question.
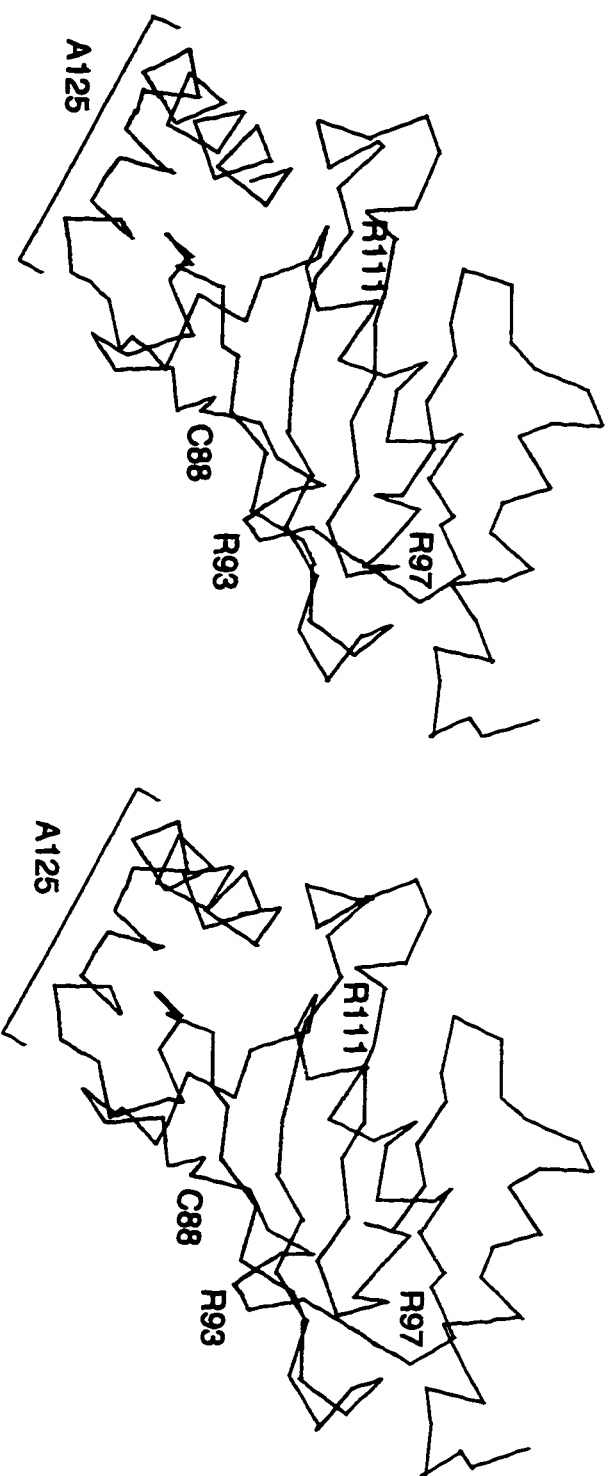
Figure 5.1. **Amino acid substitutions introduced into UBC1Δ.** Shown is the crystal structure of the RAD6 homologue from *A. thaliana* (Cook *et al.*, 1992) which was used here as a model for the structure of UBC1Δ. Amino acid substitutions were introduced into two structural regions highlighted in red and blue. Within the structural region highlighted in red the main chain positions of key residues are marked in green. These include the active site cysteine C88, and the positions at which the amino acid substitutions K93R (R93), S97R (R97), and A111R (R111) were introduced. Similarly, within the structural region highlighted in purple the main chain positions of the five amino acids substitutions introduced are also highlighted in green and include E125A, H129A, L131A, R132A, E135A. As these five alterations were introduced into UBC1Δ simultaneously this derivative has been designated by the first member of the group, namely A125.
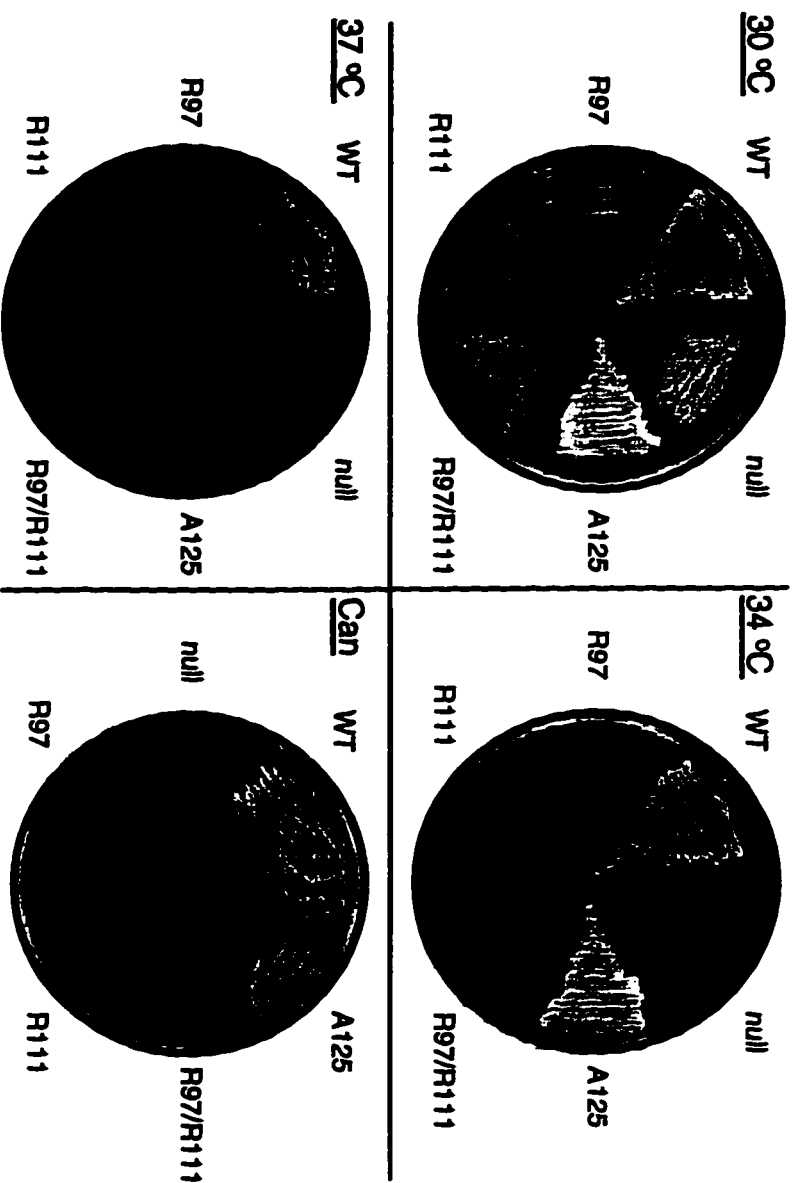
Figure 5.2. Functional complementation of a *UBC4/5* disruption mutant by various UBC1Δ derivatives. High copy yeast overexpression plasmids carrying no UBC1Δ coding sequence (null) or the coding sequence for one of the various UBC1Δ derivatives (WT, R97, R111, R97/R111, and A125) were transformed into a yeast strain in which both the UBC4 and UBC5 genes have been disrupted. The ability of cells transformed with these plasmids to remain viable at various temperatures (30 °C, 34 °C, and 37 °C), or in the presence of the amino acid analog canavanine (Can) was tested.

129

E2	Viability				Canavanine
	25°	30°	34°	37°	
WT	++	++	++	+/−	+
Null	+	+	−	−	−
R97	+	+	−	−	−
R111	+	+	−	−	−
R97/R111	+	+	−	−	−
A125	++	++	++	−	+

Figure 5.3. **The UBC1Δ derivatives R97, R111, and R97/R111, are unable to functionally complement a *UBC4/5* disruption mutant.** The results of the complementation experiment shown in Figure 5.2 are summarized. Cell viability was scored in terms of overall growth rate and colony size by comparison to cells grown at 25 °C in the presence of WT UBC1Δ. A ++ score indicates an identical growth rate and colony size while + and +/− scores indicate successively slower growth rates and smaller colony sizes. A − score indicates no growth.

— E2-Ub$_3$

— E2-Ub$_2$

— E2-Ub

— Ub$_2$

— Ub

E2:   WT   R93   R97 R111 R97/ A125
                               R111
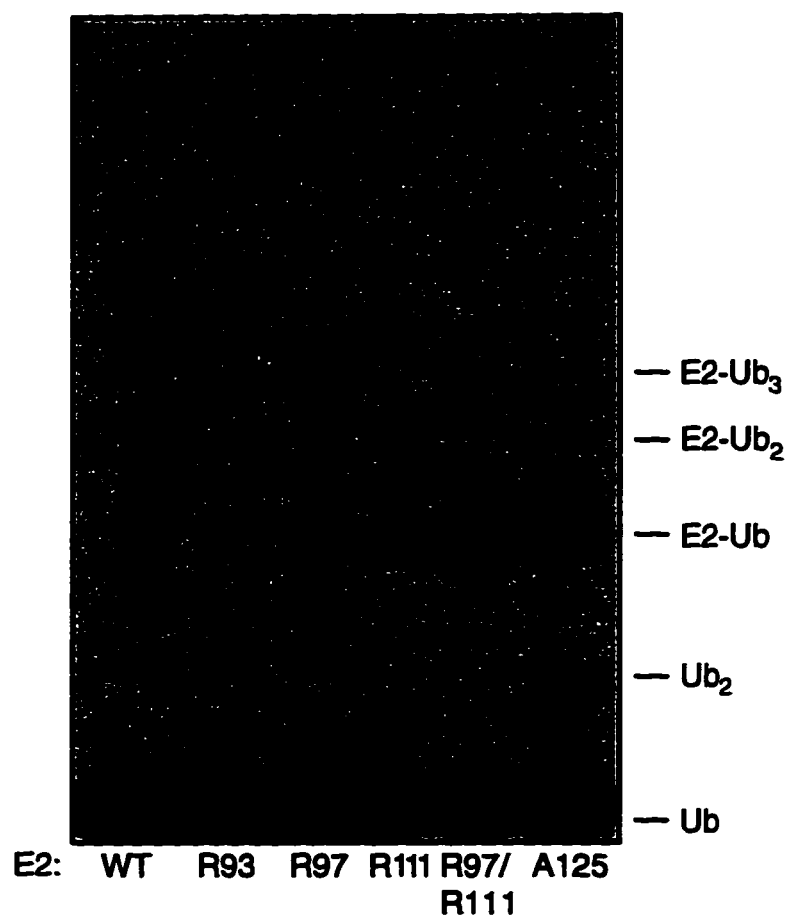
Figure 5.4. *In vitro* ubiquitination assays using wheat E1.
Purified ^{35}S-Ub and a crude extract of recombinantly expressed wheat E1
were incubated together with one of the various UBC1Δ derivatives.
Reaction products containing ^{35}S-Ub were separated using SDS-PAGE
and visualized by autoradiography. Band assignment for Ub, Ub$_2$, and the
various UBC1Δ-Ub conjugates (E2-Ub$_n$) were based on the criteria
described in the results section (5.3.3).

131

A

15

23 kDa

% Total CPM

10

7 kDa

5

0

35 45 55 65 75 85 95

Fraction

B

E2-Ub$_2$ —
E2-Ub —

Ub$_2$ —

Ub —

Fraction: 60 61 62 63 64 65 66 67 68 69 70 71 72 73 74 75
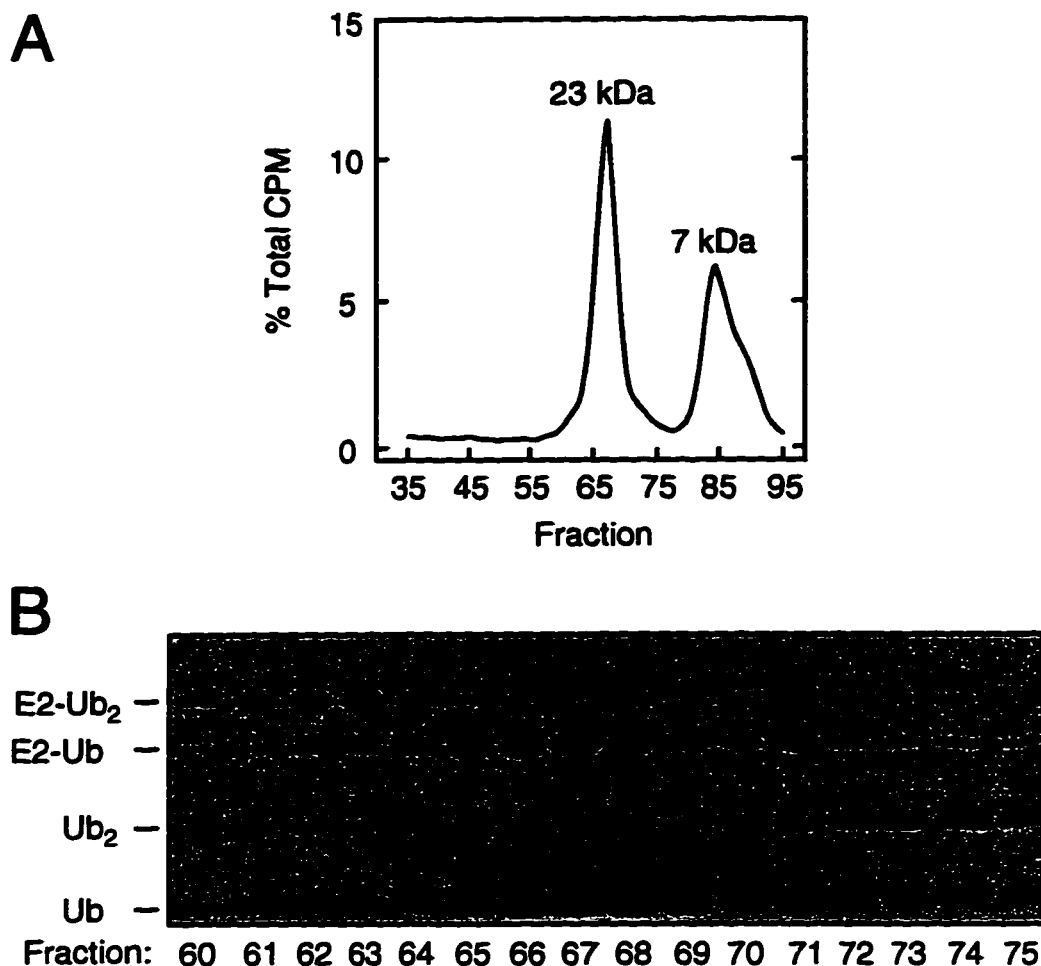
Figure 5.5. Separation of the Ub thiolester and conjugate forms of UBC1Δ from free Ub using gel filtration chromatography. Shown in part A is the elution profile of ^{35}S-Ub from an *in vitro* ubiquitination assay that included WT UBC1Δ, ^{35}S-Ub, and wheat E1. ^{35}S-Ub counts observed in each fraction were expressed as a percentage of the total counts summed over fractions 35-95. Molecular mass determinations were made for each peak based on the elution position of known molecular mass standards identifying a 23 kDa and a 7 kDa peak. In Part B components of fractions 60-75 which make up the 23 kDa peak were determined using SDS-PAGE followed by autoradiography identifying the UBC1Δ~Ub thiolester (Ub) and the UBC1Δ-Ub conjugate (E2-Ub) as the principal components of this peak. Other reaction products including free Ub$_2$ and UBC1Δ-Ub$_2$ are also observed and contribute to the tailing seen on either side of the 23 kDa peak.
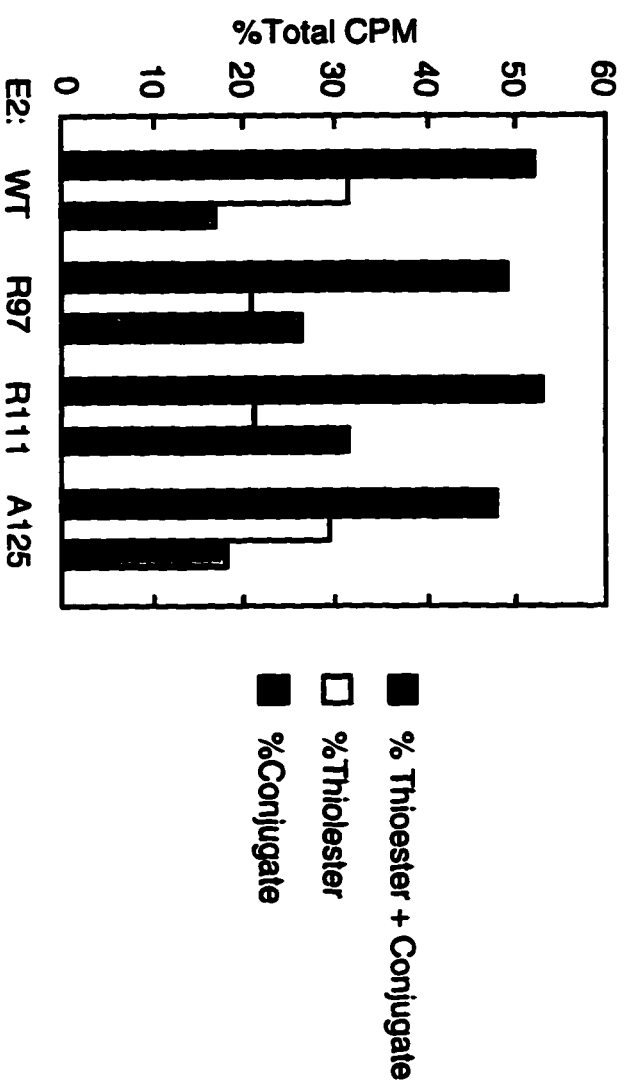
Figure 5.6. **Thiolester and conjugate composition of the 23 kDa peak.** *In vitro* ubiquitination reactions employing the UBC1Δ derivatives were carried out and subsequently analyzed using gel exclusion chromatography followed by SDS-PAGE and autoradiography as described for WT UBC1Δ in Figure 5.5. The amount of 35S-Ub found in the thiolester and conjugate forms of the various UBC1Δ derivatives in fractions 60-75 was quantitated and expressed as a percentage of total 35S-Ub found in fractions 35-95. These values are shown individually (% thiolester-white and % conjugate-gray) or as a sum (% thiolester + conjugate; black).
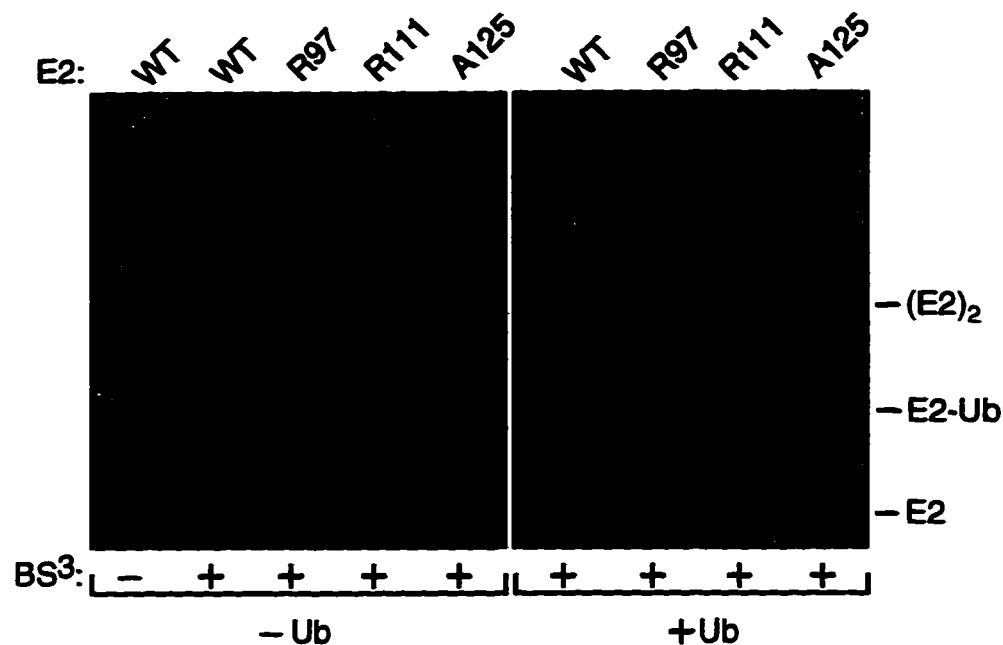
Figure 5.7. **Self-association of UBC1Δ and its interaction with Ub as detected by crosslinking.** Crosslinking reactions which included ^{35}S-labeled versions of the UBC1Δ derivatives, 1mM of the lysine crosslinker BS^3 were incubated in the presence (+Ub) or absence (-Ub) of Ub. Reaction products were separated using SDS-PAGE and visualized by autoradiography. Band assignments for crosslinked (E2)$_2$ and E2-Ub were made based on the relative migration of these species to the migration of known molecular mass standards.

134
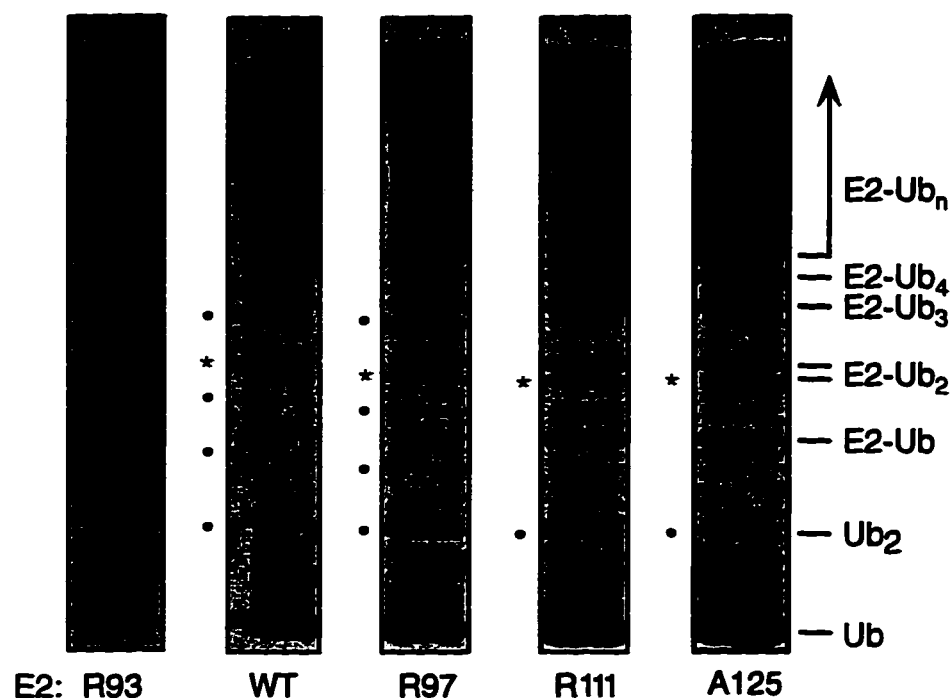
Figure 5.8. *In vitro* ubiquitination assays using bovine E1.
Purified ^{35}S-Ub and bovine E1 were incubated together with one of the
various UBC1Δ derivatives. Reaction products containing ^{35}S-Ub were
separated on an SDS-polyacrylamide gel and visualized using
autoradiography. Band assignment were made based on the criteria
described in section 5.3.3. Free multiUb chains are identified by a dot for
all other reactions. As R93 is unable to conjugate Ub to itself all of the
bands seen in this lane correspond to free multiUb chains. Free multiUb
chains are identified by a dot for all the other reactions. The remaining
bands comprise Ub conjugates of the UBC1Δ derivatives (E2-Ub to E2-
Ub$_n$). The E2-Ub$_2$ conjugate has been previously identified to consist of
two distinct species (Hodgins et al., 1996) the less abundant of which has
been marked by an asterix.

135

5.5. Bibliography.

Chen, P., Johnson, P., Sommer, T., Jentsch, S., and Hochstrasser, M. (1993). Multiple ubiquitin-conjugating enzymes participate in the *in vivo* degradation of the yeast MATα2 repressor. *Cell* **74**, 357-369.

Cook, W. J., Jeffery, L. C., Sullivan, M.L., and Vierstra, R. D. (1992). Three-dimensional strycture of a ubiquitin-conjugating enzyme (E2). *J. Biol. Chem.* **21**, 15116-15121.

Cook, W. J., Jeffery, L. C., Xu, Y., and Chau, V. (1993). Tertiary structures of class I ubiquitin-conjugating enzymes are highly conserved: crystal structure of yeast UBC4. *Biochemistry* **32**, 13809-13817.

Girod, P. A., Vierstra, R. D. (1993). A major ubiquitin conjugation system in wheat germ extracts involves a 15 kDa ubiquitin-conjugating enzyme (E2) homologous to the yeast *UBC4/UBC5* gene products. *J. Biol. Chem.* **268**, 955-960.

Gwozd, C. S., Arnason, T. G., Cook, W. J., Chau, V., and Ellison, M. J. (1994). The yeast UBC4 ubiquitin conjugating enzyme monoubiquitinates itself in vivo: evidence for an E2-E2 homointeraction. *Biochemistry* **34**, 6296-6302.

Haas, A. L., and Bright, P. M. (1988). The resolution and characterization of putative ubiquitin carrier protein isozymes from rabbit reticulocytes. *J. Biol. Chem.* **263**, 13258-13267.

Hatfield, P. M., Callis, J., and Vierstra, R. D. (1990). Cloning of ubiquitin activating enzyme from wheat and expression of a functional protein in Escerichia coli. *J. Biol. Chem.* **26**, 15813-15817.

Hodgins, R., Gwozd, C., Arnason, T., Cummings, M., and Ellison, M. J. (1996). The tail of ubiquitin-conjugating enzyme redirects multi-ubiquitin chain synthesis from the lysine 48-linked configuration to a novel nonlysine-linked form. *J. Biol. Chem.* **271**, 28766-28771.

Pickart, C.M., and Rose I.A. (1985). Functional heterogeneity of ubiquitin carrier proteins. *J. Biol. Chem.* **260**, 1573-1581.

Pitluk, Z. W., McDonough, M., Sangan, P., and Gonda, D.K. (1995). Novel *CDC34 (UBC3)* ubiquitin-conjugating enzyme mutants obtained by charge to alanine scanning mutagenesis. *Mol. Cell. Biol.* **15**, 1210-1219.

Prendergast, J. A., Ptak, C., Arnason, T. G., and Ellison, M. J. (1995). Increased ubiquitin expression suppresses the cell cycle defect associated with the yeast ubiquitin conjugating enzyme, CDC34 (UBC3): evidence for a noncovalent interaction between CDC34 and ubiquitin. *J. Biol. Chem.* **270**, 9347-9352.

Ptak, C., Prendergast, J. A., Hodgins, R., Kay, C. M., Chau, V., and Ellison, M. J. (1994). Functional and physical characterization of the cell cycle ubqiutin-conjugating enzyme CDC34 (UBC3): Identification of a functional determinant within the tail that facilitates CDC34 self-association. *J. Biol. Chem.* **42**, 26539-26545.

Seufert, W., McGrath J. P., and Jentsch, S. (1990). *UBC1* encodes a novel member of an essential subfamily of yeast ubiquitin-conjugating enzymes involved in protein degradation. *EMBO J.* **9**, 4535-4541.

Sherman, F., Fink, G. R., and Hicks, J. B., (1986) *Methods in Yeast Genetics*. Cold Spring Harbor Laboratory Press, Cold Spring Harbor, NY.

Silver, E. T., Gwozd, T. J., Ptak, C., Goebl, M., and Ellison M. J. (1992). A chimeric ubiquitin conjugating enzyme that combines the cell cycle properties of CDC34 (UBC3) and the DNA repair properties of RAD6 (UBC2): implications for the structure, function, and evolution of the E2s. *EMBO J.* **11**, 3091-3098.

Tabor, S., and Richardson, C. C. (1985). A bacteriophage T7 RNA poymerase/promoter system for controlled exclusive expression of specific genes. *Proc. Natl. Acad. Sci. USA* **82**, 1074-1078.

Chapter 6

Conclusions

One of the principal aims of this work was to identify those amino acids or peptide regions within ubiquitin conjugating enzymes which defined either conserved or distinct E2 functions. Two E2s were chosen for this study namely CDC34 and the carboxy terminal deletion derivative of UBC1, UBC1Δ. Each of these enzymes was useful for such analysis as they both have distinct *in vivo* functions and both may be utilized in *in vitro* ubiquitination reactions. In particular, CDC34 is a key enzyme which functions to allow yeast cells to pass through the G1 phase into the S phase of the cell cycle. The *in vivo* function of UBC1Δ overlaps with that of UBC4 and UBC5 within the stress response pathway. *In vitro*, each of these enzymes also carries out typical E2 activities such as E2~Ub thiolester formation and may also autoubiquitinate themselves. This latter property allows each enzyme to also function as a target for ubiquitination. By introducing amino acid substitutions or peptide deletions the affect of these changes on the *in vivo* and *in vitro* functions of these E2s could be assessed.

CDC34 is unique among E2s in that it possess both a carboxy terminal extension or tail as well as a catalytic domain insertion. The absence of these particular elements from the primary sequences of other E2s suggested that they impart unique properties to CDC34 which allowed it to carry out its cell cycle function. In fact, deletion of either the catalytic domain insertion or the tail domain eliminated the ability of CDC34 to carry out its cell cycle function *in vivo*. Using a series of CDC34 tail deletion derivatives it was determined that the first 39 residues of the tail domain (residues 171-209) were necessary and sufficient for full cell cycle function *in vivo*. Furthermore, these same residues were required for CDC34 self-association *in vitro*. These observations indicated that the cell cycle function of CDC34 is dependent upon its ability to self-associate.

The role self-association plays in defining this function remains to be determined. We have suggested that one possible role is to facilitate the assembly of multiUb chains (see Figure 2.7). The observation that the UBC1Δ~Ub thiolester could support minimal multiUb chain assembly provides some evidence that E2-E2 complexes may function in this way (see section 4.3.3). An alternative possibility is that self-association functions to generate a binding site on the surface of CDC34. CDC34 targets a number of different proteins for degradation *in vivo* (Bai*et al.*, 1996; Willems *et al.*, 1996; Deshaies *et al.*, 1995; Yaglom *et al.*, 1995; Schwob *et al.*, 1994). The degradation of these targets appears to require the formation of a multisubunit complex. Some of these components, in

138

particular CDC53, are thought to provide an E3 function thereby bringing CDC34 and its targets into close proximity. As such, if CDC34 self-association generates a novel binding surface it is most likely that an E3, potentially CDC53 rather than the actual protein targets would bind at such a site. Current studies in the lab of M. Goebl are addressing whether any of the CDC34 tail deletion derivatives presented in chapter 2 affect the ability of CDC34 and CDC53 to interact *in vivo* (N. Mathias, pers. comm.)

Deletion of the CDC34 catalytic domain insertion apart from eliminating the ability of CDC34 to carry out its cell cycle function *in vivo*, also significantly altered its *in vitro* activity. The observation that deletion of the insert results in a hyper-autoubiquitination activity also suggests that the transfer of Ub from the CDC34 active site to a target lysine residue is regulated by the catalytic domain insertion.

The need for regulating CDC34 function *in vivo* is suggested by the observations that it is both phosphorylated and ubiquitinated *in vivo* (Goebl *et al.*, 1994). Regulating CDC34 function through its degradation does not appear to be a key process as deletion of the principal autoubiquitination sites at the carboxy terminus of the tail domain does not affect its cell cycle function (see Figure 2.1). Furthermore, CDC34 appears to be a long lived protein, suggesting that it is not rapidly degraded by the ubiquitin system or only a fraction of all CDC34 molecules are degraded in this fashion.

As a long lived protein it may be necessary to modulate the ubiquitination activity of CDC34 to ensure that its targets are not degraded prematurely. *In vitro*, it appears that the catalytic domain insertion does in fact limit this activity. Liu *et al.*, (1995) identified a genetic interaction between the catalytic domain insertion and residue S97 also present in the catalytic domain (see Figure 3.9). Furthermore, the amino acid substitutions S97D or S97A were not tolerated by CDC34 resulting in a loss of its cell cycle function. The genetic interaction and need for residue S97 suggest that phosphorylation of S97 may function to remove the block in CDC34's ubiquitination activity. Such a hypothesis would predict that S97 is a phosphorylation site, second CDC34 phosphorylation is cell cycle dependent, and third CDC34 phosphorylation increases its activity. With respect to the third point, Kong and Chock (1992) have already shown *in vitro* that protein ubiquitination by the rabbit reticulocyte E2-32K is increased 2.4 fold upon phosphorylation of the E2.

Unlike CDC34, UBC1Δ closely resembles the active sites of most E2s in that it lacks a catalytic domain insertion. In this study it was shown that two amino acid substitutions introduced at positions close to and on the carboxy terminal side of the active site cysteine affected the ability of UBC1Δ to assemble multiUb chains. One derivative, R97 increased the rate of chain synthesis, while the second A111 showed a defect in chain extension. The catalytic domain insertion of CDC34 also occurs just on the carboxy terminal side of its

139

catalytic domain. In fact, the insertion is found adjacent to the loop structure in which UBC1Δ R97 is found (see Figure 5.1). Like the R97 and R111 UBC1Δ derivatives, the catalytic domain deletion derivative cdc34M showed a distinct ability from CDC34 in its ability to synthesize multiUb chains. These results indicate that structures found on the carboxy terminal side of an E2s active site function to control protein ubiquitination and multiUb chain assembly. Thus, sequence differences between E2s within this region may in fact function to regulate these activities.

Studies employing UBC1Δ also showed that E1 may play an integral role in multiUb chain assembly along with E2s. It was found that bovine E1 could preferentially utilize the UBC1Δ-Ub conjugate over unmodified UBC1Δ in the formation of an E2-Ub thiolester. This indicated that E2s could regulate multiUb chain assembly via E2 specificity. Current studies in the lab are addressing the question of whether an E1-E2 complex forms in the process of chain assembly. Large multisubunit complexes such as the APC or cyclosome have already been identified as being responsible for the ubiquitination of B-type cyclins (King et al., 1995; Sudakin et al., 1995). It will interesting to see if these complexes also contain E1s thereby allowing the entire process of protein ubiquitination to occur within a large multisubunit complex. Identification of a bovine E1-UBC1Δ complex that was responsible for UBC1Δ autoubiquitination would support the existence of such ubiquitination complexes.

6.1 Bibliography

Bai, C., Sen, P., Hofmann, K., Ma, L., Goebl, M., Harper, W., and Elledge, S. J. (1996). *SKP1* connects cell cycle regulators to the ubiquitin proteolysis machinery through a novel motif, the F-box. *Cell* **86**, 263-274.

Deshaies, R. J., Chau, V., and Kirschner, M. (1995). Ubiquitination of the G1 cyclin Cln2p by a Cdc34p-dependent pathway. *EMBO J.* **14**, 303-312.

Goebl, M. G., Goetsch, L., and Byers, B. (1994). The Ubc3 (Cdc34) ubiquitin-conjugating enzyme is ubiquitinated and phosphorylated *in vivo*. *Mol. Cell. Biol.* **14**, 3022-3029.

King, R. W., Peters, J-M., Tugendreich, S., Rolfe, M., Hieter, P., and Kirschner, M. W. (1995). A 20S complex containing CDC27 and CDC16 catalyzes the mitosis-specific conjugation of ubiquitin to cyclin B. *Cell* **81**, 279-288.

Kong, S. K., and Chock., P. B. (1992). Protein ubiquitination is regulated by phosphorylation. *J. Biol. Chem.* **267**, 14189-14192.

Liu, Y., Mathias, N., Steussy, N., and Goebl, M. G. (1995). Intragenic suppression among *CDC34 (UBC3)* mutations defines a class of ubiquitin-conjugating catalytic domains. *Mol. Cell. Biol.* **15**, 5635-5644.

Schwob, E., Bohm, T., Mendenhall, M. D., and Nasmyth, K. (1994). The B-type cyclin kinase inhibitor p40^{SIC1} controls the G1 to S transition in S. cerevisiae. *Cell* **79**, 233-244.

Sudakin, V., Ganoth, D., Dahan, A., Heller, H., Hershko, J., Luca, F. C., Ruderman, J. V., and Hershko, A. (1995). The cyclosome, a large complex containing ubiquitin ligase activity, targets cyclins for destruction at the end of mitosis. *Mol. Biol. Cell* **6**, 185-198.

Willems, A. R., Lanker, S., Patton, E. E., Craig, K. L., Nason, T. F., Mathias, N., Kobayashi, R., Wittenberg, C., and Tyers, M. (1996). Cdc53 targets phosphorylated G1 cyclins for degradation by the ubiquitin proteolytic pathway. *Cell* **86**, 453-463.

Yaglom, J., Linskens, M. H. K., Sadis, S., Rubin, D. M., Futcher, B., and Finley, D. (1995). p34^{cdc28}-mediated control of Cln3 cyclin degradation. *Mol. Cell. Biol.* **15**, 731-741.

Appendix I

Growth repression of a *cdc34* mutant strain is dependent upon the GTPase activation domain of SAC7

The ubiquitin conjugating enzyme CDC34 plays a critical role in allowing yeast cells to pass from the G1 phase to the S phase of the cell cycle (Goebl *et al.*, 1988). In this capacity CDC34 has been implicated in targeting a number of key cell cycle regulators for degradation by the ubiquitin dependent proteolytic pathway. Counted among these targets are FAR1 (McKinney *et al.*, 1993), CLN2 (Willems *et al.*, 1996; Deshaies *et al.*, 1995), CLN3 (Yaglom *et al.*, 1995) and SIC1 (Bai *et al.*, 1996; Schwob *et al.*, 1994). These proteins control the passage of cells through START, the G1 to S phase transition, as well as the onset of replication during S phase.

The activities of these cell cycle regulators are themselves controlled through covalent modifications such as phosphorylation and ubiquitination. Given that CDC34 functions in the cell cycle as a regulator it is reasonable to expect that its function is also controlled in some fashion. The *in vivo* ubiquitination and phosphorylation of CDC34 (Goebl *et al.*, 1994) as well as the identification of UBS1 as a positive regulator of CDC34 function (Prendergast *et al.*, 1995) lend credence to this idea.

This section describes the results of a genetic selection scheme which was used to identify negative regulators of CDC34 function. The approach used builds upon the observation that the tail deletion derivative cdc34Δ_{185} could restore CDC34 function to a *cdc34* ts strain but not a *cdc34* disruption strain (Ptak *et al.*, 1994). These results demonstrate that within the ts strain both cdc34Δ_{185} and the cdc34 ts polypeptide are required in order for CDC34 function to be restored at the non-permissive temperature. While cdc34Δ_{185} restores growth at the non-permissive temperature a large proportion of the *cdc34* ts/*cdc34Δ_{185}* cells still exhibited the multibudded phenotype associated with a loss of CDC34 function. Thus, cdc34Δ_{185} only partially complements the ts mutation.

These results indicated that even in the presence of cdc34Δ_{185} these ts cells were precariously close to losing their ability to grow. It was expected that any negative perturbation in the activity of either cdc34Δ_{185} or the cdc34 ts polypeptides would eliminate the ability of these cells to grow at the non-permissive temperature. Based on this premise, gene product(s) whose overexpression had a negative affect on the activity of cdc34Δ_{185}, cdc34 ts, or both polypeptides would eliminate CDC34 function from these cells.

To identify such a gene product a high copy yeast genomic library was transformed into the *cdc34-2* ts strain that was also expressing cdc34Δ_{185}. Transformed cells were tested

for growth at both 25 °C and 37 °C. Colonies able to grow at the permissive temperature of 25 °C, but not at the non-permissive temperature of 37 °C were identified and retained for further analysis. Of the 2×10^5 colonies screened, library plasmids from two were retained based on their abilities to render cells completely inviable upon subsequent transformations. Ten other plasmids were also retained but were not analyzed further as they did not consistently eliminate cell growth or did so partially.

On the basis of restriction, and southern analysis these two library plasmids were shown to contain identical genomic fragments (results not shown). One of these plasmids was subcloned by partial Sau 3A digestion to produce a set of plasmids carrying different sized DNA fragments. From this set of plasmids four plasmids were retained of which three were shown to inhibit growth at the non-permissive temperature (Figure A.1). Sequencing showed that plasmids A3.1 and A4.1 contained identical Sau 3A fragments while plasmid A1.4 contained a larger fragment which spanned the sequence found in the other two. As A3.1 contained a smaller sized genomic fragment that could cause inhibition it was used in all subsequent experiments.

Using the BLAST database search (Altschul *et al.*, 1990) a single truncated ORF was identified within the genomic fragment contained in plasmid A3.1. According to the yeast genome project, a fragment corresponding to the first 1270 nucleotides of a 1962 nucleotide ORF was present in A3.1. A conflicting sequence had been presented previously by Dunn and Shortle (1990). In this work, an 822 nucleotide ORF referred to as *SAC7* was identified as a suppressor of actin mutations. Comparison of these sequences shows that the genome project sequence contains additional nucleotides at both the 5' and 3' ends of the ORF.

3' differences result from the absence of a C nucleotide in the Dunn and Shortle sequence. Lack of this residue causes a frame shift in the ORF introducing a stop codon which shortens the ORF relative to the genome project ORF. In the 5' region these ORFs different start codons were employed. As a result the genome project *SAC7* sequence was 1140 nucleotides longer than that of Dunn and Shortle.

In both this work and that of Dunn and Shortle a 3' truncation of *SAC7* was shown to be sufficient for the repressive and suppressive affects observed respectively. The truncation occurs in the sequence prior to the point in the sequence where the two *SAC7* ORFs differ. This shows that the 3' end of SAC7 is dispensable with respect to its function.

Translation of the genome project sequence and a subsequent protein database search (Altschul *et al.*, 1990) identified regions within SAC7 showing significant homology to RHO-GAP proteins. These proteins are characterized by three polypeptide regions (Figure

A.2A) which are conserved between RHO-GAPs from different organisms (Boguski and McCormick, 1993). As such, *SAC7* as defined by the genome project will be referred to as GAP-SAC7 (Figure A.2B).

Use of a distinct start codon by Dunn and Shortle results in a translated gene product lacking the first two of these RHO-GAP homology regions. As such, the Dunn and Shortle sequence will be referred to as SAC7 (Figure A.2B). Also, the carboxy terminal truncations of both versions are identified as SAC7Δ and GAP-SAC7Δ.

To determine whether the RHO-GAP homology regions were required for growth repression plasmids carrying the *SAC7Δ* and *GAP-SAC7Δ* coding sequences were transformed into the *cdc34-2* ts/*cdc34Δ$_{185}$* yeast strain and tested for growth at the non-permissive temperature. Plasmids containing no SAC7 sequence (control) and the A3.1 plasmid were also transformed into this strain. Both the control and the *SAC7Δ* plasmids were unable to repress cell growth (Figure A.3). As such, SAC7Δ as defined by Dunn and Shortle was not the repressor identified in this work. On the other hand, both the *GAP-SAC7Δ* and the A3.1 plasmids did cause repression of cell growth. This identified that the *GAP-SAC7Δ* sequence defined by the genome project and contained within the A3.1 plasmid defined the repressor. Furthermore, the presence of the RHO-GAP domain was essential in order for GAP-SAC7Δ to carry out its repressive function.

It remains to be seen how SAC7 carries out its repressive affect. The requirement of the RHO-GAP domain in this activity suggests a possibility. RHO proteins such as CDC42 and RHO1-4 in yeast are small GTPases of the RAS superfamily, implicated in defining cell polarity and bud assembly during the yeast cell cycle. As GTPases, they function within signal transduction pathways. In particular, RHO proteins carry out their signaling functions in association with the cytoskeleton (reviewed by Drubin and Nelson, 1996).

These proteins cycle through an active GTP-bound state and an inactive GDP-bound state. Control of these states is defined by GTPase exchange factors (RHO-GEF) which stimulate the exchange of GDP bound by the RHO protein with GTP thereby activating RHO. Stimulation of RHO's GTPase activity by GTPase activating proteins (RHO-GAP) results in the hydrolysis of GTP to GDP thereby inactivating RHO. As such RHO-GAPs are negative regulators of RHO function.

SAC7 possesses the regulatory GAP sequences and has also been found to associate with actin, an integral component of the cytoskeleton and a key component of bud assembly. This suggests that GAP-SAC7 may modulate the activity of one or more yeast RHO proteins. Furthermore, this activity could be dependent upon its ability to interact with the cytoskeleton during bud assembly.

Connections between bud assembly at the plasma membrane and CDC34 found in the nucleus are suggested by the occurrence of multiple, elongated buds as a terminal phenotype associated with *cdc34* mutations (Byers and Goetsch, 1973). Signals between the growing bud and the nucleus may act to modulate CDC34 function. Such a signal could induce ubiquitination or phosphorylation of CDC34 thereby down regulating its activity. Alternatively, the signal could increase the levels of a CDC34 target. Previous studies have shown that increased levels of a CDC34 target inhibits growth of a *cdc34* ts mutant. This likely results from cdc34 being sequestered through interactions with the target reducing cdc34's effective concentration.

On the other hand, degradation of targets by CDC34 is required for passage from the G1 to the S phase of the cell cycle. Increased expression of a key CDC34 target within the mutant *cdc34-2* ts/*cdc34Δ_{185}* background could increase the overall half-life of this target. The inability of the cdc34-2 ts and cdc34Δ_{185} polypeptides to effectively remove such a target could also account for the repression of cell growth.

As SAC7 was identified as a repressor of CDC34 function it was expected that this function could be rescued by CDC34 suppressors. In fact compared to a null control plasmid, plasmids expressing wild type CDC34, Ub and UBS1 all were able to rescue growth of *cdc34-2* ts/*cdc34Δ_{185}* cells that also contained the *GAP-SAC7Δ* plasmid. In the presence of CDC34 the cells also showed no aberrant morphologies at the non-permissive temperature. Cells expressing Ub and UBS1 on the other hand still exhibited a large proportion of cells having multiple, elongated buds. Thus, suppressors of the *cdc34-2* ts mutation were unable to fully restore CDC34 function to this strain in the presence of GAP-SAC7Δ.

While the homology of SAC7 to other RHO-GAP proteins is striking it remains to be definitively identified as such. Simple *in vitro* assays may be used to identify whether SAC7 is in fact a RHO-GAP. If in fact SAC7 turns out to have this activity these assays may also help to identify which RHO protein from yeast functions best as its target and also within which signal transduction pathway it is involved.
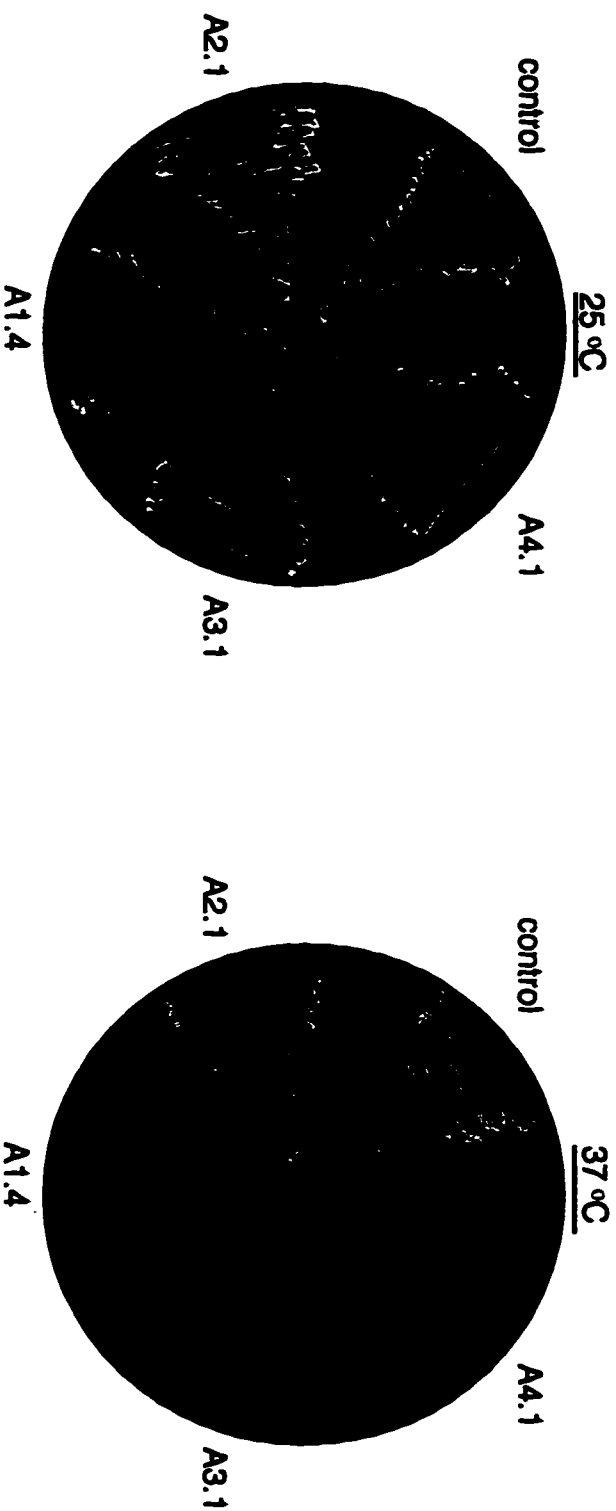
Figure A.1. **Growth inhibition of a *cdc34* mutant.** Plasmids used here included A1.4, A2.1, A3.1, and A4.1 which carry yeast genomic DNA fragments subcloned from a yeast genomic library plasmid. Also used was a control plasmid identical in every respect to the others except that it lacks a genomic DNA fragment. Each plasmid was transformed into the *cdc34-2* ts yeast strain already harboring a plasmid possessing the *cdc34Δ185* coding sequence. From each transformation a single colony was picked, grown in liquid culture to mid log phase, after which 10^5 cells of each was spotted onto plates and streaked out. Plates were grown at either 25 °C or 37 °C for three days to allow for colony development.
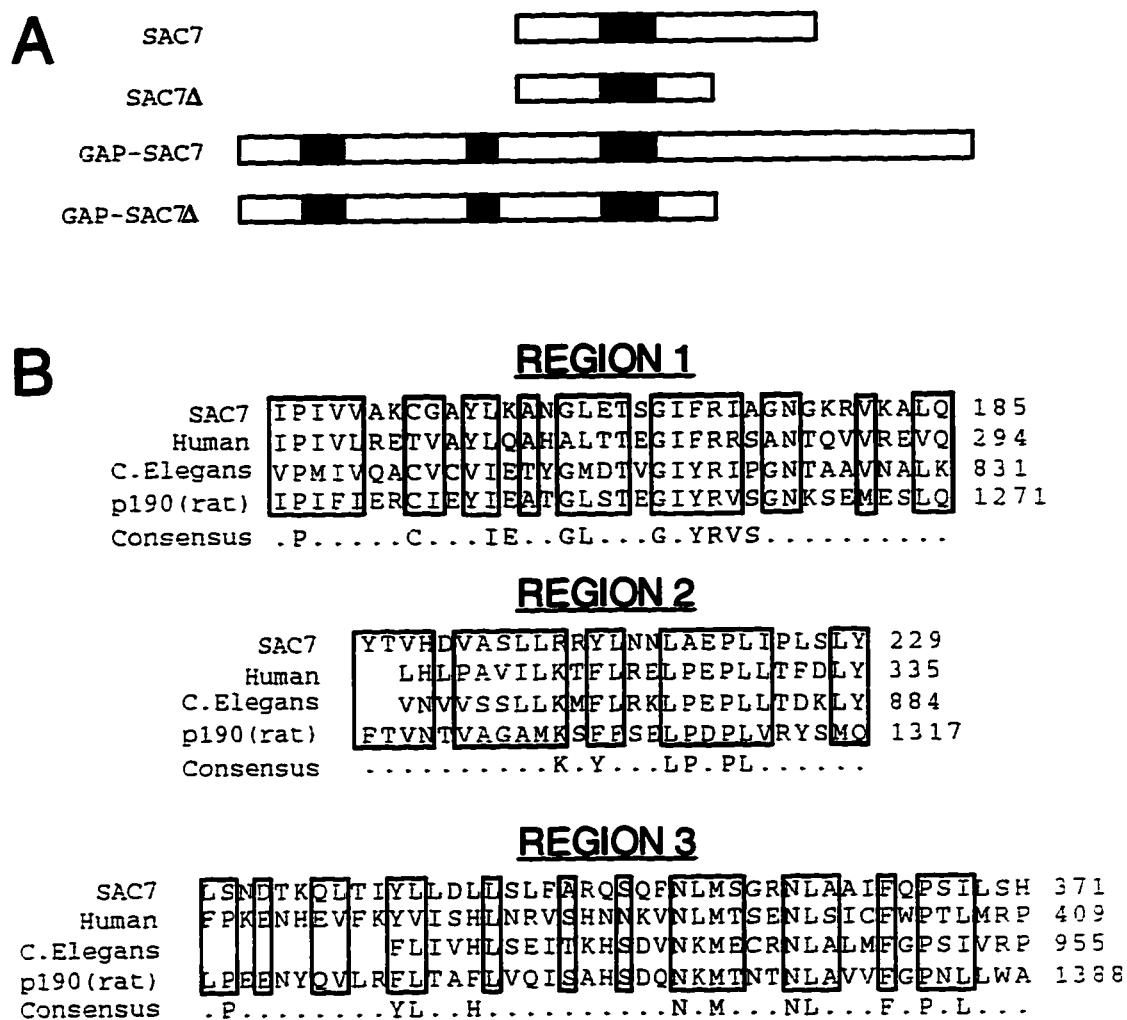
146

A

SAC7

SAC7Δ

GAP-SAC7

GAP-SAC7Δ

B

REGION 1

```
      SAC7  IPIVVAKCGAYLKANGLETSGIFRIAGNGKRMKALQ  185
     Human  IPIVLRETVAYLQAHALTTEGIFRRSANTQVVREVQ  294
 C.Elegans  VPMIVQACVCVIETYGMDTVGIYRIPGNTAAVNALK  831
 p190(rat)  IPIFIERCIEYIEATGLSTEGIYRVSGNKSEMESLQ  1271
 Consensus  .P.....C...IE..GL...G.YRVS..........
```

REGION 2

```
      SAC7  YTVHDVASLLRRYLNNLAEPLIPLSLY  229
     Human  LHLPAVILKTFLRELPEPLLTFDLY     335
 C.Elegans  VNVVSSLLKMFLRKLPEPLLTDKLY     884
 p190(rat)  FTVNTVAGAMKSFESELPDPLVRYSMQ  1317
 Consensus  ...........K.Y...LP.PL......
```

REGION 3

```
      SAC7  LSNDTKQLTIYLLDLDSLFARQSQFNLMSGRNLAAIFQPSILSH  371
     Human  FPKENHEVFKYVISHLNRVSHNNKVNLMTSENLSICFWPTLMRP  409
 C.Elegans  FLIVHLSEIIKHSDVNKMECRNLALMFGPSIVRP  955
 p190(rat)  LPEENYQVLRFLTAFLVQISAHSDQNKMTNTNLAVVEGPNLLWA  1388
 Consensus  .P........YL..H..........N.M...NL...F.P.L...
```

Figure A.2. **SAC7 gene products.** Part A shows differences in the SAC7 gene product as published by Dunn and Shortle (1990; SAC7) when compared to that identified by the yeast genome project (GAP-SAC7). Both in this work and that of Dunn and Shortle the same carboxy terminal trunction was isolated. This truncation produces the SAC7Δ and the GAP-SAC7Δ gene products respectively. The GAP-SAC7 gene product showed homolgy to three distinct ploypeptide stretches found in other proteins previously identified as RHO GTPase activating proteins or RHO-GAPs. These regions of homolgy are shown in Part B. Boxes identify residues showing sequence conservation between at least three of the four proteins. The consensus sequence identifies those residues which have previously been identified as characteristic of RHO-GAPs (Boguski and McCormick, 1993). Numbers refer to the final amino acid of each sequence shown identifying its position within the overall protein sequence. The location of these three homology regions within the gene products identified in Part A are shown in black.
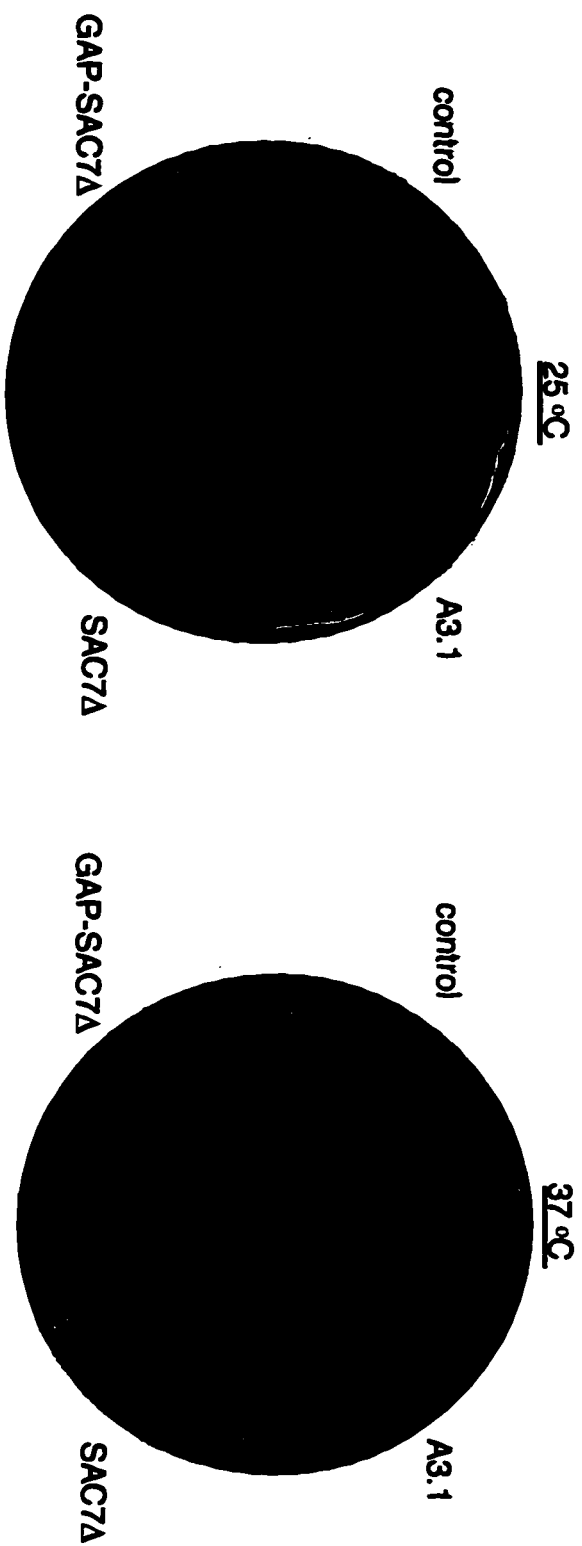
147

Figure A.3. Growth inhibition of a *cdc34* mutant requires the RHO-GAP domain of SAC7. Plasmids carrying the coding sequences for SAC7Δ and GAP-SAC7Δ shown in Figure A.2 along with the control plasmid and plasmid A3.1 shown in Figure A.1 were all transformed into the *cdc34-2* ts yeast strain already harboring a plasmid possessing the *cdc34Δ185* coding sequence. From each transformation a single colony was picked, grown in liquid culture to mid log phase, after which 10⁵ cells of each was spotted onto plates and then streaked out. Plates were grown at either 25 °C or 37 °C for three days to allow for colony development.
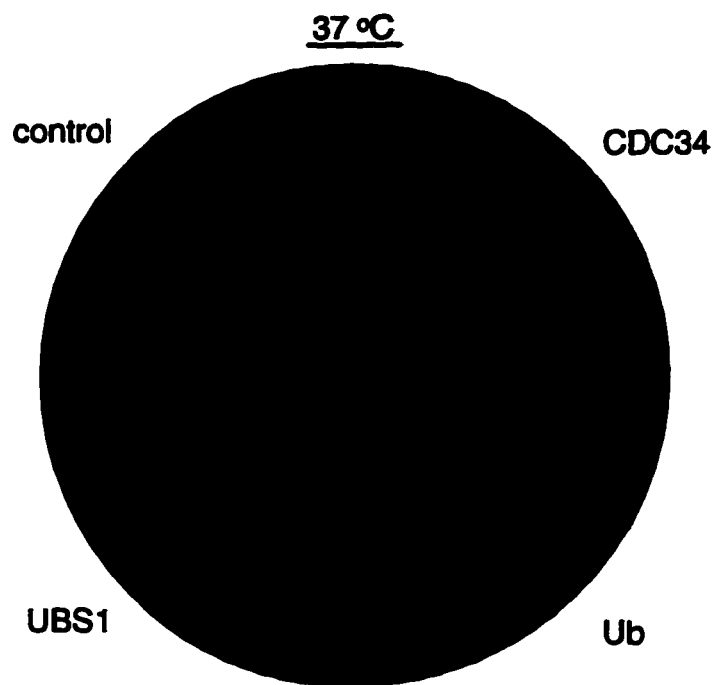
37 °C

control

CDC34

UBS1

Ub

Figure A.4. **Suppressors of** cdc34 **mutations complement the growth inhibition phenotype mediated by SAC7.** Plasmids carrying the coding sequence for CDC34 and the cdc34-2 supressors Ub and UBS1 were used here. These plsmids were transformed into the cdc34-2 ts yeast strain already harboring two plasmids of which one contained the cdc34Δ185 coding sequence, and the other contained the GAP-SAC7Δ coding sequence. From each transformation a single colony was picked, grown in liquid culture to mid log phase, after which 10^5 cells of each was spotted onto plates and then streaked out. Plates were grown at either 25 °C or 37 °C for three days to allow for colony development. Only the plate grown at 37 °C is shown.

A.1. Bibliography

Altschul, S. F., Gish, W., Miller, W., Myers, E. W., and Lipman, D. J. (1990). Basic local alingment search tool. *J. Mol. Biol.* **215**, 403-410.

Bai, C., Sen, P., Hofmann, K., Ma, L., Goebl, M., Harper, W., and Elledge, S. J. (1996). *SKP1* connects cell cycle regulators to the ubiquitin proteolysis machinery through a novel motif, the F-box. *Cell* **86**, 263-274.

Boguski, M. S., and McCormick, F. (1993). Proteins regulating Ras and its relatives. *Nature* **366**, 643-654.

Byers, B., and Goetsch, L. (1973). Duplication of spindle plaques and integration of the yeast cell cycle. *Cold Spring Harbor Symp. Quant. Biol.* **38**, 123-131.

Deshaies, R. J., Chau, V., and Kirschner, M. (1995). Ubiquitination of the G1 cyclin Cln2p by a Cdc34p-dependent pathway. *EMBO J.* **14**, 303-312.

Dunn, T. M., and Shortle, D. (1990). Null alleles of *Sac7* suppress temperature-sensitive actin mutations in *Saccharomyces cerevisiae*. *Mol. Cell. Biol.* **10**, 2308-2314.

Drubin, D. G., and Nelson, W. J. (1996). Origins of cell polarity. *Cell* **84**, 335-344.

Goebl, M. G., Yochem, J., Jentsch, S., McGrath, J. P., Varshavsky, A., and Byers, B. (1988). The yeast cell cycle gene *CDC34* encodes a ubiquitin-conjugating enzyme. *Science* **241**, 1331-1335.

Goebl, M. G., Goetsch, L., and Byers, B. (1994). The Ubc3 (Cdc34) ubiquitin-conjugating enzyme is ubiquitinated and phosphorylated *in vivo*. *Mol. Cell. Biol.* **14**, 3022-3029.

Prendergast, J. A., Ptak, C., Kornitzer, D., Steussy, C. N., Hodgins, R., Goebl, M., and Ellison, M. J. (1996). Identification of a positive regulator of the cell cycle ubqiutin-conjugating enzyme Cdc34 (Ubc3). *Mol. Cell. Biol.* **16**, 677-684.

Ptak, C., Prendergast, J. A., Hodgins, R., Kay, C. M., Chau, V., and Ellison, M. J. (1994). Functional and physical characterization of the cell cycle ubqiutin-conjugating enzyme CDC34 (UBC3): Identification of a functional determinant within the tail that facilitates CDC34 self-association. *J. Biol. Chem.* **42**, 26539-26545.

Schwob, E., Bohm, T., Mendenhall, M. D., and Nasmyth, K. (1994). The B-type cyclin kinase inhibitor p40^{SIC1} controls the G1 to S transition in S. cerevisiae. *Cell* **79**, 233-244.

Willems, A. R., Lanker, S., Patton, E. E., Craig, K. L., Nason, T. F., Mathias, N., Kobayashi, R., Wittenberg, C., and Tyers, M. (1996). Cdc53 targets phosphorylated G1 cyclins for degradation by the ubiquitin proteolytic pathway. *Cell* **86**, 453-463.

Yaglom, J., Linskens, M. H. K., Sadis, S., Rubin, D. M., Futcher, B., and Finley, D. (1995). p34^{cdc28}-mediated control of Cln3 cyclin degradation. *Mol. Cell. Biol.* **15**, 731-741.